SYNTHESIS AND CHARACTERIZATION OF POLYMERIC AND INORGANIC MATERIALS FOR BIOMEDICAL APPLICATIONS

By

Georgina Annette Comiskey

A DISSERTATION

Submitted to
Michigan State University
in partial fulfillment of the requirements
for the degree of

Chemistry-Doctor of Philosophy

2013

ABSTRACT

SYNTHESIS AND CHARACTERIZATION OF POLYMERIC AND INORGANIC MATERIALS FOR BIOMEDICAL APPLICATIONS

By

Georgina Annette Comiskey

The need of safe biodegradable materials for drug delivery has been an increasing demand. Polylactide is a biodegradable and bioresorbable polyester. Polylactide has the disadvantage of hydrophobicity and little functionality. Scientists have taken on the task of modifying polylactide to overcome its shortcomings while retaining its good properties. Herein, we explore the synthesis of substituted polylactides and their applications. We formed stereocomplexes of isotactic poly(isopropyl glycolide), a semicrystalline polyester. Stereocomplexes will have different thermal and crystallinity properties different from the homopolymers. We also explored the modification of poly(propargyl glycolide) (PPGL) via click chemistry and further crosslinking of PPGL clicked with PEG chains using a simple alkyl diazide or a diazide containing a disulfide bond to obtain reductively degradable PPGL nanoparticles. We compared the reductive degradation of the two types of nanoparticles obtained. Using click chemistry, we modified PPGL with azide ligands containing various functional groups, which were then crosslinked. We tested the interaction of the various surface functional groups with a cell membrane lipid bilayer mimic. Similarly, we synthesized reductively degradable PPGL clicked with amines and we assessed their use as siRNA delivery vehicles. We found out that these polymeric siRNA delivery

vehicles were inefficient. In order to elucidate the reasons of the unsuccessful results of the previous attempt to deliver siRNA, we turned to surface modified silica nanoparticles containing dextran, which are very efficient siRNA delivery vehicles capable of triggering silencing of EGFP in human lung carcinoma cells without causing toxicity. We attempted to elucidate why these nanoparticles had such great silencing efficiency.

ACKNOWLEDGEMENTS

I would like to thank my advisor Dr. Gregory Baker for taking me under his wing and teaching me the basics of polymer science and how to be a problem solver. You will always be missed. Thanks to Dr. Milton Smith for becoming my advisor and helping me through a difficult time. Thanks to Dr. Cristina Chan and Dr. S. Patrick Walton for conversations that led to a better understanding of my project. Special thanks, to Amanda Malefyt for being an excellent collaborator in this intriguing and challenging project. Thanks to Olivia Chesniak and Daniel Vocelle for stepping up to the plate for the project. I would also like to thank my committee members Dr. Babak Borhan, Dr. Ned Jackson and Dr. Merlin Bruening for their guidance and support. I would like to thank past and present lab group members for all the conversations that led to better insight of my research and their help: Erin, DJ, Quanxuan, Hui, Tom, Qin, Sampa, Yiding, Heyi, Greg, Salinda, Zhe and Wen. I would also like to thank all my friends that made my experience in MSU very enjoyable. Thanks to Richard Staples, Dan Holmes, Kermit Johnson, Kathy Severin, Xudong Fan, Alicia Pastor, Abby Vanderberg, Rui Huang for teaching me different characterization techniques. Thanks to Dr. Jetze Tepe, Dr. Xuefei Huang, Dr. Kevin Walker for allowing me into their labs to use their equipment. Thanks to Dr. Medha Kamat for meaningful conversations and for teaching me important tools in a new area of my research. Thanks to my parents and sister for their support love and encouragement, also thanks to James, the person in my life that kept me motivated throughout this journey. This would not have been possible without all of you.

TABLE OF CONTENTS

LIST OF TABLES

LIST OF FIGURES

LIST OF SCHEMES

ABBREVIATIONS

A12	N-(3-Azidopropyl)-1,3-diaminopropane
Ac	Acetyl
APTES	3-aminopropyltrietoxysilane
ATRP	Atom transfer radical polymerization
Boc_2O	*tert*-Butyl dicarbonate
br	Broad
Cbz	Benzyloxy carbonyl group
CLSM	Confocal laser scanning microscopy
d^6-DMSO	Deuterated dimethylsulfoxide
Da	Daltons
DCC	Dicyclohexylcarbodiimide
DCC	Dicyclohexycarbodiimide
DLS	Dynamic light scattering
DMACA	7-Dimethylaminocoumarin acetic acid
DMAP	4-Dimethylaminopyridine
DMF	Dimethyl Formamide
DNA	Deoxyribonucleic acid
dsRNA	Double stranded RNA
DTT	Dithiothreitol
ECM	Extracellular matrix

EDC	1-Ethyl-3-(3-dimethylaminopropyl)carbodiimide
EGFP	Enhanced green fluorescence protein
FM	Functional monomer
FTIR	Fourier transform infrared spectroscopy
FTP	Freeze-pump-thaw
GPC	Gel permeation chromatography
HEPES	4-(2-Hydroxyethyl)-1-piperazineethanesulfonic acid
kDa	Kilodaltons
LF2K	Lipofectamine 2000
M	Multiplet
MHz	Megahertz
MMA	Methyl methacrylate
M_n	Number average molecular weight
M_w	Weight average molecular weight
MWCO	Molecular weight cutoff
N/P ratio	Nitrogen to phosphorous ratio
NAG	N-acetylgalactosamine
NHS	N-hydroxysuccinimide
NMR	Nuclear magnetic resonance
PBAVE	Poly(butylaminovinylether)
PBS	Phosphate buffer saline

PDI	Polydispersity index
PDMAEMA	Poly((2-dimethylamino)ethyl)methacrylate
PEG	polyethylene glycol
PGL	Propargyl glycolide
PLA	Polylactide
PLGA	Poly(lactide-*co*-glycolide)
PLL	Poly(L-lysine)
PMAA	Poly(methacrylic acid)
PPGL	Poly(propargyl glycolide)
PPM	Post-polymerization modification
ppm	parts per million
p-TsOH	*para*-Toluenesulfonic acid
RAFT	Reversible addition-fragmentation chain transfer polymerization
RISC	RNA-induced silencing complex
RNA	Ribonucleic acid
RNAi	RNA interference
ROP	Ring opening polymerization
SDS	Sodium dodecyl sulfate
SiNP	Silicon nanoparticle
siRNA	Small interfering RNA
TEOS	Tetraethyl orthosilicate (Tetraethoxy silane)

TGA	Thermogravimetric analysis
THF	Tetrahydrofuran
Ts	*para*-Toluenesulfonyl

Chapter 1: Introduction

Importance of polylactides

Polylactide is an important aliphatic polyester. Due to its biodegradability and biocompatibility, applications of polylactide materials range from the biomedical field to packaging. Polylactide has been used in sutures[1], tissue scaffolds[2] and bone engineering,[3] for orthopedics, drug controlled release[4-6] and gene therapy.[7-10] Polylactide is also a commodity chemical first commercialized by a venture of Cargill Inc. and The DOW Chemical Company.[5] Fermentation of sugar beets, cane sugar, potatoes, and corn[11] provides lactic acid, the starting material. Lactic acid is converted into polylactide.

Poly(L-lactide) (PLLA) and Poly(D-lactide) PDLA can be obtained from the corresponding lactide as mentioned before. Poly(L-lactide) and Poly(D-lactide) are both isotactic and semicrystalline polymers. Since the properties of PLLA/PDLA are different from racemic PLA, they are suitable for different applications. For example racemic PLA has a higher hydrolytic degradation rate which makes it suitable for biomedical applications. The slower degradation rate and the higher melting point of semicrystalline PLLA and PDLA could make them suitable for thermoplastic applications.

PLA has a pendant methyl group on each monomer subunit. If the pendant groups in the polyester chain are modified, the properties of the polymer change as well. Baker et al. synthesized high molecular weight substituted polylactides, gaining control over their thermal properties **(Scheme 1)**.[12, 13] When a cyclic bulky group was used,

the T_g increased. Acyclic aliphatic groups decreased the T_g. In the case of mixed lactides, the T_g was in between the T_gs of polylactide and the other substituted homopolymer **(Figure 1)**.

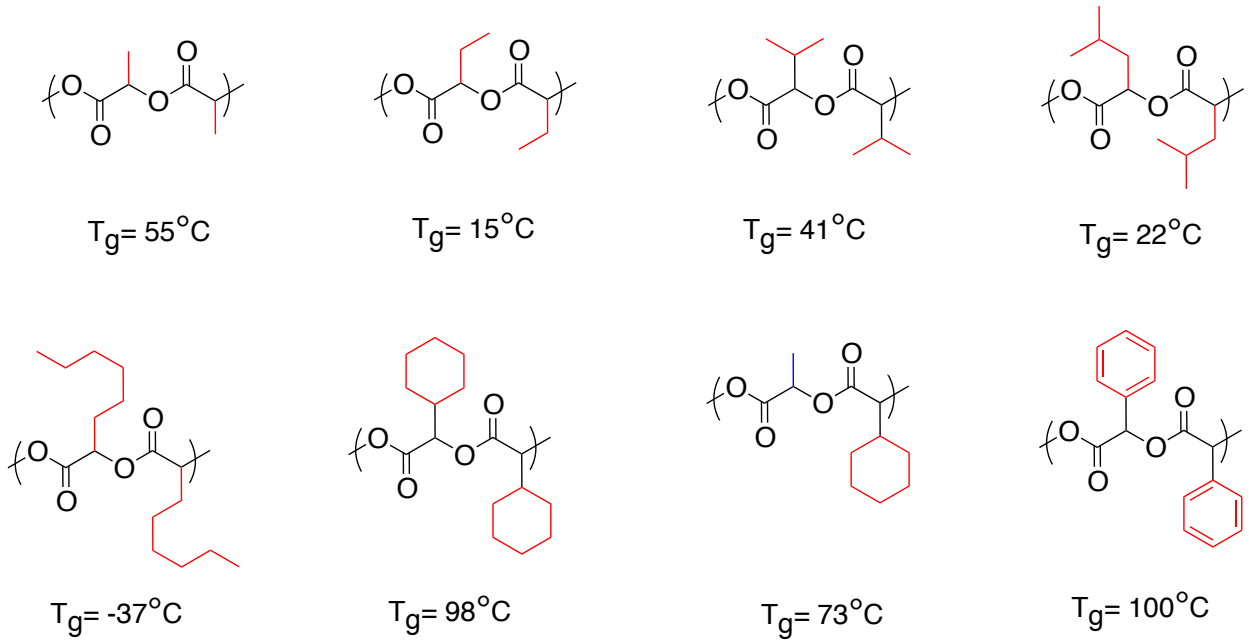

Figure 1 Racemic polylactide derivatives synthesized by Baker et al and their glass transition temperatures.[12, 13] For interpretation of the references to color in this and all other figures, the reader is referred to the electronic version of this dissertation.

Substituted polylactides are obtained using the functional monomer approach **(Scheme 1)**.[12, 13] In order to introduce chirality to the polymer, we must start with a chiral monomer. The most accessible chiral monomers are the ones derived from essential amino acids like valine, leucine, isoleucine and phenylalanine.

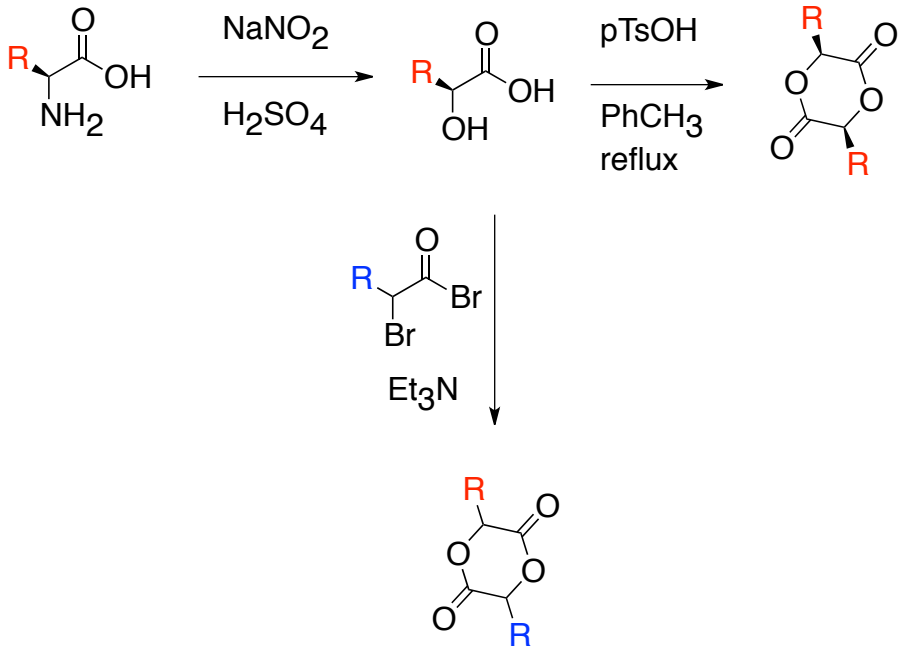

Scheme 1 General scheme for racemic lactide derivative monomer synthesis used by Baker et al.

Accessing modified polyglycolides

There are two main strategies for accessing modified polylactides, the functional monomer (FM) approach and post-polymerization modification (PPM) **(Figure 2)**.[14] In the FM approach, monomers are synthesized that contain hydroxyl, carboxyl, amino or other functional groups, and then polymerized. Usually, the functional groups require protection-deprotection steps during synthesis and polymerization. In the PPM approach, a latent functional group is incorporated into a monomer, and after polymerization, functional groups are appended to the polymer by coupling reactions.

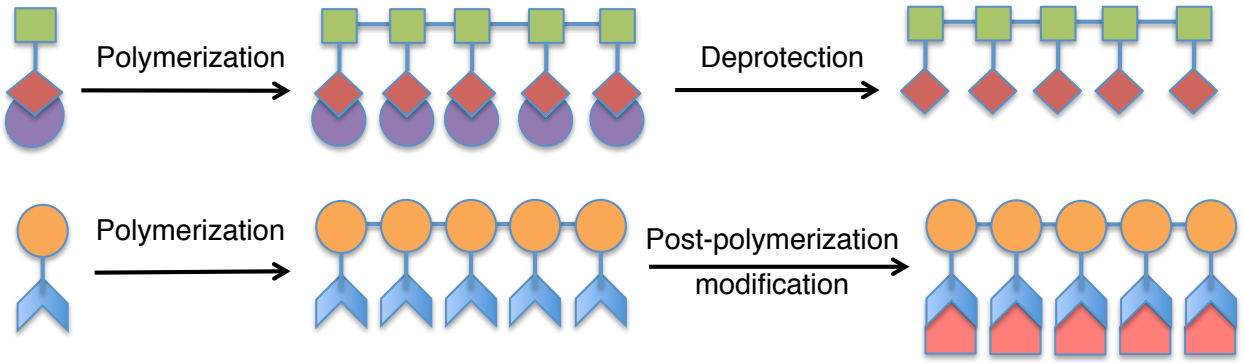

Figure 2 Two strategies used to introduce functionality in modified polylactides. Top: Functional monomer approach. Bottom: post-polymerization modification

In a general example of the FM approach, Baker and coworkers controlled the polylactide glass transition temperature (T_g) by synthesizing polylactide derivatives[12, 15] **(Figure 1)**. Racemic substituted lactide monomers were synthesized and then polymerized to high molecular weight poly(ethylglycolide), poly(*iso*-butylglycolide), and poly(hexylglycolide), with T_g's of 12, 22 and -37 °C respectively.[13] These examples show that the physical properties of polylactide can be tuned by the proper choice of the polymer backbone substituents. However, these polylactide derivatives have properties different from PLA, they lack the chemical functionality required for applications in biomaterials and medicine. Several functional polylactides have been described in the literature. One example is the work of Gerhardt and coworkers, where lactide and glycolide monomers were synthesized with protected amino, hydroxyl, and carboxylic acid groups from amino acids[16] **(Scheme 2)**. The main limitation of the functional monomer approach is that most monomers require multi-step syntheses, which limits rapid optimization of polymer properties.

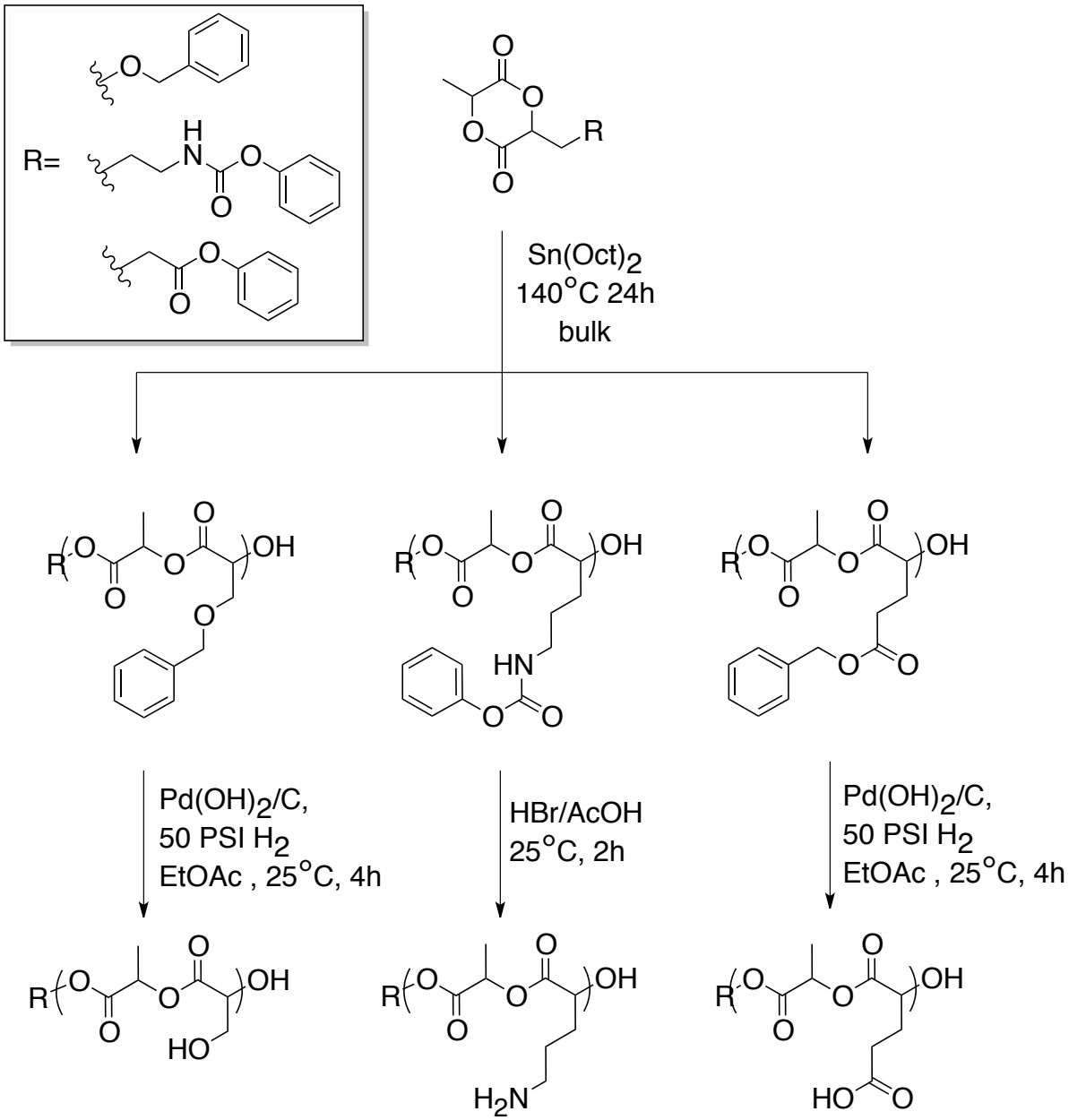

Scheme 2 Functional polylactides synthesized by the Gerhardt group.

An alternative strategy, PPM, is based on the synthesis of a common polymer that can be modified with various functional groups. PPM allows for facile synthesis of new polymers, and avoids the need to synthesize a new monomer for each new polymer. Examples of PPM include carbodiimide coupling reactions,[17-20] olefin cross-

metathesis,[21, 22] click chemistry, ketoximine coupling,[23-27] and Michael additions.[28, 29] Of these methods, carbodiimide coupling and click chemistry are most pertinent to the scope of this report.

In a recent report, PLGA was conjugated to poly(ε-carbobenzoxy-L-lysine) via DCC coupling.[18] The block copolymer was used to encapsulate growth factors such as vascular endothelial growth factor (VEGF) and ciliary neurotrophic factor (CNTF). Compared to PLGA PLGA-PLL (PLL = poly(L-lysine) conjugates were more efficient in releasing growth factors. Noga et al. copolymerized lactide with a benzyl-protected lactide derived from serine. Deprotection yielded a hydroxy-substituted PLA that was then treated with succinic anhydride to afford pendant carboxylic acid groups. Using NHS and EDC, the carboxyl-functionalized PLA was then conjugated to an RGD-containing peptide **(Scheme 3)**.[30]

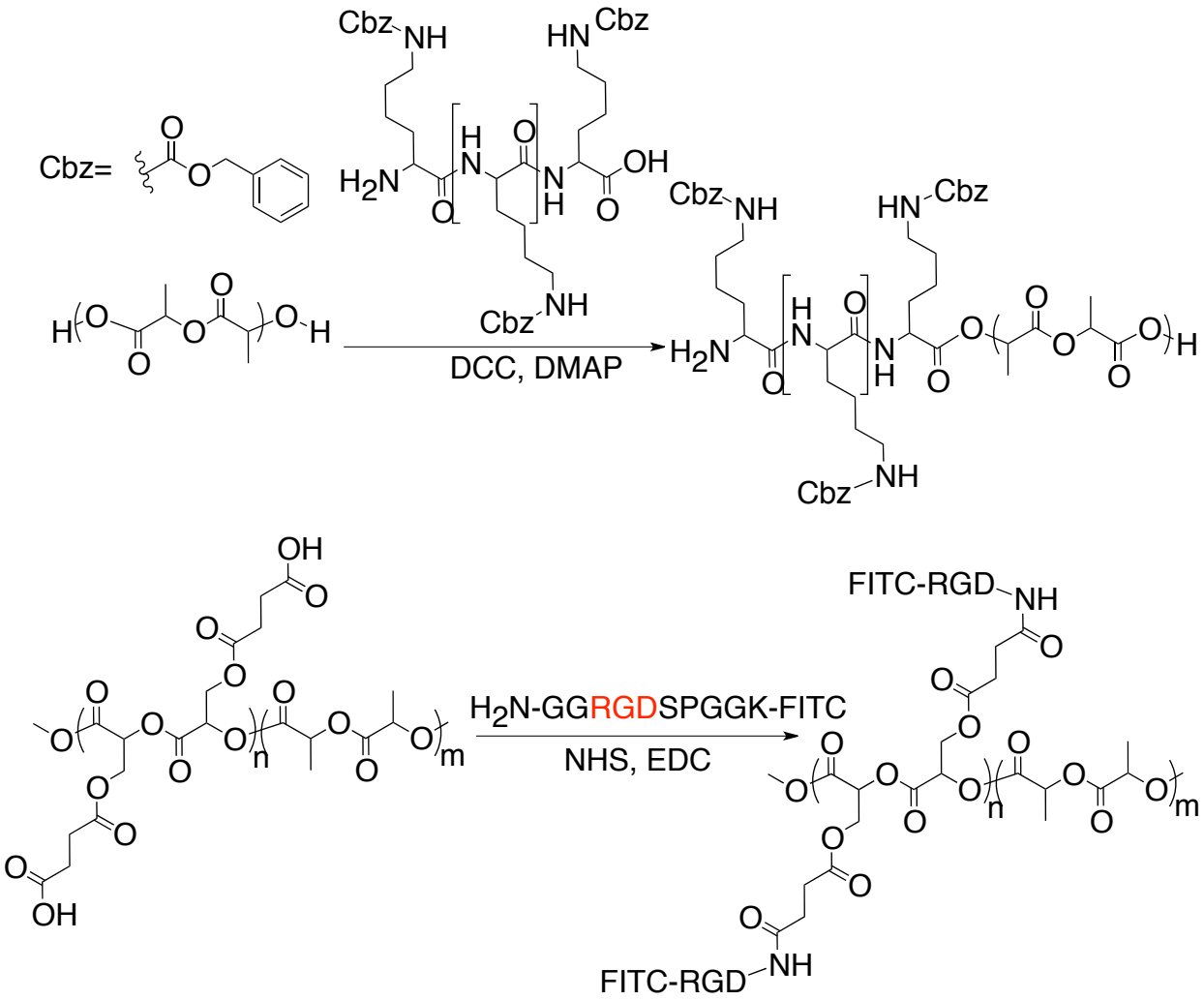

Scheme 3 An example of using carbodiimide to couple polylactide to Cbz-protected poly(L-lysine) (top).[18] Carboxyl-modified PLA was conjugated to an RGD-containing peptide (bottom).[30]

Click Chemistry

The Cu^{I} catalyzed 1,3-dipolar cycloaddition of an alkyne with an azide (CuAAc), commonly termed “Click chemistry”, is a member family of modular reactions that have high yields, occur under mild reaction conditions, and generate only harmless side products.[31-33] The reaction is highly regioselective, yielding only the 1,4-disubstituted products, and is also tolerant to a wide variety of functional groups and stable to water

and oxygen **(Scheme 4)**.[34] The use of click chemistry for materials synthesis has become ubiquitous. Its use in dendrimer synthesis is described as representative examples. **Scheme 5** shows the synthesis of one member of a library of dendrimers, where “click” chemistry was used to attach functional groups to the periphery of a common intermediate.[26] Click chemistry also was used to build dendritic structures. In one example, an AB_2 monomer, which contained two terminal alkynes and an alkyl halide was clicked to azides **(Scheme 6)**.[35] Converting the alkyl halide to an azide enables additional click reactions. The dendrimers generated by this method were claimed to have well-defined structures, and can be obtained in high purity and high yields. These examples show that click chemistry is a powerful technique for introducing diversity in a wide range of architectures.

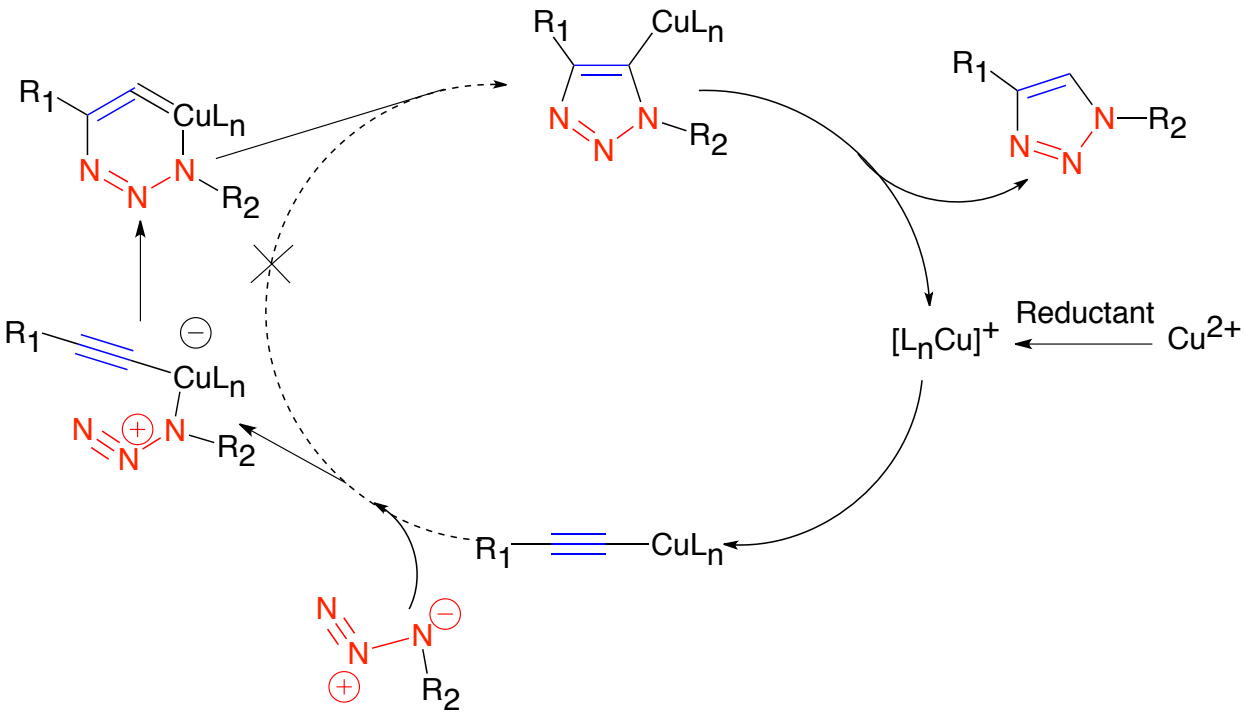

Scheme 4 Proposed mechanism of the Cu(I)-catalyzed 1,3-cycloaddition of azides and alkynes.[34]

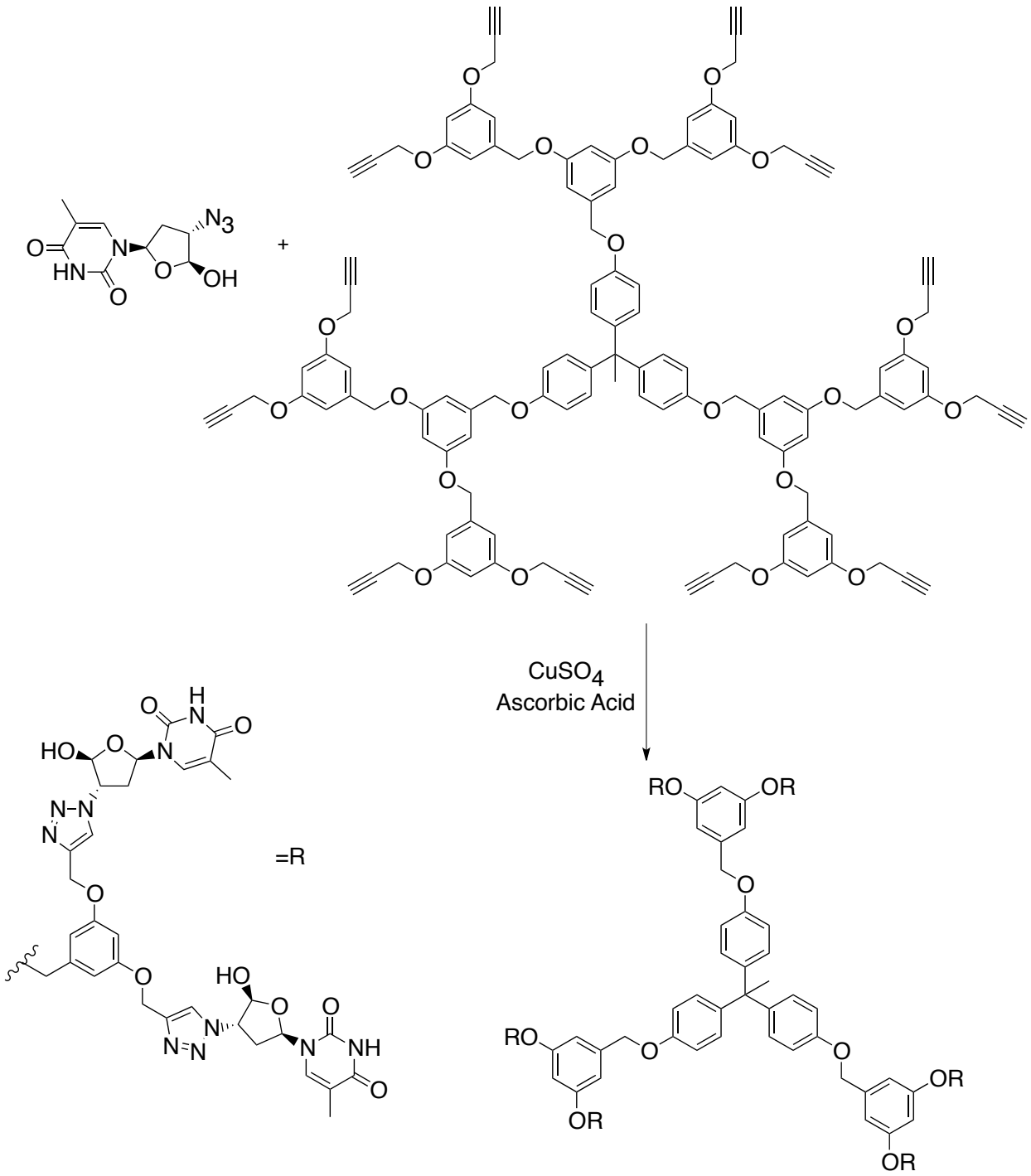

Scheme 5 Functionalization of dendrimers via click chemistry.[26]

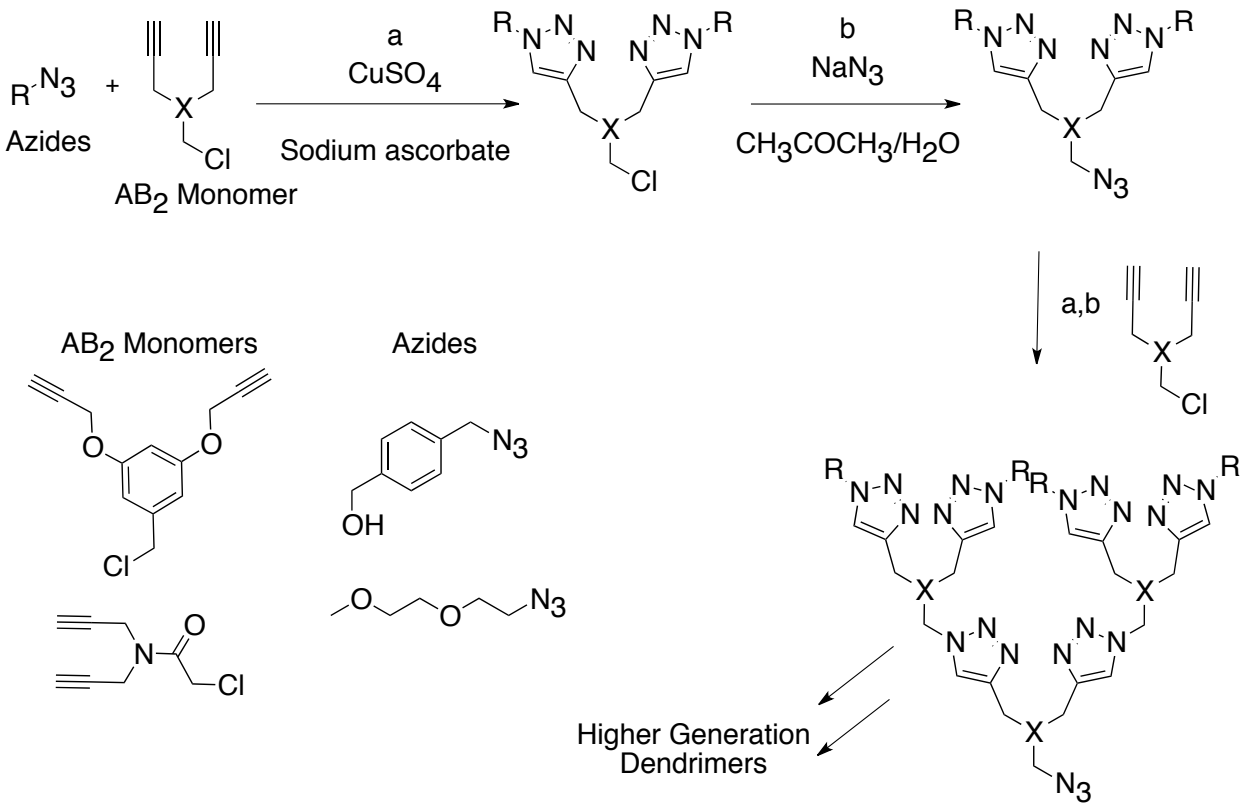

Scheme 6 Synthesis of dendritic structures via click chemistry.

"Click" chemistry has been widely applied to polymer synthesis. One of its most useful applications is PPM. Under standard click conditions, polymethacrylates with pendant azide groups reacted with alkynes such as propargyl alcohol and propargyl 2-bromoisobutyrate[36] **(Scheme 7)**. The latter could not be incorporated into the monomer since the 2-bromoisobutyrate ester reacts under radical polymerization conditions, causing uncontrolled cross-linking.

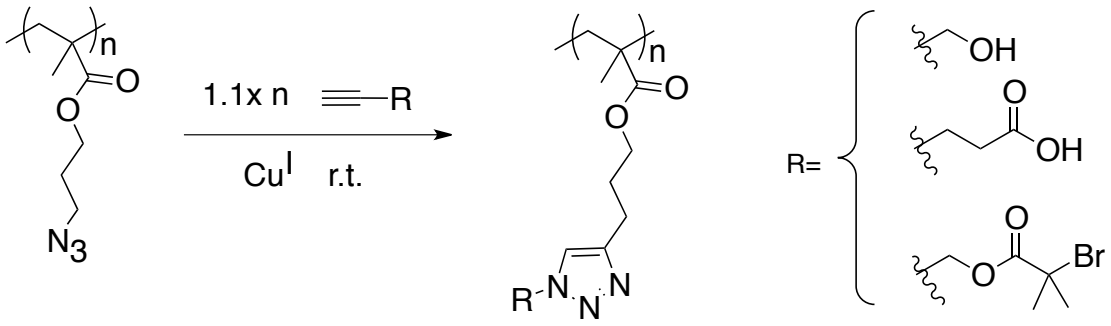

Scheme 7 Clickable azide modified methacrylates.[36]

The benefits of click chemistry can be applied to polyglycolides. In 2008, Jiang et al. described the synthesis of propargyl glycolide, (PGL), an alkyne-functionalized lactide, which can be polymerized via ring opening polymerization (ROP) to poly(propargyl glycolide) (PPGL). The resulting polyester contains one pendant acetylene per repeat unit **(Scheme 8)**, and can be modified by "clicking" different azide ligands to the pendant alkynes. Experimentally, it was discovered that preparing the Cu(I) catalyst *in situ* in the presence of a reducing agent, such as sodium ascorbate, afforded better yields and no side reactions were observed. This technique allows for fast modification of the chemical and physical properties of PPGL in a single step. Functional groups such as amino and hydroxyl groups, which need to be protected in the functional monomer approach, are easily appended to the polyester backbone by click reactions without the use of protective schemes. Being able to quickly modify a common polymer backbone is a great advantage when evaluating new materials for the biomedical applications.

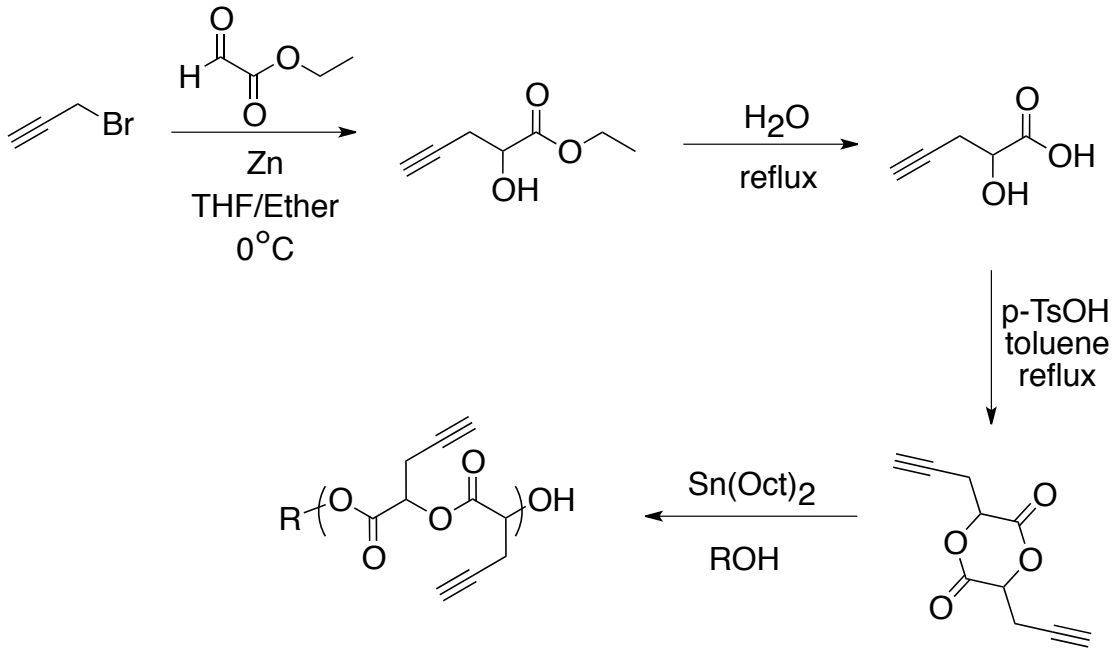

Scheme 8 Synthesis and polymerization of PGL

Tacticity and crystallinity of polymers

The tacticity of a polymer is defined as the possible spatial arrangements of substituents on the backbone of the chain; it can be isotactic when each chiral center in the polymer chain has the same configuration. A polymer is syndiotactic when the configuration of each stereocenter alternates (e.g R, S, R, S….). When a polymer contains no discernable pattern of stereochemistry, it is said to be atactic (**Figure 3**). [37]

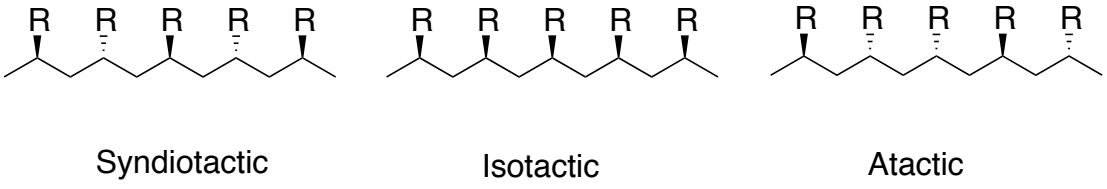

Figure 3 Three configurations of a monosubstituted polyethylene.

The crystallinity of a polymer can be dictated by its stereochemistry, syndiotactic and isotactic polymers are usually crystalline or semicrystalline, whereas atactic polymers are almost always amorphous with the exception of polymers with very small or highly polar side groups, and comb polymers with long alkyl side chains. A polymer is said to be crystalline when it diffracts X-rays and undergoes a melting transition. Regularity in the polymer chain increases the melting temperature and aids the formation of crystals, while monomer units of the wrong tacticity can disrupt the crystallinity of a polymer. Semicrystalline polymers also diffract X-rays and exhibit a melting transition but they also have a glass transition. The glass transition temperature (T_g) is a second order transition, where the slope changes in volume-temperature dependence. The T_g can be described as the change in the mobility of the polymer chains. Below T_g the polymer chains will behave as a rigid solid, above T_g the polymer chains are mobile.

Ziegler-Natta catalysts are highly regiospecific and are used to synthesize highly crystalline polymers. For example isotactic[38, 39] and syndiotactic polystyrene[40], syndiotactic and isotactic polypropylene[41], have been prepared by catalysts of this nature (**Figure 4**). Ziegler-Natta catalysts are employed for the synthesis of these polymers because common cationic or radical polymerizations yield atactic, amorphous polymers.

Polyamides are highly crystalline materials that are atactic; they are crystalline due to hydrogen-bonding and polarity properties (**Figure 5**).

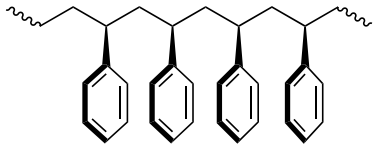

via

$TiCl_3$-$Al(CH_3)_3$

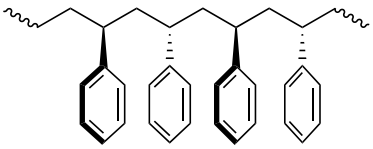

via

Bz_4-Ti-$Al(CH_3)_3$

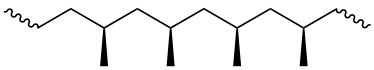

via

$TiCl_3$-$Al(C_2H_5)_2Cl$

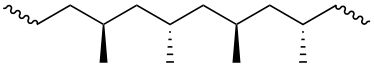

via

VCl_4-$Al(C_2H_5)_2Cl$

Figure 4 Syndiotactic and isotactic polymers prepared using Ziegler-Natta catalysts.

Examples of these polymers are poly(*m*-phenylene isophthalamide), commercially known as Nomex®, and poly(*p*-phenylene terephthalamide), known as Kevlar®[42]. Polyamides are prepared by condensation of diacyl chlorides and diamines at low temperature or from diacids and diamines at high temperatures. Polyamides can also be aliphatic like Nylon 6® or Nylon 6,6 which have the same chemical composition but are derived from different monomers.[43]

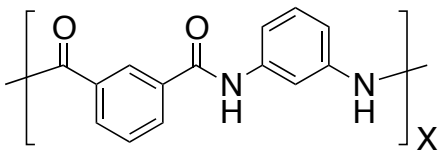

Nomex®

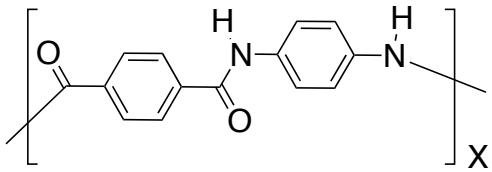

Kevlar®

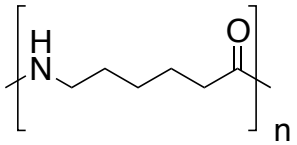

Nylon 6 ®

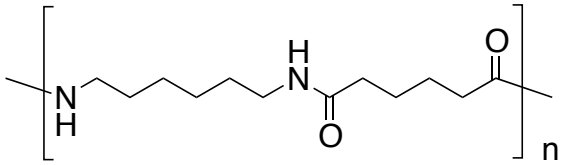

Nylon 6,6

Figure 5 Some commercial polyamides.

Other polymers have stereochemistry inherently given by their monomers (**Figure 6**). Such is the case of poly(α-aminoacids). They are able to form ordered arrays like α-helices and β-sheets.[44] Poly(α-amino acids) can be synthesized with the same configuration in each repeating unit by condensing enantiopure amino acids by peptide synthesis. One example is poly(γ-benzyl-glutamate), the crystal structure has been determined for the racemic poly(γ-benzyl-glutamate) from microbial origin,[45] and poly(γ-benzyl-L-glutamate) has been investigated for its liquid crystalline properties.[46] Another example where a polymer stereochemistry can arise from chiral monomers is polylactide (PLA). Polylactide is synthesized by ring opening polymerization of lactide. Lactide is a monomer that contains two chiral centers and has three stereoisomers, the configurations are (R, R), (S, S) and (R, S), which is a meso compound. Isotactic PLA is polymerized from the R, R or the S, S monomers and polylactide from the meso-lactide will be atactic unless a chiral catalyst is used.[47, 48] Isotactic PLA has a regular structure

that makes it semicrystalline; it has a melting transition at 180 °C[49] and it exhibits a T_g at ~60 °C.[11]

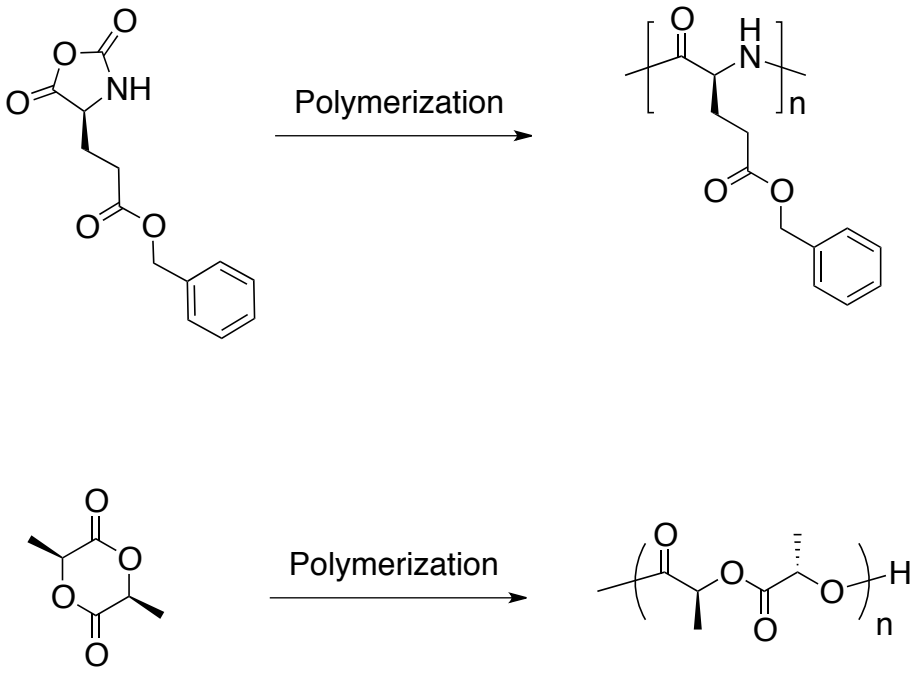

Figure 6 Polymers prepared from chiral monomers.

Applications of modified polyglycolides

An interesting and novel area of gene therapy is RNA interference (RNAi). Mello and Fire discovered that RNAi regulates endogenous gene expression in the nematode worm *Caenorhabditis elegans.* Mello and Fire received the Nobel Prize in Physiology or Medicine in 2006 for this work.[50-52] RNAi is activated when double stranded RNA (dsRNA) ~21 nucleotides long is introduced to the cell. Dicer, an RNAkinase III, then cleaves the dsRNA into a small interfering RNA duplex (siRNA) with two nucleotide overhangs **(Figure 7)**. The siRNA complexes with Slicer, a protein of the Argonaut family with an RNAase H-like domain PIWI, to form an RNA-induced silencing complex

known as RISC. RISC unwinds the double stranded siRNA into single stranded siRNA, and in a sequence specific manner, single stranded siRNA binds to mRNA, cleaves it in half, and unbinds. Finally, the cleaved mRNA is degraded by nucleases, which results in sequence-specific silencing of gene expression.[50-54]

Gene therapy has great potential for treating various diseases such as cancer and Alzheimer's disease, and the critical step in gene therapy is the delivery of the desired nucleic acid to the cell. Different types of delivery vehicles have been developed, with viral vectors the earliest delivery vehicles. Adenoviruses,[55] retroviruses,[56] and adeno-associated viruses[57] are among the preferred vectors but they have several disadvantages including low cargo capacity, safety, immune response and resistance to repeated infection.[55, 58, 59] Alternatives to viruses are non-viral vectors such as gene guns,[60] electroporation, ultrasound,[61] cationic lipids, liposomes, peptides and cationic polymers.[62] The latter can be conjugated to nucleic acids via electrostatic interactions between cationic groups in polymers, usually amines, and the phosphate groups of the nucleic acid backbone.

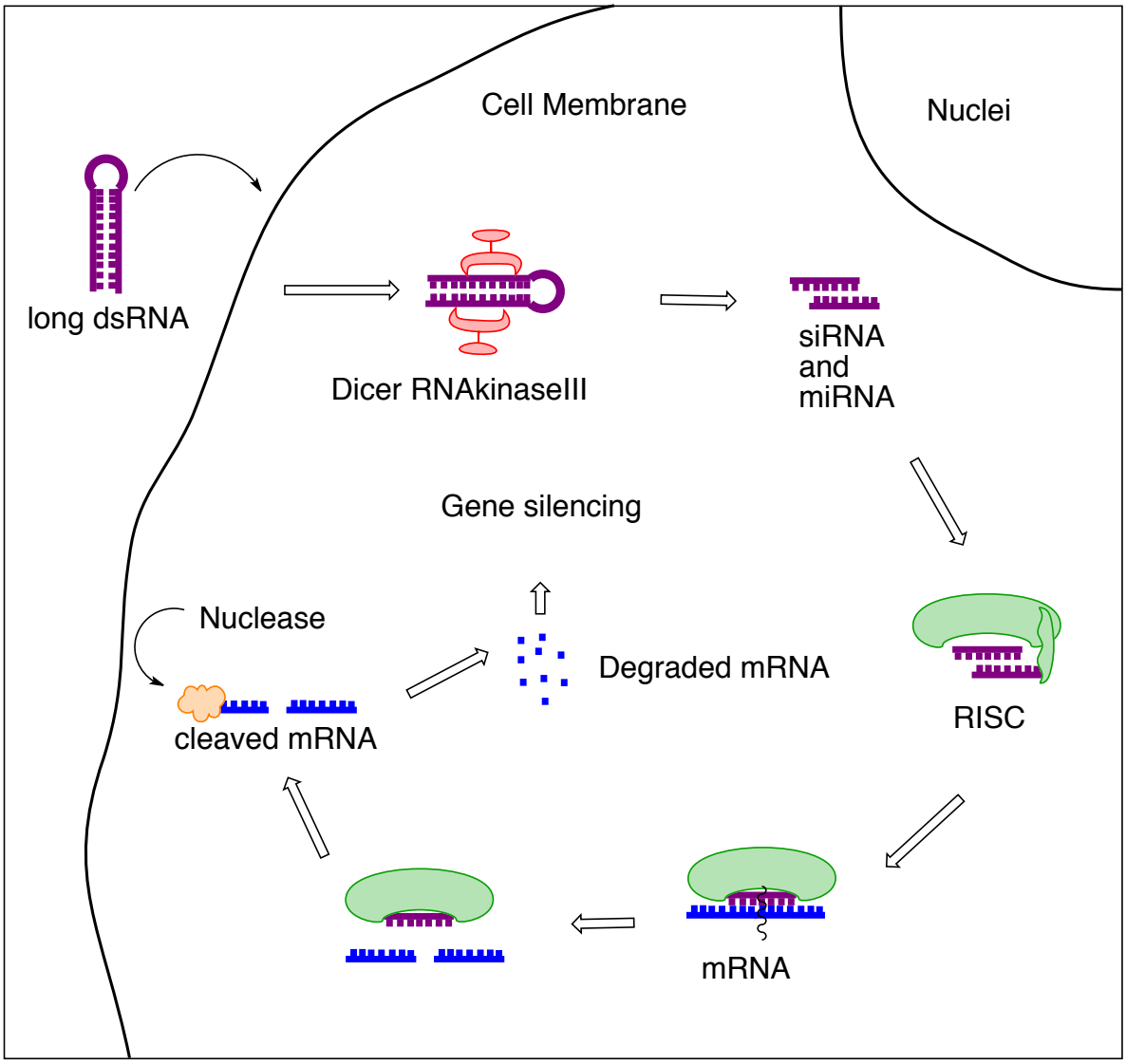

Figure 7 Gene silencing via RNA interference (RNAi)

The goal of this research is to synthesize and characterize polycationic delivery vectors for siRNA delivery to activate the RNAi machinery. The delivery vehicle must possess certain qualities to be suitable for siRNA delivery: It must soluble in water or aqueous buffer, bind electrostatically to the phosphate groups of nucleic acids, be biodegradable, and have a high binding efficiency, low toxicity, and high transfection efficiency. The reported polycationic vectors have common qualities and motifs.

Several polycations used in siRNA delivery utilize amino groups grafted to the polymers,[63-65] and polyethylene glycol (PEG) is a common component in delivery nanoparticles.[64, 66, 67] PLGA,[63] poly(ε-caprolactone),[64] and other polyesters are components of polyconjugates for siRNA delivery vehicles, however, simple polyesters lack amino groups and are unable to bind to nucleic acids. Amino groups are capable of binding to nucleic acids electrostatically and therefore have largely become the preferred motifs for binding to nucleic acids, examples are shown in **Figure 8.**

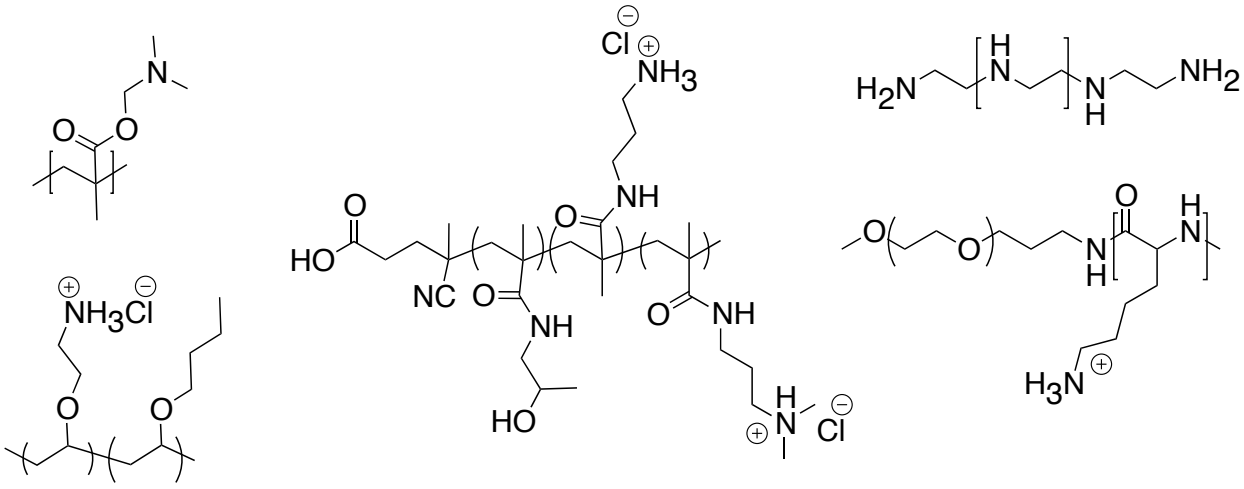

Figure 8 Examples of synthetic polycationic vectors for siRNA delivery.

Different types of polycationic vehicles have been reported, including poly(2-(dimethylamino)ethyl methacrylate) (PDMAEMA) which has been widely studied. Long and coworkers established the molecular weight dependent toxicity of PDMAEMA,[68] showing that 43 KDa PDMAEMA was less toxic than 915 KDa PDMAEMA. However, the plasmid DNA transfection efficiency and binding affinity were higher for high molecular weight PDMAEMA. In order to reduce the toxicity of PDMAEMA while maintaining transfection efficiency, a comb-shaped PDMAEMA copolymer was

synthesized by initiating atom transfer radical polymerization (ATRP) of DMAEMA from hydroxypropyl cellulose.[69] The comb polymer showed lower toxicity and higher transfection efficiency than the PDMAEMA homopolymer.

In another report, enhanced stability and longer systemic circulation were achieved when PDMAEMA initiated by a cholesterol oxyanion was used in combination with a PEG-PMAA block copolymer which was modified to contain pendant thiol groups that would later be crosslinked upon oxidation.[70] The polyion complex bound to plasmid DNA, released the nucleic acid under the reducing environment of the cell.

PDMAEMA is representative of the many polymers synthesized for gene therapy vehicles. However, most polymers are not biodegradable, and there are very few examples of gene delivery using PLA. In one example, poly(lactide-*co*-glycolide) (PLGA) was used to deliver plasmid DNA for transgene expression into injured spinal cords and nerve regeneration.[7, 8] The complex was coated with fibronectin, an extracellular matrix protein (ECM), which aided its immobilization to the surface. In another example, PLGA/PEI (PEI = polyethyleneimine) nanoparticles (200-250 nm) were complexed with plasmid DNA encoded for antigen 85B of *Mycobacterium tuberculosis*. The complexes had high plasmid loading efficiency and low cytotoxicity.[71] In previous examples, PLGA nanoparticles and complexes required an additive such as TransFast® a commercially available transfection agent,[7] chitosan,[72] or PEI.[8, 71, 73, 74,75] In these cases the additives contained a chemical functionality such as an amine or carbohydrate that increased the uptake of the nanoparticle into the cell. Some additives lack chemical

functional groups, but aid in transfection. For example, poly(vinyl acetate) PVA was used as an emulsifier to form PLA/PLGA and plasmid DNA composites, and successfully delivered plasmid DNA encoding for firefly luciferase to breast cancer and prostate cancer cell lines.[76]

Polylactides are attractive for gene delivery because of their biocompatibility and degradability. Previously, PLA and its copolymers have been used for tissue[2] and bone engineering,[3] orthopedics and sutures,[1] controlled drug release[4-6] and gene therapy.[7-10] Nonetheless, the lack of chemical functionality and hydrophobic nature of polylactide are major disadvantages, and in some instances, have limited the scope of polylactide applications.[16] Therefore, several investigators modified the polylactide structure to obtain physical and chemical properties more suitable for biomedical applications.

Modification of PPGL modification has been explored in the Baker laboratory, with a goal of developing polymers that function as nucleic acid delivery agents. These PPGL derivatives must have good binding affinity, compatibility with RNA or DNA, water solubility, and low toxicity to cells and tissue. The inherent hydrolytic degradability of the polyester backbone is an advantage over most polymeric delivery agents since it can be cleared from the body. In the first studies, PPGL was clicked with short PEG oligomers and other azide ligands in the search for adequate properties for delivery.

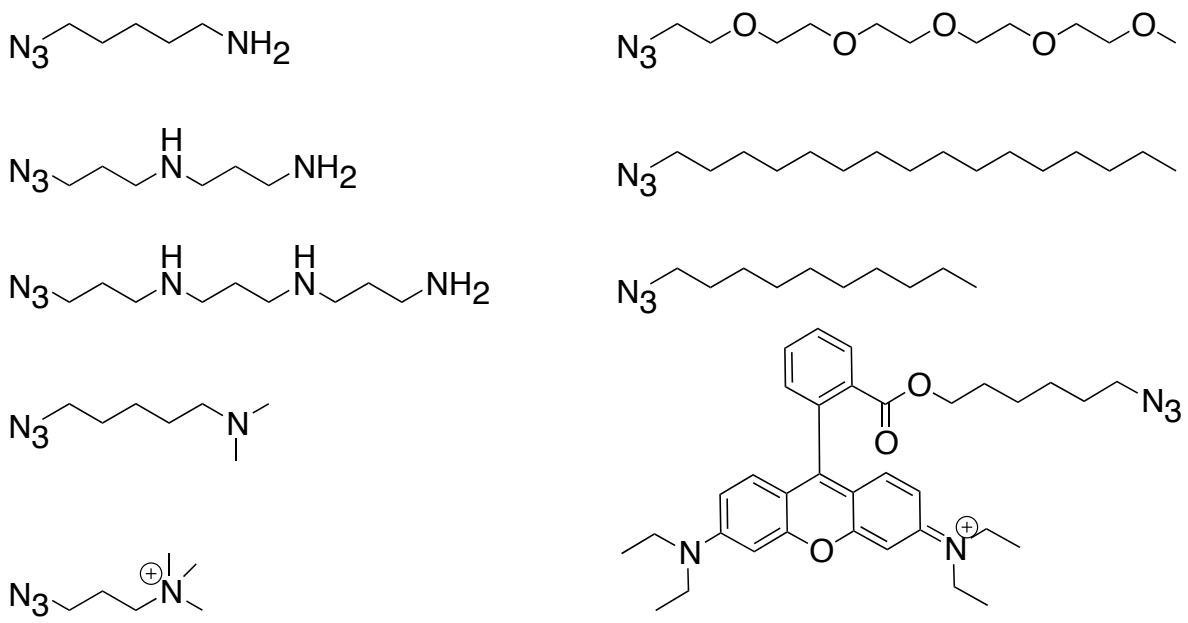

Figure 9 Examples of azide ligands used to change and tune the properties of PPGL at the Baker laboratory.

Azide ligands were clicked to PPGL in order to tune its properties (**Figure 9**). Since the nomenclature for the clicked polymers is complicated, a systematic abbreviation scheme was developed. For example, $PEG_8PG_{45}[A12_{80}C10_{20}]$ defines a poly(propargyl glycolide) chain with a degree of polymerization of 45, initiated by a PEG segment with a degree of polymerization of 8. $A12_{80}C10_{20}$ indicates that the alkynyl groups of the poly(propargyl glycolide) chain were modified by click chemistry with 80% of the amine A12 (N-(3-azidopropyl)-1,3-diaminopropane a diamine) and 20% of the C10 (1-azidodecane). Amine ligands were added to PPGL to explore the binding affinity to nucleic acids. PEG oligomers are appended to the PPGL to increase the solubility in aqueous media and circulation time of the polymer in the bloodstream they also control immunogenicity. The *n*-alkyl groups were found to increase the binding affinity of polymer particles or micelles. Azide-modified Rhodamine B, a red fluorescent dye,

enabled imaging polymers and particles in cells by confocal laser scanning microscopy (CLSM). Vogel found that A12 provides the highest binding affinity, due to 1,3 spacing of the amines that enables chelation with phosphate groups in the nucleic acid backbone. Also, adding PEG to PPGL enhanced the hydrolytic degradation rate. PPGL, 100% clicked with PEG chains, dissolved in PBS at 37^{o}C, lost 85% of its mass in seven days, whereas PLA showed insignificant mass loss under identical conditions.[14]

Conclusion

Modification of polylactide and its properties has allowed the development of more biomedical applications using biodegradable materials. Herein, we explore the synthesis and properties of polylactide derivatives. We developed stereoregular poly(isopropyl glycolide) and we formed stereocomplexes using the two enantiomeric forms of the homopolymer. We crosslinked clicked poly(propargyl glycolide) and we studied the interactions of multiple surface functional groups on a lipid bilayer cell membrane mimic. The uses and application of modified poly(propargyl glycolide) via click chemistry as a nucleic acid delivery vector were studied. And finally, we synthesized surface modified inorganic silicon nanoparticles for siRNA delivery.

Chapter 2: Formation of Poly(isopropyl glycolide) Stereocomplexes

Introduction

Polymer-polymer complexes with favorable chemical interactions can be formed from two chemically different polymers. These favorable interactions include; polyelectrolyte complexation between a polyanion and a polycation,[77, 78] hydrogen-bonding complexation,[79, 80] and charge transfer complexation between polymer acceptor and donor pairs.[81] A **stereocomplexation** can occur between two polymers of the same chemical composition but with opposite stereochemistry. The properties of stereocomplexed materials are often significantly different from those of the single enantiomer polymers. Thermal, crystal, viscoelastic and rheological properties are some of the properties that can be modified by stereocomplexation. The polymer pair in a stereocomplex is racemic and optically inactive.[82]

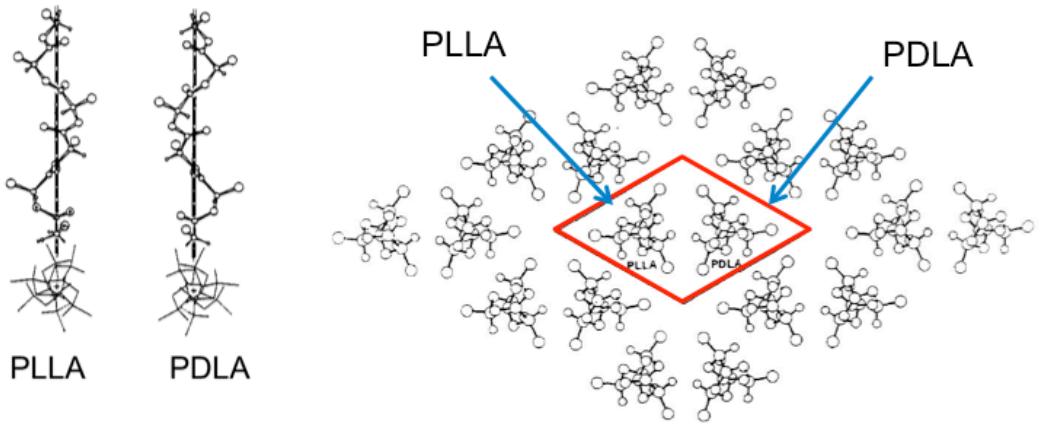

Figure 10 Models of equimolar PDLA and PLLA stereocomplex by Okihara et al

The Ikada group reported a polylactide stereocomplex in 1987. The formation of the stereocomplex was assessed by differential scanning calorimetry (DSC), which

indicated that the melting temperature increased from 180 °C in the homopolymer to 230 °C in the stereocomplex.[83] Stereocomplexes of PLA have been widely investigated with Tsuji and Ikada being major contributors in the area.[83-93] In 1991, Okihara and coworkers elucidated the crystal structure of PLA stereocomplexes **(Figure 10)**. PLA stereocomplexes have been obtained from film casting,[83, 85, 94] precipitation,[86] fiber spinning[91] and crystallization from melt.[90] Although PLA stereocomplexes have been explored widely, reports of stereocomplexes formed from other substituted polylactides are scarce. One instance is the work on poly(2-hydroxybutyrate) also known as poly(ethylglycolide) by Tsuji. Stereocomplexes were formed using R- and S- Poly(2-hydroxybutyrate)[95] The T_m increased 100 °C (110 °C→ 212 °C) over that of the homopolymers of M_n ca. $3.5x10^3$ g/mol **(Figure 11)**.

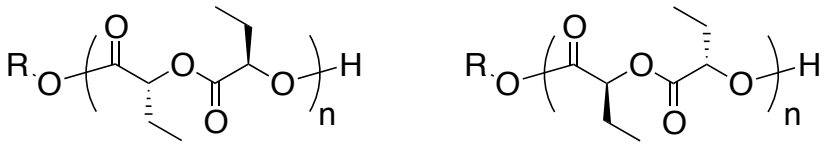

Figure 11 Poly(2-hydroxy butyrate) or poly(ethyl glycolide) in both stereochemical configurations.

Although traditionally stereocomplexes are thought to be a binary blend of homopolymers with opposite stereochemistry, atactic and isotactic polymers can form a stereocomplex. Tsuji and Ikada combined racemic PLA with PLLA and studied the crystallization effects of the atactic component on PLLA. PLLA crystallized at mole fractions (X_c) higher than 0.2 PLLA, and at X_c higher than 0.5 the crystal growth was no

longer spherulite like.[92] Annealing the stereocomplex blend affects the thermal and mechanical properties and morphology of the blend. Annealing the stereocomplex increases the T_m and crystallinity, and affects spherulite size.[93]

Besides PLA, other stereocomplexes have been reported **(Figure 12)**; Poly(γ-benzyl glutamate) forms a stereocomplex that has an endothermic thermal transition at 135 °C; whereas enantiomers melt at 95 °C.[96] A 1:1 mixture of (R)- and (S)- Poly(α-methyl benzyl methacrylate) exhibited an endothermic transition at 230 °C, which was attributed to the melting transition. Also, the glass transition temperature at 81 °C disappeared upon complexation **(Table 1)**.[97] Stereocomplexes of poly(methyl methacrylate) (PMMA) have been extensively explored. PMMA stereocomplexes were formed from isotactic PMMA and syndiotactic PMMA.[98-102] PMMA stereocomplexes are able to form gels and were found to be thermoreversible, which means that the gelation process is reversible with temperature changes.[100, 103]

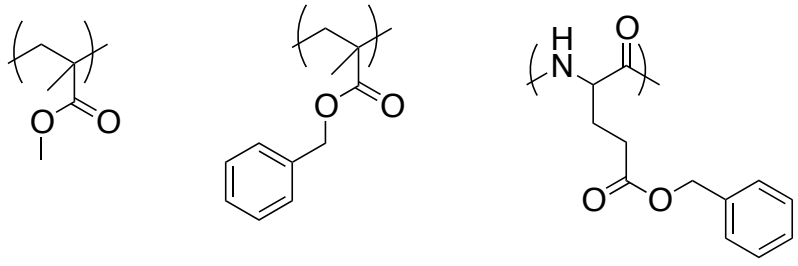

Figure 12 Polymers known to form stereocomplexes: Syndiotactic and isotactic poly(methyl methacrylate), R- and S- poly(α-methylbenzyl methacrylate), R- and S- poly(γ-benzyl glutamate)

Table 1 Comparison of melting temperatures of known stereocomplexes

Polymer	T_m Homopolymer	T_m Stereocomplex	Composition
Poly(γ-benzyl glutamate)	95	132	1:1 R and S
Poly(α-methyl benzyl methacrylate)	266	230	1:1 R and S
Poly(methyl methacrylate)	na	92.7[a]	1:1 Syndiotactic
Polylactide	180	230	1:1 R and S
Poly(ethyl glycolide)	110	212	1:1 R and S

[a]Gelation point

Stereocomplexes that are formed between two or more chemically different polymers are called hetero-stereocomplexes. Slager and coworkers have explored hetero-stereocomplexes of PDLA and PLLA entrapping peptides such as leuprolide,[104-106] and insulin.[107] Polybutadiene-block-syndiotactic PMMA and isotactic PMMA formed hetero-stereocomplexes at low molecular weights of PMMA.[108] Syndiotactic poly(isobutyl methacrylate) and isotactic PMMA formed a complex with similar characteristics of a stereocomplex.[109] Hetero-stereocomplexes also form between PLA and poly(ethyl glycolide) as block copolymers.[110] Homo and hetero-stereocomplexes of poly(ethyl glycolide) were used as crystallization accelerating agents for PLLA.[111]

The properties of stereocomplexes make them appealing for applications in biomedicine and material processing. The high thermal stability of PLA stereocomplexes

would make them suitable to make fibers, films, rods etc.[112] PLA stereocomplexes can enhance the crystallization of PLLA and improve its thermal stability.[113] Industrially, PLA stereocomplexes are not used due to the unavailability of PDLA in bulk quantities. Some biomedical applications of stereocomplexes have been explored. In one instance, Dexamethasone was encapsulated in a stereocomplex of PDLA and PLLA-PEG-PLLA block copolymer.[114] Stereocomplexed PLA has been used for encapsulation and release of insulin.[107] Dextran hydrogels that can then be used as protein release agents where PDLA and PLLA stereocomplexes act as crosslinking agents.[115-118] Bovine serum albumin can be adsorbed into poly(methyl methacrylate) stereocomplexes formed from isotactic PMMA and syndiotactic PMMA, this has been used as hollow fiber membranes for artificial dialysis.[119] PLLA-PEG-PLLA and PDLA-PEG-PDLA triblock compolymers formed a thermo-responsive hydrogel by stereocomplexation,[120, 121] PEG-PLA hydrogels by stereocomplexation were also generated as star-shaped polymers.[122]

Stereocomplexation of PLA has been widely studied since the late 1980's. However, the potential of other substituted polylactides as stereocomplex candidates remains unexplored. The objective of this project is the synthesis and characterization of isotactic poly(isopropyl glycolide) (PiPG) from R,R- and S,S- isopropyl glycolide. The formation and characterization of stereocomplexes is reported.

Results and Discussion

Polylactide stereocomplexes have been extensively explored since the late 1980's. So far, the only substituted polylactide studied is poly(ethyl glycolide), whose stereocomplex had a T_m of 200 ^{o}C compared to the T_m of the homopolymers of ca. 100^{o}C.[95] Poly(isopropyl glycolide) (PiPG) is an easily accessible substituted polylactide. PiPG can be obtained in both enantiomeric forms, and isotactic PiPGs can be blended to form stereocomplexes. The properties of these PiPG stereocomplexes are explored, herein.

Monomer Characterization

Poly(isopropyl glycolide) is synthesized from isopropyl glycolide via ring opening polymerization. Isopropyl glycolide is easily synthesized from valine in two steps (**Scheme 9**). The first step consists in a diazotization reaction to change the amino acid into an α-hydroxy acid with the retention of stereochemistry via a double S_N2 mechanism. The second reaction is a condensation in the presence of an acid catalyst, which also affords retention of stereochemistry. The water byproduct is removed using a Dean Stark trap. One of the first reports of the synthesis of the α-hydroxy acid was the work by Iwakura where he performed the synthesis of the L configuration monomers and he also synthesized optically active polymers.[123, 124] However, the conditions used in these reports were too harsh. The reaction conditions for the monomer synthesis are a modified procedure from Baker et al.[12, 125] All the reactions gave moderate to high yields.

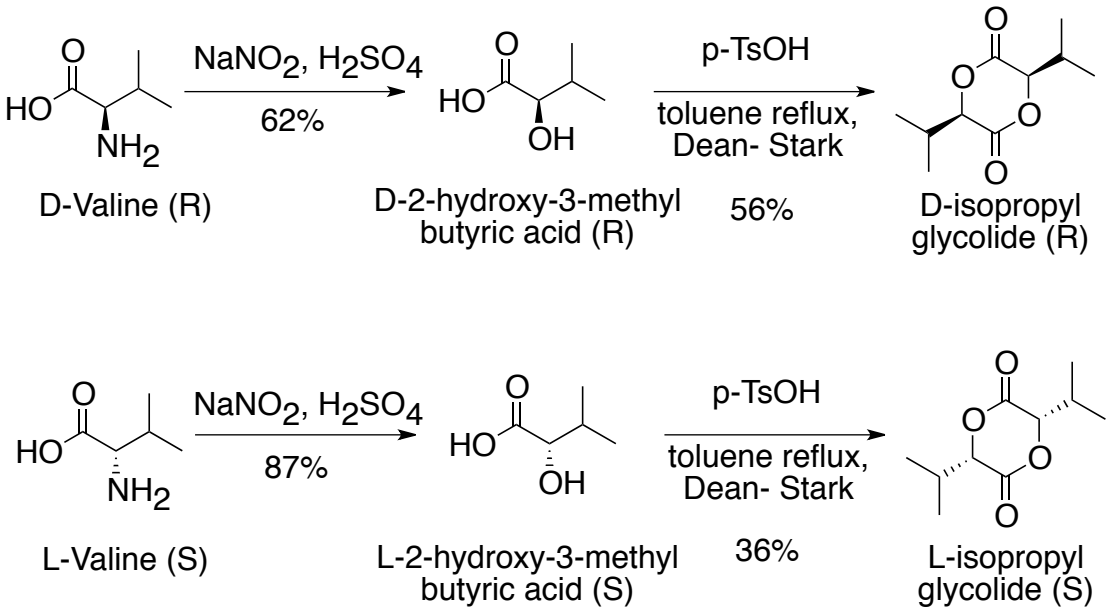

Scheme 9 Synthesis of D- and L- Isopropyl Glycolide

The α-hydroxy acids were prepared with retention of stereochemistry. L-valine has an S configuration and the hydroxyacid yielded had S configuration as well. Likewise, D-valine yielded the R configuration. The optical rotation obtained for both R- and S- 2-hydroxy-3-methyl butyric acids were consistent with the data from literature references (**Table 2**). X- Ray crystallography also confirmed the absolute stereochemistry (**Figure 13**).

Table 2 Optical rotation data for α-hydroxyacids and glycolides

Compound	[α]	[α] Literature	Configuration
D-2-hydroxy-3-methylbutyric acid	-14.8	-13.7[126]	R
L-2-hydroxy-3-methylbutyric acid	+13.8	+18.3[127]	S
D-isopropyl glycolide	+257.2	NA	R,R
L-Isopropyl glycolide	-256.5	-256[124]	S,S

Optical rotation measurements done in triplicate, 589nm, 20°C, $CHCl_3$, 10mg/mL

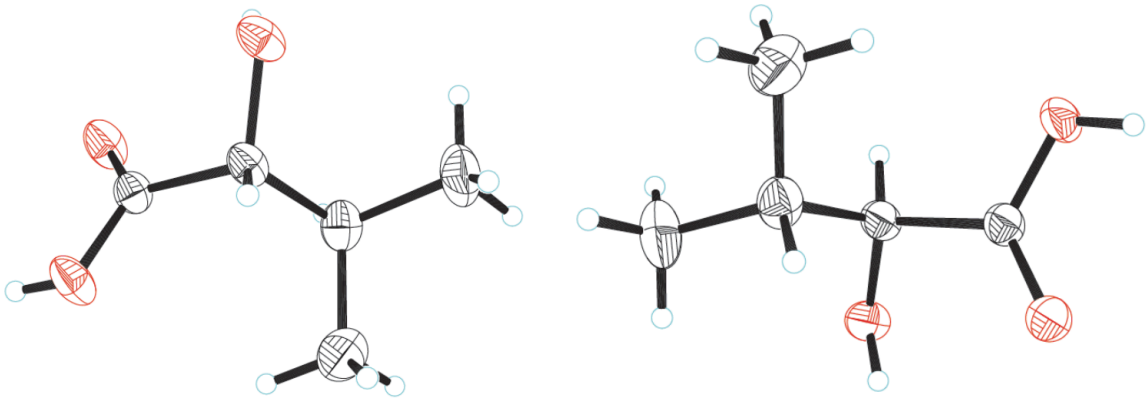

Figure 13 Crystal structures of R- (left) and S- (right) 2-hydroxy-3-methyl butyric acid.

The synthesis of isopropyl glycolide was also carried on with retention of stereochemistry since the reaction does not take place on the stereocenter. This condensation reaction was catalyzed by para toluene sulfonic acid under reflux conditions. Per every molecule of isopropyl glycolide formed, two molecules of water are generated. In order to push the equilibrium forward, the water is removed using a Dean Stark trap. The absolute stereochemistry of each of the monomers was determined

using X-Ray crystallography (**Figure 2**). The optical rotation of the monomers is in agreement with the literature for S,S- monomer, the optical rotation of the R,R monomer has not been reported before but the rotation power is the same as the S,S- monomer with opposite sign.

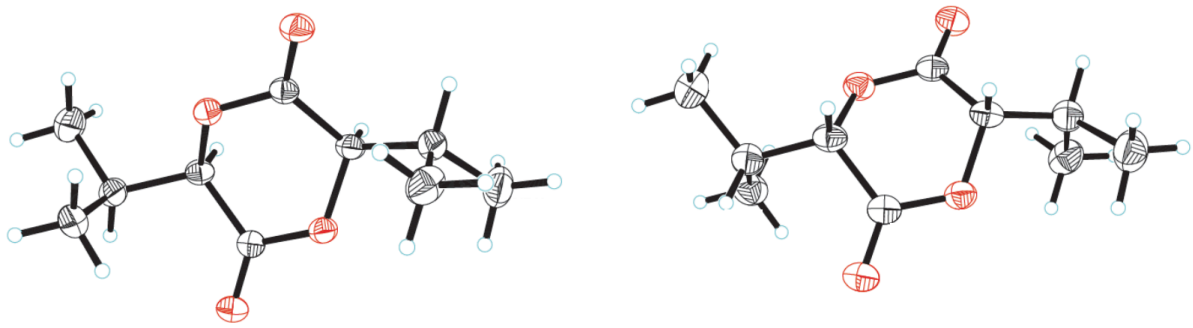

Figure 14 Crystal structure of isopropyl glycolide monomers (3R, 6R)-3,6-diisopropyl-1,4-dioxane-2,5-dione (left) (3S, 6S)-3,6-diisopropyl-1,4-dioxane-2,5-dione (right)

Both enantiomers of isopropyl glycolide are readily accessible from the corresponding aminoacids. The ability to obtain the monomer easily, is a motivation to explore the potential of poly(isopropyl glycolide) in stereocomplexation.

Synthesis and Characterization of optically active Poly(isopropyl glycolide)

Poly(isopropyl glycolide) is a polymer made from renewable resources. Optically active poly(isopropyl glycolide) can be synthesized with both configurations. Using either configuration the resulting polymer is isotactic. If the meso isopropyl glycolide is used an atactic polymer is obtained. Isotactic poly(isopropyl glycolide) is a semi crystalline polymer.

We obtained poly(isopropyl glycolide) via ring opening polymerization in bulk using tert-butyl benzyl alcohol (BBA) as initiator and tin (II) 2-ethylhexanoate as our catalyst **(Scheme 10)**. The polymerization was carried out at 180 ^{o}C for 1-2 hours but by 30 min the reaction mixture had already crystallized. The crystallization of the polymer did not affect the degree of polymerization. The targeted degree of polymerization was achieved without evidence of racemization of the polymer **(Figure 15)**, as shown by the ^{13}C NMR and ^{1}H NMR spectra. Because the polymerization conditions used are somewhat harsh, polymerizations in solution were examined.

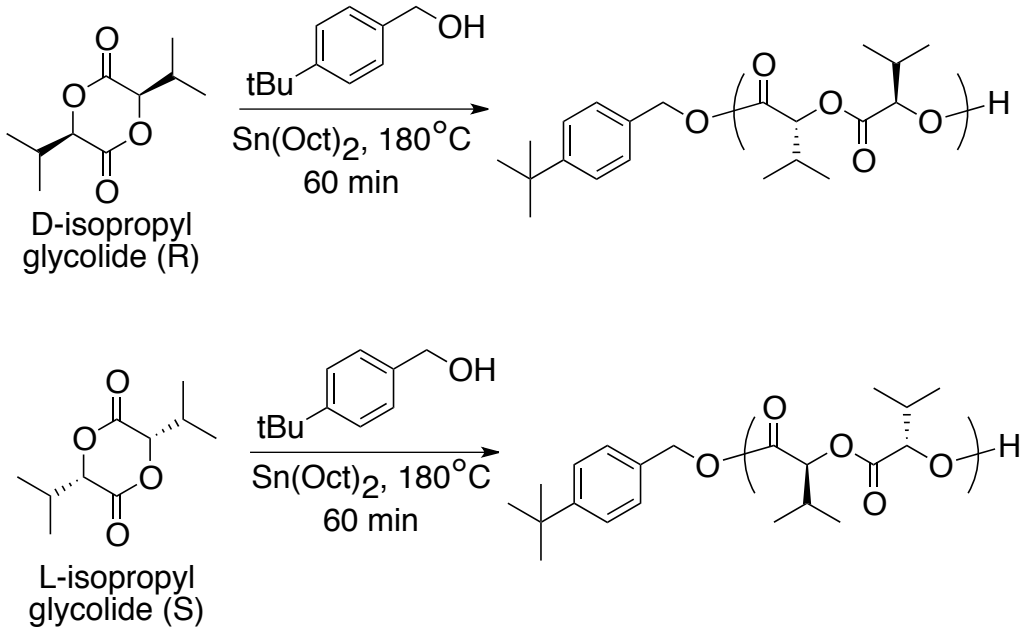

Scheme 10 Ring opening polymerization of isopropyl glycolide

There was no conversion when isopropyl glycolide was subject to BBA and tin II 2-ethylhexanoate in toluene at 90 ^{o}C. Two organocatalysts were explored for the polymerization reaction in solution. Dimethyl amino pyridine (DMAP) in toluene at 90 ^{o}C

and in chloroform at 60°C did not show conversion of monomer even after 4 days. DMAP is able to polymerize lactide under these conditions.[128] Evidently, DMAP and tin II 2-ethylhexanoate were not able to polymerize isopropyl glycolide in solution is because isopropyl glycolide is too sterically hindered and the conditions were too mild. 1,8-diazabicycloundec-7-ene (DBU) in toluene at 60 °C was able to polymerize isopropyl glycolide, but the polymerization was slow and it showed evidence of racemization **(Figure 16)**.

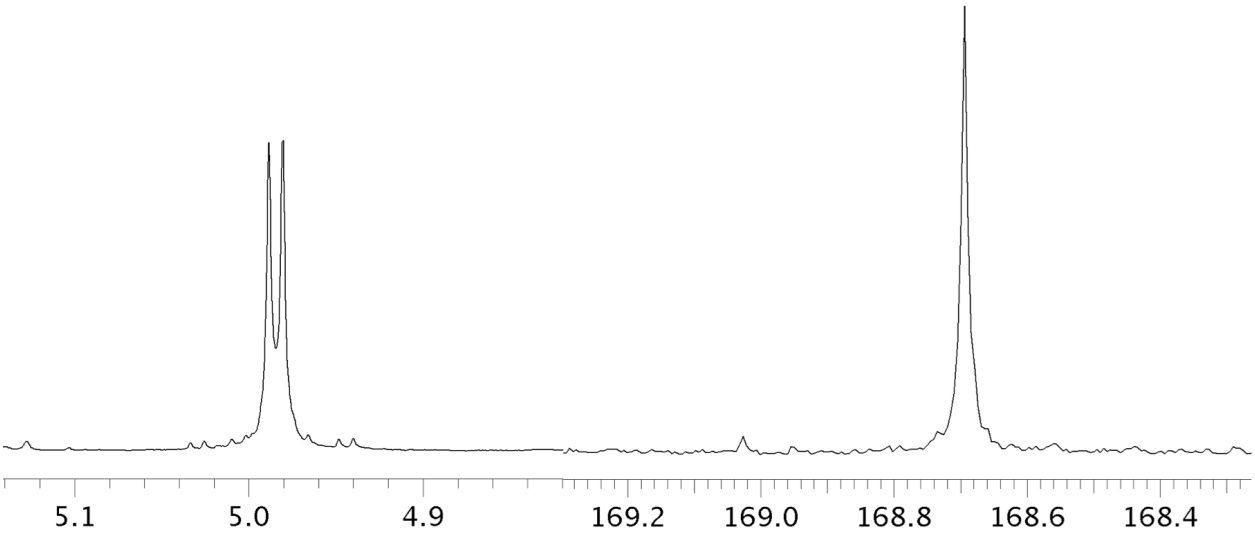

Figure 15 Methine region of isotactic D-Poly(isopropyl glycolide) in $CDCl_3$ ^{1}H NMR 500 MHz (left) ^{13}C NMR 125 MHz(right)

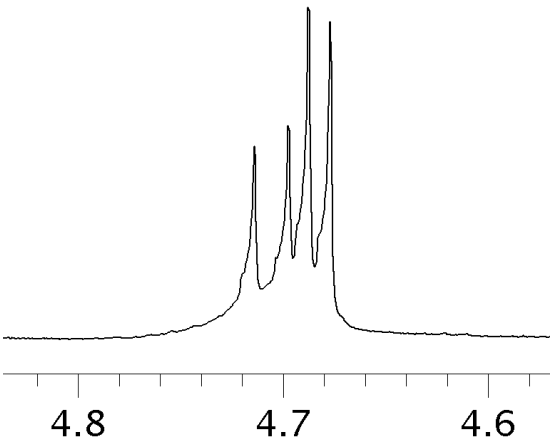

Figure 16 Methine region in ^{1}H NMR of isopropyl glycolide during polymerization using DBU as catalyst showing racemization.

The thermal properties of poly(isopropyl glycolide) were explored. Poly(isopropyl glycolide) exhibited a melting transition, a glass transition and a crystallization transition, which indicated the polymer is semicrystalline in nature. The melting temperature and crystallization temperature increased with increasing molecular weight **(Figure 17, table 3)**, but the glass transition temperature did not seem to be affected by the molecular weight. The ΔH_f of melting is not affected by the change in molecular weight (**Table 3**). The ΔH_f showed some fluctuation, which is due to differences in crystallinity between the different polymer chains. A lower degree of crystallinity in the polymer chain can be evidence of the wrong tacticity of the repeating unit due to racemization. However, this was not evident from the NMR data.

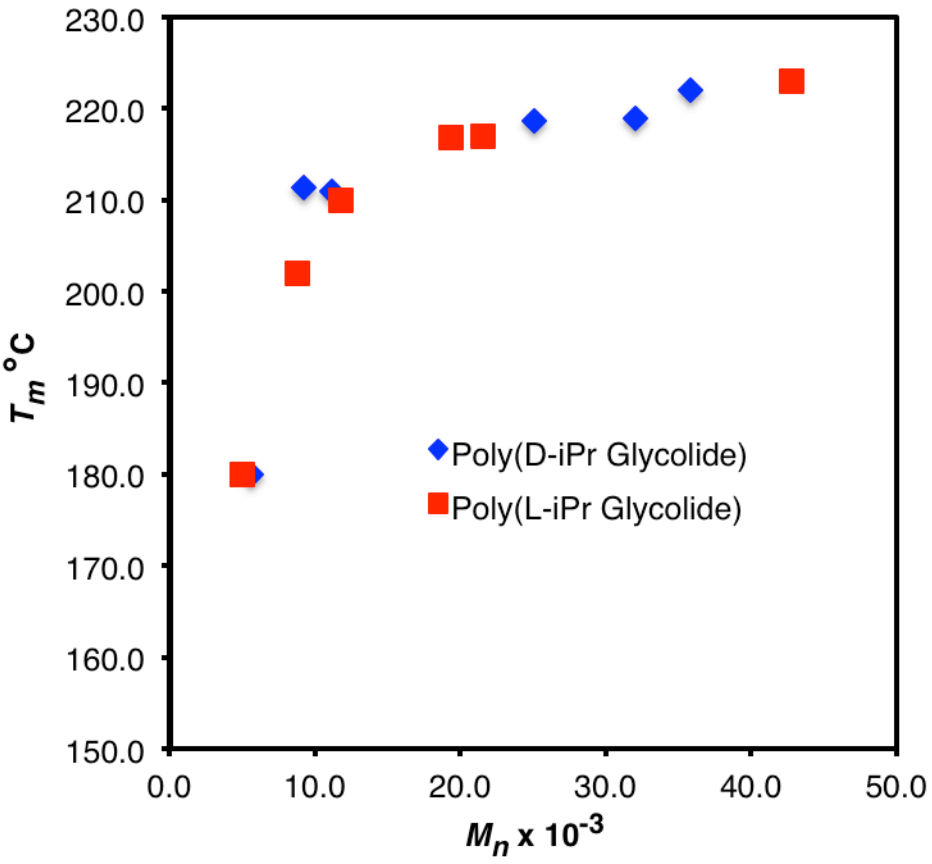

Figure 17 Melting temperature T_m and number average molecular weight M_n relationship of Poly(isopropyl glycolide)

Table 3 Thermal properties of Poly(Isopropyl Glycolide) as a function of molecular weights

Configuration	X_n	M_n x 10^{-3}	T_m °C	ΔH_f J/g	T_g °C	T_c °C	ΔH_c J/g
L	25	5.0	200.0	27.2	38.6	150.4	28.3
D	28	5.6	200.0	30.8	35.4	155.0	29.9
L	44	8.8	202.0	23.5	28.8	150.7	22.7
D	46	9.2	211.4	17.0	46.0	159.1	16.5
D	56	11.2	211.0	28.1	36.9	163.4	28.9
L	59	11.8	210.0	30.8	40.7	157.6	29.9
L	97	19.4	216.9	27.7	44.7	160.4	26.3
L	108	21.6	217.0	30.0	47.8	168.4	28.5
D	126	25.1	218.6	30.1	43.6	166.4	20.5
D	158	32.0	219.0	29.2	50.0	169.4	27.9
D	179	35.8	222.0	28.7	51.1	180.7	27.7
L	214	42.8	223.0	28.9	48.7	181.7	28.9

[a,b] M_n calculated from chain-end count from ^{1}H NMR

We analyzed samples of the polymers using GPC **(Table 4)** equipped with a multiangle light scattering and refractive index detectors to obtain the M_n and the polydispersity of the homopolymers. The polydispersity of poly(isopropyl glycolide) was narrow for all the examples (1.1-1.4). For the lower molecular weight examples both measurements are within agreement. However, with higher molecular weight polymers the discrepancy between the two molecular weights is greater. Counting the chain ends

becomes difficult and unreliable at high molecular weight because the signal to noise ratio of the chain end unit is very small thus the integration of the signal is inaccurate.

Table 4 Comparison of number average molecular of ^{1}H NMR and GPC data

Configuration	$^{a}X_n$	$^{a}M_n$ x 10^{-3}	$^{b}M_n$ x 10^{-3}	$^{b}M_w/M_n$
L	25	5.0	6.52	1.201
D	28	5.6	5.91	1.2
L	44	8.8	9.6	1.436
D	46	9.2	15.4	1.153
D	56	11.2	11.08	1.17
L	59	11.8	14.4	1.152
L	97	19.4	29.0	1.214
L	108	21.6	21.6	1.188
D	126	25.1	27.8	1.257
D	158	32.0	24.5	1.123
D	179	35.8	66.8	1.34
L	214	42.8	65.34	1.207

[a]Calculated from ^{1}H NMR [b]Calculated from GPC in THF using 2 PLgel 10μm mixed b columns with MALS, RI, and viscometer detectors.

Formation of Poly(Isopropyl Glycolide) Stereocomplexes

We explored three methods for the formation of the stereocomplexes of Poly(Isopropyl Glycolide); precipitation, film casting and slow evaporation to a pellet. The first step is the same for all methods; we measured equal masses of polymers of

each configuration, and dissolved them to a 10% w/v solution in CH_2Cl_2 and stirred at room temperature for 24 hours. Then some of the polymer blends were cast into films by pipetting the solution onto glass microscope slides and allowing them to air dry. A different blend was precipitated into ice-cold methanol.

Table 5 Melting temperature transitions for pairs of stereocomplexes of different molecular weights

Entry	Method	D M_n x 10^{-3}	L M_n x 10^{-3}	T_m °C	ΔT_m °C	ΔH_m J/g
1a	Film*	5.6	5.0	214	14	36.67
2a	Precipitated	11.2	11.8	225	15	35.83
3a	Pellet	9.2	8.8	205	3	27.98
3a*	Pellet*	9.2	8.8	225	23	32.87
3b	Film	9.2	8.8	205	3	27.31
		9.2	8.8	227	25	0.6221
3b*	Film*	9.2	8.8	206	4	13.91
		9.2	8.8	225	23	11.13
4a	Pellet	25.1	19.4	234	17	27.54
4b	Film	25.1	19.4	NA	NA	NA

* DSC data from the first heating/cooling cycle. DSC method: heat to 240 °C at 10°C/min, cool to -10 °C at 10 °C/min

Lastly, other blend solutions were placed in vials loosely capped inside of a TLC glass chamber and they were allowed to evaporate slowly thus forming a pellet. DSC analysis confirmed that stereocomplexes were formed, the stereocomplexes exhibited

an increase in T_m of 10 to 20 °C (**Table 5**). Formation by film casting was possible only at low molecular weights (entries 1a, 3b). The precipitation method was also successful (entry 2a), the sample presented good thermal stability. The slow evaporation method was the most successful.

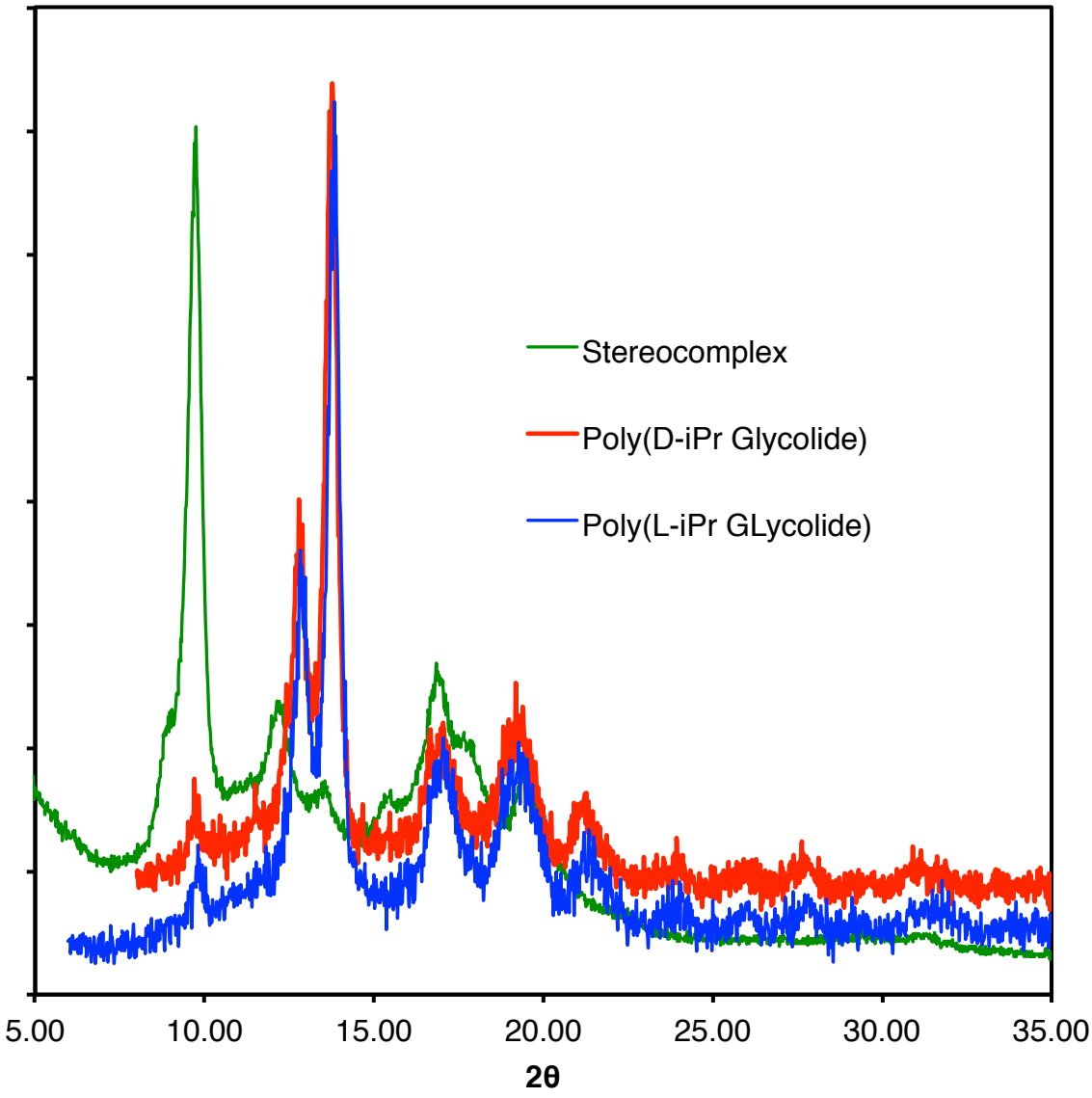

Figure 18 Powder X-Ray traces of D- and L- poly(isopropyl glycolide) (M_n = 5.6 x10^{-3} and 5.0x10^{-3} respectively) and the corresponding stereocomplex from film

Stereocomplexes formed by slow evaporation had better thermal stability than the stereocomplexes made by film casting and precipitation. The film samples only showed a T_m increase on the first heating scan, the T_c could not be determined. The T_m went back to the T_m that of the homopolymer pairs. The precipitated and the pellet samples had better thermal stability than the cast films. The pellet sample 3a stereocomplex showed an increase in T_m on the first heating cycle, however the T_m decreased on the second cycle. The thermal stability of the stereocomplexes increases with increasing molecular weight. A pellet formed by slow evaporation method (4a) presented a T_m of 233 ^{o}C after several heating and cooling cycles; the homopolymers had a T_m of 217 and 219 ^{o}C respectively. Although stereocomplexes of higher molecular weight have better thermal stability, the co-crystallization of the homopolymer pairs is very slow, thus higher molecular weight homopolymer pairs fail to complex by casting a film or by precipitation. This indicates that the rate of stereocomplexation decreases with increasing molecular weight. Poly(isopropyl glycolide) stereocomplexes had an increase in ΔH, the increase was not as high as stereocomplexes made from polylactide, which had a ΔH of 65 J/g[129] compared to 27 J/g for poly(isopropyl glycolide). One reason for the lower ΔH is that the pendant isopropyl groups shield the dipole interaction of the carbonyl groups between chains.

With the help of powder X-Ray crystallography, we determined that the X-ray patterns (**Figure 18**) of poly(isopropyl glycolide) and the respective stereocomplex were

significantly different. As expected, the X-ray patterns of the R,R- and S,S-poly(isopropyl glycolide) were identical. The X-Ray pattern is not resolved enough to obtain information about the unit cell. However, X-ray diffraction confirms that the crystal structure of the material has changed and it is evidence of stereocomplex formation. The stereocomplex showed an increase in % crystallinity from 54-57 to 60%.

Using a microscope with polarized light we can observe crystallites formed on stereocomplex 3b but a film of amorphous material would not show up light diffraction. SEM micrographs of the film's surface show circular structures with radial streaks from the center, these structures are crystallites. The crystallites had a diameter 60-67 μm. The cross-section images also showed circular crystallites, this indicates that the crystals formed are spherical **(Figure 19)**.

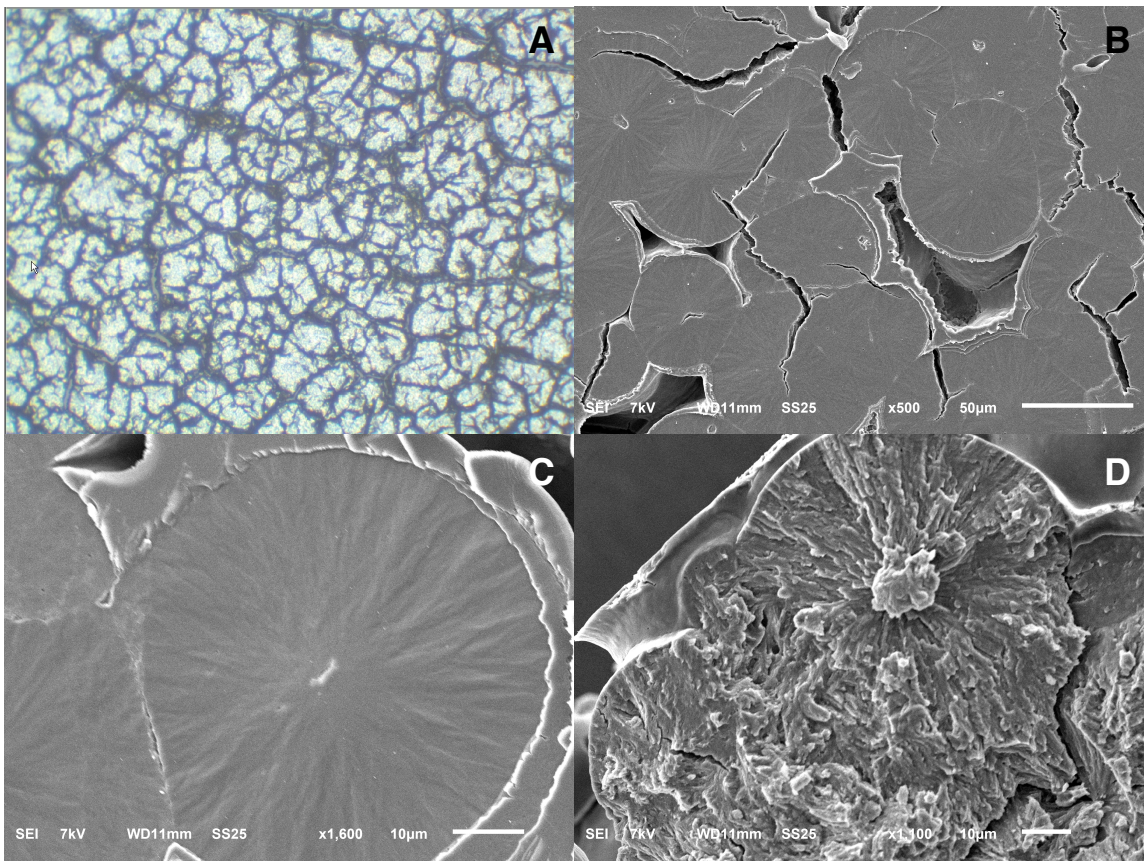

Figure 19 Microscopy of poly(isopropyl glycolide) stereocomplex 3b. **A** Cross-polarized light microscope image. **B** SEM image of crystallites in the film (scale bar 50µm). **C** Enlarged SEM image of crystallite (scale bar 10µm). **D** SEM image of crystallite film cross-section (scale bar 10µm).

SEM of stereocomplex 4b did not show crystallites as the ones in stereocomplex 3b, the film of 4b showed a very smooth surface without any interesting morphology suggesting that stereocomplexation had not occurred. Examination of the cross sectional area we can identify a porous structure of 105-µm thickness, no crystallites were found either (**Figure 20**).

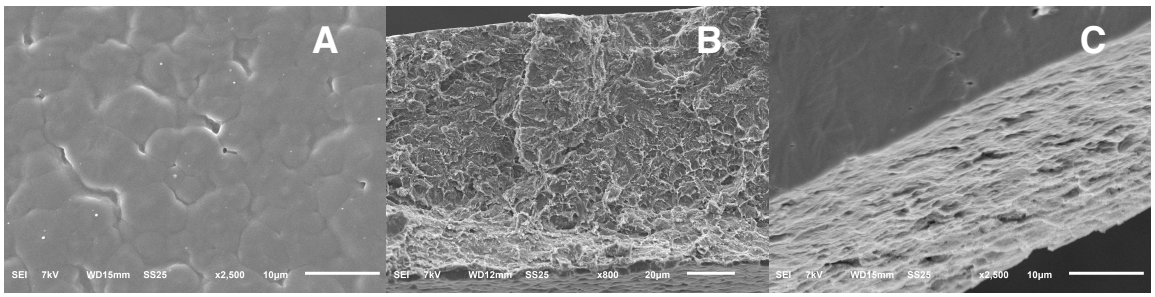

Figure 20 SEM micrographs of stereocomplex film 4b surface scale bar 10µm (A) cross-section scale bar 20µm (B) cross-section scale bar 10µm (C)

Conclusion

Isopropyl glycolide was synthesized in two steps. Diazotization reaction of D- and L- valine gave the corresponding α-hydroxy acids with conservation of stereochemistry. In an acid catalyzed condensation, Isopropyl glycolide was synthesized in two configurations R,R and S,S. Crystal structures of the two α-hydroxy acids and the two isopropyl glycolides were obtained, this proved the absolute stereochemistry of the compounds. Isopropyl glycolide was polymerized via ring opening polymerization using Tin II 2-ethylhexanoate and 4-tert-butyl benzyl alcohol as catalyst and initiator respectively. Other catalysts such as DMAP and DBU were screened, for the polymerization but they resulted in no conversion or they would racemize the polymer chain. D- and L- poly(isopropyl glycolide) exhibited increasing T_m with increasing molecular weight, the ΔH was independent of molecular weight. The polymers had T_m and T_g transitions that indicate the semicrystalline nature of the polymers. The formation of poly(isopropyl glycolide) stereocomplex was successful. We used several tools to confirm the formation of the stereocomplexes; powder X-ray crystallography, SEM, and DSC. Three different methods of the stereocomplexation were applied. Film casting was

able to form stereocomplexes but only of low molecular weight polymers. Precipitation was also employed and it was able to form a thermally stable stereocomplex. For higher molecular weight materials the best method was slow evaporation. In conclusion, poly(isopropyl glycolide) successfully formed stereocomplexes with the two isotactic configurations.

Experimental

General All reagents were purchased from Aldrich unless noted otherwise. Toluene was dried over sodium and benzophenone.

Characterization ^{1}H NMR spectra were measured on a 500 MHz Varian instrument, ^{13}C NMR was taken in a 125 MHz Varian instrument. Gel permeation chromatography (GPC) was performed in THF using 2 PLgel 10μm mixed b columns with MALS, RI, and viscometer detectors. Relative molecular weights were measured against polystyrene standards. Differential Scanning Calorimetry was obtained in a TA Instruments DSC in crimped aluminum pans and lids. The DSC method used for all samples was three heat cycles, with heating to 240 ^{o}C then cooling to -10 ^{o}C at 10 ^{o}C/min. Scanning electron microscopy was done using a JEOL JSM-6610LV SEM. The SEM samples were prepared on aluminum stubs with carbon tabs and coated with osmium tetroxide to make them conductive.

Synthesis of D-2-hydroxy-3-methylbutyric acid (1a) D-valine (0.1 mol) was added to a 1L round-bottom flask and dissolved in 133 mL of 1.5 M H_2SO_4 and cooled to in an ice water bath. A 2 M solution of $NaNO_2$ (0.4 mol, 200 mL) in deionized water was added dropwise through an addition funnel. The ice bath was removed after addition and the reaction mixture was stirred at room temperature for twelve hours. The aqueous mixture was extracted with 100 mL of diethyl ether (4x), and then washed with 100 mL (2x) brine. The organic layer was dried over $MgSO_4$, filtered and the solvent removed under reduced pressure. The greenish liquid was recrystallized with toluene to give colorless crystals. 62% yield; $[\alpha]^{20}$ -14.8 (c=1.0, $CHCl_3$); ^{1}H NMR ($CDCl_3$, 500 MHz) δ: 4.12 (d, *J*=3.17 Hz, 1H), 2.15-2.11 (m, 1H), 1.04-1.03 (d, *J*= 6.8 Hz, 3H), 0.91-0.89 (d, J= 6.8 Hz, 3H) ppm; ^{13}C NMR ($CDCl_3$, 125 MHz) δ: 179.3, 74.84, 31.6, 18.76, 15.84 ppm

Synthesis of L-2-hydroxy-3-methylbutyric acid (1b) L-valine (0.5 mol) was added to a 1L round-bottom flask and it was dissolved in 666 mL of 1.5 M H_2SO_4 and it was cooled to 0^{o}C in an iced water bath. A 2 M solution of $NaNO_2$ (2.0 mol, 1000 mL) in deionized water was added dropwise through an addition funnel. The ice bath was removed after addition and the reaction mixture was stirred at room temperature for twelve hours. The aqueous mixture was extracted with 200 mL of diethyl ether (4x), and then washed with 200 mL (2x) brine. The organic layer was dried over $MgSO_4$, filtered and the solvent removed under reduced pressure. The greenish liquid was recrystallized with toluene to give colorless crystals. 58% yield; $[\alpha]^{20}$ +13.9 (c=1.0, $CHCl_3$); ^{1}H NMR ($CDCl_3$, 500

MHz) δ: 4.13-4.12 (d, *J*= 3.42 Hz, 1H), 2.15- 2.12 (m, 1H), 1.05-1.03 (d, *J*=7.08, 3H), 0.91-0.89 (d, *J*=6.83 Hz, 3H) ppm; ^{13}C NMR ($CDCl_3$, 125 MHz) δ: 178.8, 74.78, 31.96, 18.76, 15.82 ppm

Synthesis of D-isopropyl glycolide (2a) 7.0 grams of **1a** (59 mmol) and 5 mol% of p-toluene sulfonic acid (2.9 mmol) were combined and dissolved in toluene to 0.08M in a 1L round bottom flask equipped with a Dean-Stark trap and a reflux condenser. The reaction mixture was heated to reflux under N_2 for six days. The mixture was allowed to cool, and then washed with 2x 200ml saturated $NaHCO_3$, the organic layer was dried over $MgSO_4$, filtered and the solvent removed. The crude solid was sublimed at 60°C then recrystallized from toluene to give colorless flaky crystals. 56% yield; $[\alpha]^{20}$ +257 (c=1.0, $CHCl_3$); ^{1}H NMR ($CDCl_3$, 500 MHz) δ: 4.68 (d, *J*=3.17 Hz, 2H), 2.49-2.46 (m, 2H), 1.13-1.12 (d, *J*= 7.08 Hz, 6H), 1.03-1.02 (d, *J*=6.8 Hz, 6H) ppm; ^{13}C NMR ($CDCl_3$, 125 MHz) δ: 166.35, 79.55, 29.37, 18.55, 15.81 ppm.

Synthesis of L-isopropyl glycolide (2b) 16.8 g of **1b** (142 mmol) and 5 mol% of p-toluene sulfonic acid (7 mmol) were combined and dissolved in toluene to 0.08 M in a 2 L round bottom flask equipped with a Dean-Stark trap and a reflux condenser. The reaction mixture was heated to reflux under N_2 for six days. The mixture was allowed to cool, and then washed with 2x 200 ml saturated $NaHCO_3$, the organic layer was dried over $MgSO_4$, filtered and the solvent removed. The crude solid was sublimed at 60°C then

recrystallized from toluene to give colorless flaky crystals. 39% yield; $[\alpha]^{20}$ -256.5 (c=1.0, $CHCl_3$); ^{1}H NMR ($CDCl_3$, 500 MHz) δ: 4.69- 4.68 (d, *J*= 3.17 Hz, 2H), 2.48-2.45 (m, 2H), 1.13-1.12 (d, *J*= 7.08 Hz, 6H), 1.03- 1.02 (d, *J*=6.8 Hz, 6H) ppm; ^{13}C NMR ($CDCl_3$, 125 MHz) δ: 166.36, 79.54, 29.36, 18.54, 15.81 ppm

Polymerization of D-isopropyl glycolide An ampoule was loaded with 170 mg (0.85 mmol) of monomer and a T-shape Cajon® vacuum adapter was affixed. The ampoule was purged with vacuum/nitrogen cycles. Under a nitrogen atmosphere, respective amounts of a 0.049 M Tin Octoate ($SnOct_2$) solution in toluene and a 0.052 M tert-butyl benzyl alcohol (tBBA) in toluene were added to the ampoule via syringe according to desired degree of polymerization. The mixture was stirred for 30 minutes then the solvent was removed under vacuum. The ampoule was flame sealed. The polymerization was carried out at 180 ^{o}C for 1 hour. The polymerization was quenched in an ice bath. The polymer was dissolved in CH_2Cl_2 to 10 % w/v and then precipitated by adding the CH_2Cl_2 solution to cold methanol to purify the polymer. 95% conversion; 85% yield; degree of crystallinity 57%; $[\alpha]^{20}$ +73.6 (c=1.0, $CHCl_3$); ^{1}H NMR ($CDCl_3$, 500 MHz) δ: 4.9 (broad d, 55.7H), 4.1 (d, 2H), 2.3 (b, 59.2H) 1.39 (s, 9H), 1.1 (b, 350.6H) ppm; ; ^{13}C NMR ($CDCl_3$, 125 MHz) δ: 168.6, 125, 128, 76.7, 30.2, 18.5, 16.8 ppm

Polymerization of L-isopropyl glycolide An ampoule was loaded with 1.1 mmol of monomer and a T-shape Cajon® vacuum adapter was affixed. The ampoule was

purged with vacuum/nitrogen cycles. Under nitrogen atmosphere, respective amounts of a 0.049 M Tin Octoate ($SnOct_2$) solution in toluene and a 0.052 M tert-butyl benzyl alcohol (tBBA) in toluene were added to the ampoule via syringe according to desired degree of polymerization. The mixture was stirred for 30 minutes then the solvent was removed under vacuum. The ampoule was flame sealed. The polymerization was carried out at 180 ^{o}C for 1 hour. The polymerization was quenched in an ice bath. The polymer was dissolved in CH_2Cl_2 to 10 % w/v and then precipitated by adding the CH_2Cl_2 solution to cold methanol to purify the polymer. 97% conversion; 88% yield; degree of crystallinity 54%; $[\alpha]^{20}$ -78.3 (c=1.0, $CHCl_3$); ^{1}H NMR ($CDCl_3$, 500 MHz) δ: 4.9 (broad d, 50H), 4.1 (d, 2H), 2.3 (b, 50H) 1.39 (s, 9H), 1.1 (b, 320H) ppm; ; ^{13}C NMR ($CDCl_3$, 125 MHz) δ: 168.6, 125, 128, 76.7, 30.2, 18.5, 16.8 ppm

Stereocomplex formation by film casting Equal masses of each polymer configuration was dissolved in CH_2Cl_2 to a concentration 10mg/ml. The mixture was stirred at room temperature for 24 hours. By dropping the polymer solution slowly, a polymer film was cast onto glass microscope slides and the solvent was allowed to evaporate, then the films were dried further under vacuum. The polymer film was brittle and flaky.

Stereocomplex formation by precipitation Equal masses of each polymer configuration was dissolved in CH_2Cl_2 to a concentration 10mg/ml. The mixture was stirred at room temperature for 24 hours. The solution was precipitated into ice-cold methanol with

vigorous stirring. The precipitate was recovered by vacuum filtration and rinsed with aliquots of cold methanol, and then it was dried under vacuum.

Stereocomplex formation by evaporation Equal masses of each polymer configuration in a 20 mL vial, it was dissolved in CH_2Cl_2 to a concentration 10mg/ml. The mixture was stirred at room temperature for 24 hours. The vial was loosely capped and placed inside a TLC chamber and covered. The solution was allowed to evaporate slowly, leaving behind a polymer pellet.

Chapter 3: Poly(Propargyl Glycolide) Crosslinked Nanoparticles

Introduction

Polymeric particles have a long history of uses in biomedical applications like controlled drug release,[130, 131] and gene therapy.[132-134] Polymer particles are attractive for biomedical applications due to the facility to tune and modify their physical and chemical properties. Polymeric nanoparticles derived from homo polymers have been synthesized before by emulsion,[135, 136] spray drying or printing[137] techniques. However, these materials lack the needed functionality to encapsulate drugs or gene vectors. More functional nanoparticles have been synthesized using different polymer architectures; amphiphilic block copolymers,[138, 139] nanogels,[140] comb polymers,[69, 141, 142] hyper branched polymers,[143] star shaped polymers,[144] and dendrimers.[35, 145] Effective drug or gene delivery vectors encompass certain properties. Amphiphilic block copolymer nanoparticles are self-assembled by interactions with the appropriate solvents or drugs. Polymeric nanoparticles are used as drug delivery vehicles because of the potential to introduce desirable properties easily and cost effectively. These desired properties include: stability, non-cytotoxicity, aqueous solubility, and rapid clearance from the body. Crosslinking has been explored as a means of introducing additional stability to polymeric particles.[146] Amphiphilic polymers are especially desirable to introduce hydrophobic drugs such as Doxorubicin.[138] Here, the hydrophobic domain will interact with the drug while the hydrophilic domain renders the

micelle water solubility. Utilizing PEG as the hydrophilic domain has the advantage of increasing water solubility of the particle, extending blood circulation time and preventing protein fouling.[147]

Two main approaches for crosslinking nanoparticles are shell crosslinking[148-154] and core crosslinking.[145, 146, 155-159] Wooley and coworkers prepared the first examples of shell crosslinked nanoparticles.[148] Shell crosslinked nanoparticles can be hollowed out by degradation of the core to obtain nanocages.[149] Core crosslinked nanoparticles often contain hydrophobic crosslinking agents.

Synthesizing stimuli-responsive or "stealth" nanoparticles is a growing trend in biomaterials for controlled release. The environment of the cell is the trigger that stimulates the nanoparticle response. Cells have different features, such as pH change and reduction potential that can trigger a response. Nanoparticles with hydrolytically labile moieties have been synthesized by Wooley[149, 160] and by Stenzel.[161] Similarly, redox responsive materials have been prepared. Davis and coworkers developed a reducible hyperbranched polymer from AB_2 monomers using RAFT.[143] Crosslinked nanoparticles were synthesized in the laboratories of Renxi Zhuo,[133] Stenzel,[155] and others.[130, 131, 138, 158, 162-167] Lately, a new approach has been to have two modes of stimuli response to enhance the efficacy of the delivery vehicle. Examples of redox and pH responsive, pH and magnetic field responsive,[168, 169] and temperature and pH

responsive particles[170, 171] exist in the literature. It is important for nanomaterials used for drug therapies to have efficient release mechanisms. Another important mechanism is how the drug vehicle gains entry into the cell.

Cells have diverse mechanisms for recognition and uptake of agents and nutrients such as phagocytosis, endocytosis, and fluid phase pinocytosis.[172-174] It has been reported that due to enhanced permeability and retention, cancerous cells selectively internalize sub micrometer particles.[140, 162, 175, 176] The first barrier for internalization is the cell membrane, which is a phospholipid bilayer. Therefore, the interaction of the cell membrane with the surface or the nanoparticle must be favorable to gain entry to the cytoplasm.

In this chapter we explore the synthesis and characterization of dual stimuli crosslinked poly(propargyl glycolide) nanoparticles, the surface modification of PPGL crosslinked nanoparticles with different functional groups and their interaction with a lipid bilayer mimic.

Results and Discussion

Effect of reducible vs non-reducible cross-linker in controlled release

Poly(propargyl glycolide) is a hydrolytically degradable polyester. This is convenient because a change in pH will trigger degradation. Although PPGL is a hydrophobic material, we can introduce diverse functionality via click chemistry. Pegylated poly(propargyl glycolide) crosslinked nanoparticles have been prepared in our lab.[14] However, hydrolysis can be slow. Introducing reductively cleavable moieties

will produce a dual stimuli responsive material. A material that is hydrolytically and reductively degradable may be advantageous for drug controlled release. First, the reduction of the material will release the encapsulated drug, and then the clearance from the body would be aided by the hydrolysis of the material. Disulfide bonds are labile to reducing agents such as dithiothreitol but more importantly thioredoxin and glutathione, which are reducing agents found in the cell cytoplasm.[177]

Using click chemistry, we modified poly(propargyl glycolide) with pendant PEG chains to introduce amphiphilic groups. We added stability to the polymer by crosslinking it with either of two crosslinking agents; 1,5-diazido pentane (CL: Crosslinker) or bis-2-azidoethyl disulfide (CD: Crosslinker degradable) **(Scheme 11)**. The latter is a reductively cleavable crosslinker. The size of both types of crosslinked nanoparticles was stable as a function of concentration in MQ water **(Figure 21)**.

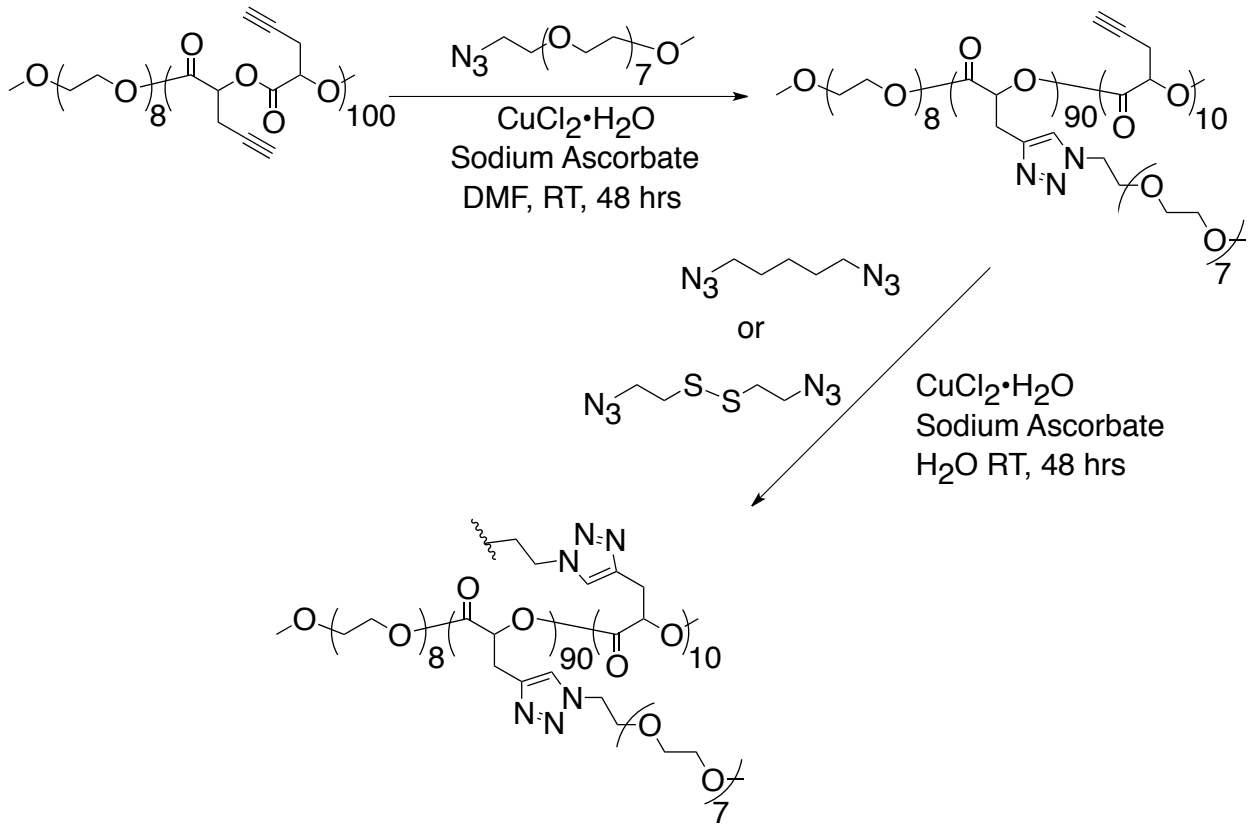

Scheme 11 Synthesis of crosslinked nanoparticles using a reducibly degradable crosslinker (CD) or a non-reducibly degradable crosslinker (CL).

To test the effect of a reducing agent on the crosslinked nanoparticles encapsulation and release of pyrene as a hydrophobic drug model was attempted post-crosslinking **(Figure 22)**. However, pyrene was not encapsulated quantitatively and interfered with the signal of the released pyrene. To remove the free pyrene, the samples were filtered through a 0.45 µm PVDF syringe filter, which also removed a fraction of particles. The study was inconclusive. Nonetheless, the effect of a reducing agent was still necessary. A second attempt was made to follow the degradation of the nanoparticles both in the presence and absence of dithiothreitol (DTT) in 4-(2-hydroxyethyl)-1-piperazineethanesulfonic acid (HEPES) pH 7.4 buffer by DLS. Initially, the samples appeared to increase in size but with the course of the experiment the data

became very noisy due to the contribution of hydrolytic degradation. Again the experiment was inconclusive.

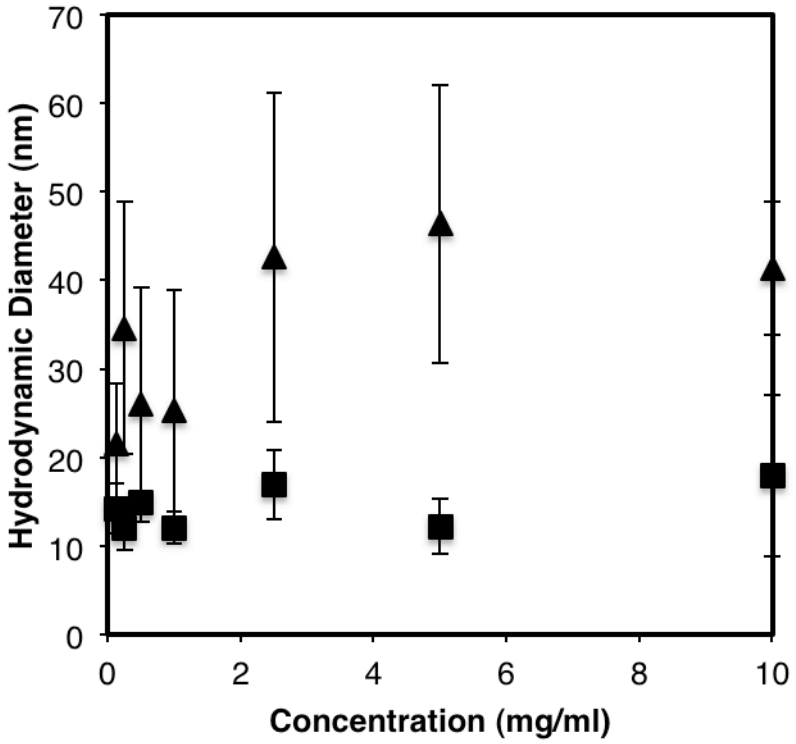

Figure 21 Hydrodynamic radius vs concentration of CD particles (■) and CL particles (▲) in MQ water using DLS.

At last, instead of attempting to replicate physiological conditions, the degradation of the particles was assayed by GPC. Samples of nanoparticles were tested in DMF prior to treatment. An identical sample was incubated in DMF containing 100 µL of DTT (1mg/mL) at 37 ^{o}C for 2 hours, and then it was tested. The GPC showed identical traces for the CL particles with and without treatment. The elution time for the CD particle after DTT treatment changed to an earlier time. This is an indication of reductive degradation of the crosslinker but not the polymer chain **(Figure 23)**. Although

this experiment does not resemble physiological conditions, it shows that the CD particles are vulnerable to reductive degradation.

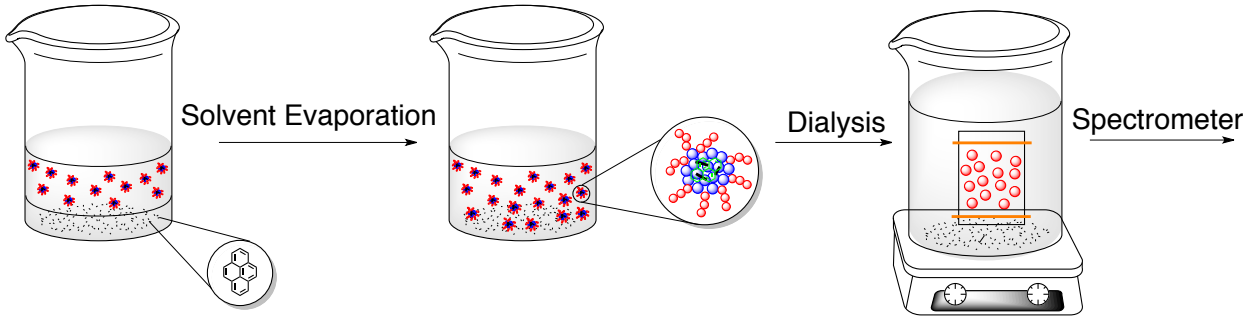

Figure 22 Pyrene was encapsulated in CLNPs and CDNPs by the solvent evaporation method. The NPs containing pyrene were dialyzed in 10 KDa MWCO reconstituted cellulose membranes against 0.1M PBS buffer pH 7.4 at 25°C in the presence or absence of 0.01M DTT. Samples were taken at time intervals and where analyzed by fluorescence and UV-Vis spectroscopy, the samples were returned after analysis to maintain NP concentration constant.

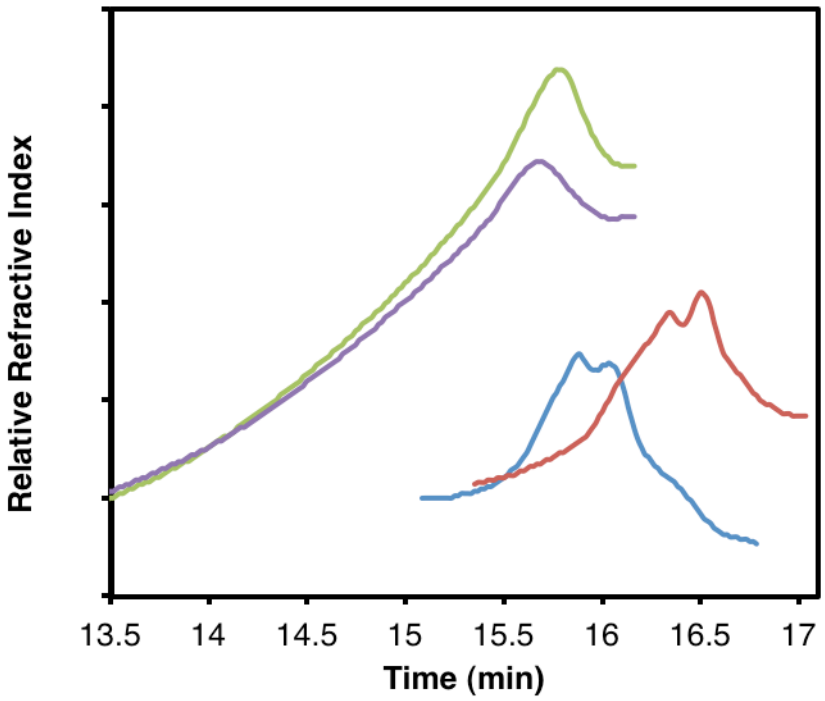

Figure 23 GPC traces of CD particles before (red), after treatment (blue) CL particles before (purple) and after treatment (green). Untreated samples in DMF, treated samples with DTT in DMF at 37°C for 2 hours.

Functional group surface modification

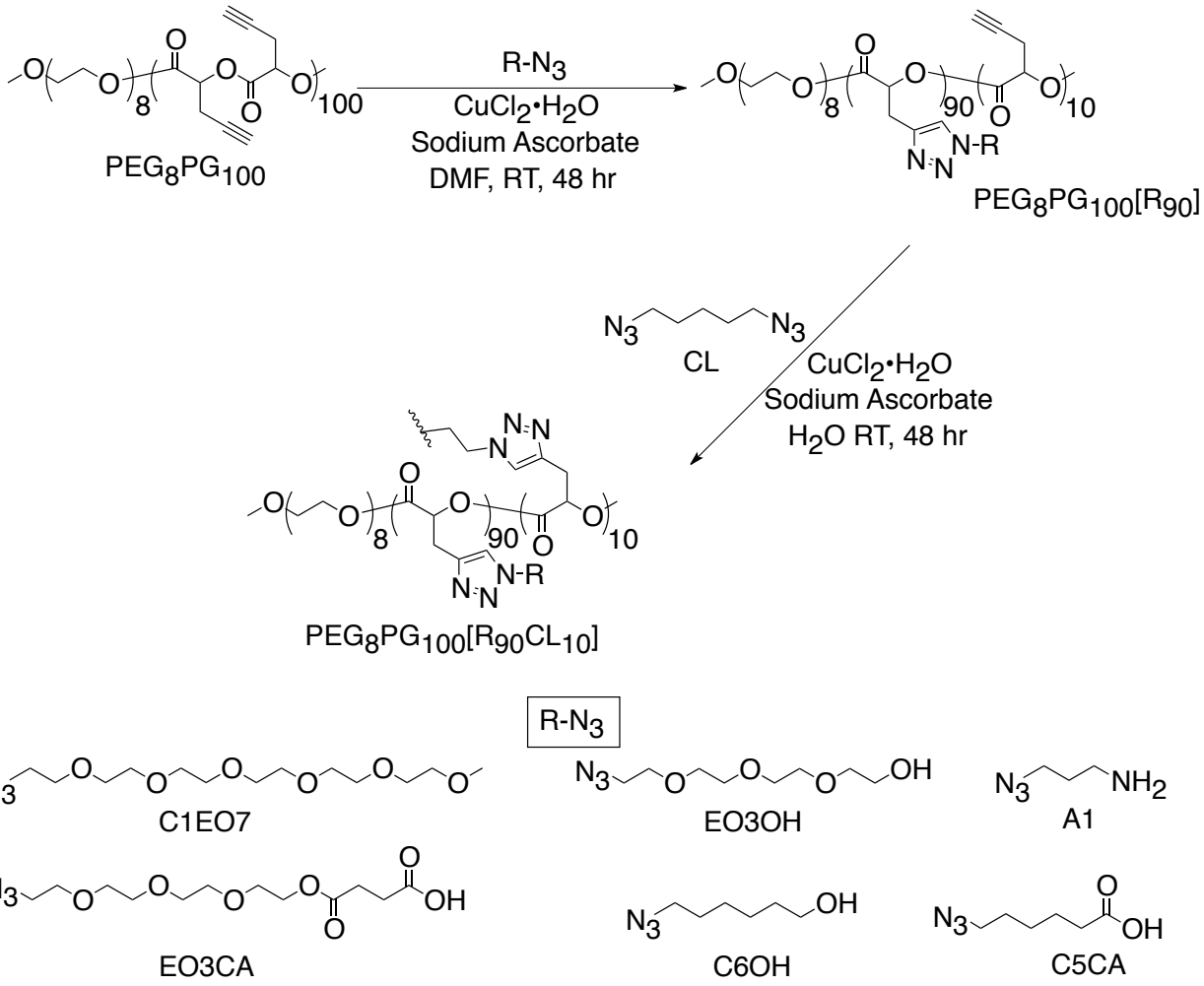

Scheme 12 Synthesis of variable functionality crosslinked Poly(propargyl glycolide) nanoparticles via click chemistry.

We modified PPGL using azides that contained different functional groups; PEG, carboxylic acids, amines and alcohols, then we crosslinked the core to add stability **(Scheme 12)**. We wanted to test the interactions between the different functional groups and a cell membrane mimic. **Figure 24** shows the ^{1}H NMR of PPGL after each chemical transformation. After click reaction using a short PEG azide, we see the appearance of the aromatic triazole peak and the pendant clicked PEGs. The polymer

was crosslinked at the core on a second click reaction. The NMR only shows the groups on the surface of the particle.

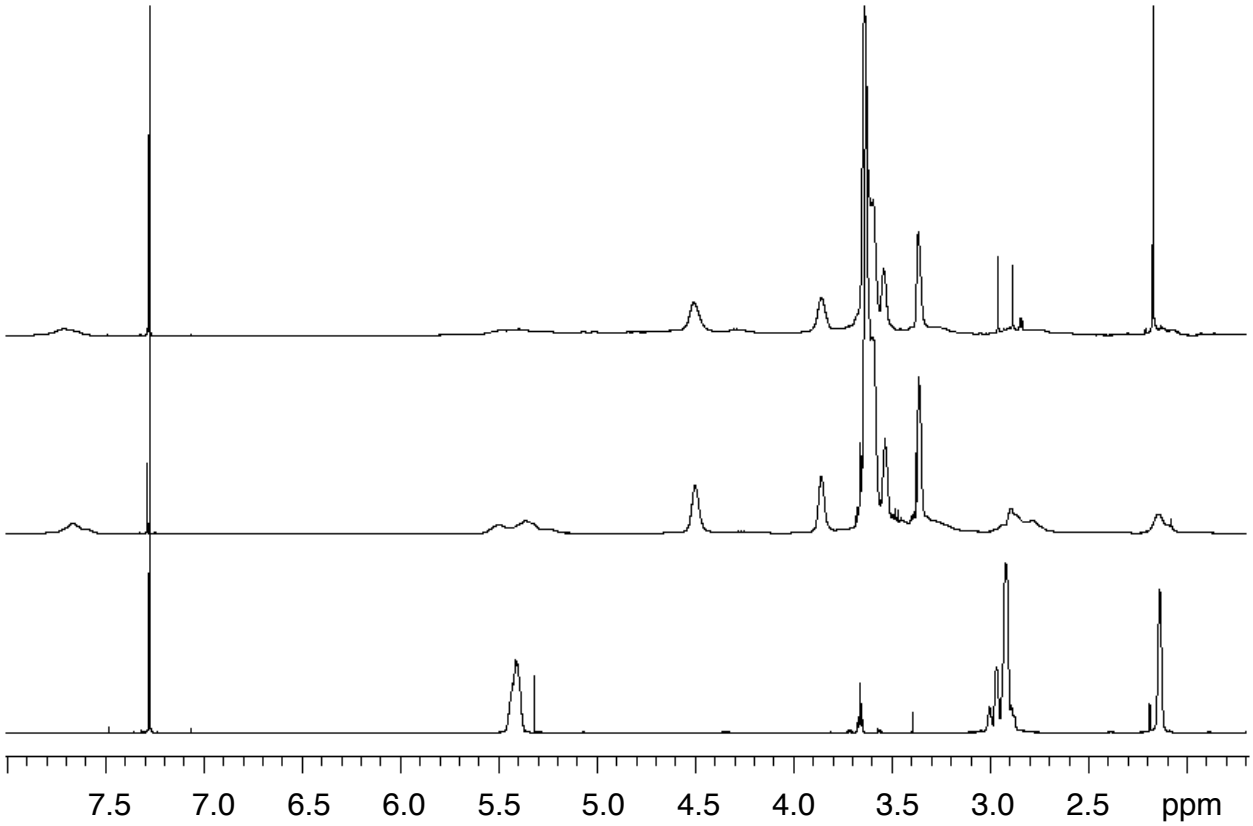

Figure 24 Characterization of crosslinked PPGL through ^{1}H NMR. Poly(ethylene glycol)-*block*-poly(propargyl glycolide) (bottom). Poly(ethylene glycol)-*block*-poly(propargyl glycolide)-*graft*-poly(ethylene glycol) (middle). Crosslinked Poly(ethylene glycol)-*block*-poly(propargyl glycolide)-*graft*-poly(ethylene glycol) (top). The disappearance of the alkyne and appearance of triazole signal protons show the completion of the click reaction. The methine on the polymer backbone are not prominent in the crosslinked particle spectrum.

We probed the hydrodynamic diameter of the particle in two media; MW water and HEPES buffer pH 7.4 at 1mg/ml particle concentration **(Figure 25)**. Overall, the particles were about the same size and there was no significant difference between the two media. Only the amine particle was different and was twice as big as the other

particles in MQ water, the size decreased in HEPES buffer. This was due to aggregation of the nanoparticles. The hydrodynamic diameter of the particles was taken using DLS with a backscattering detector at 173°. The size of the crosslinked nanoparticles by DLS is comparable to the size of the nanoparticles from TEM. **Figure 26** shows the TEM micrographs of the PEG particle. Given the diameter of the particles, we can infer that the crosslinking was intermolecular not intramolecular as initially planned.

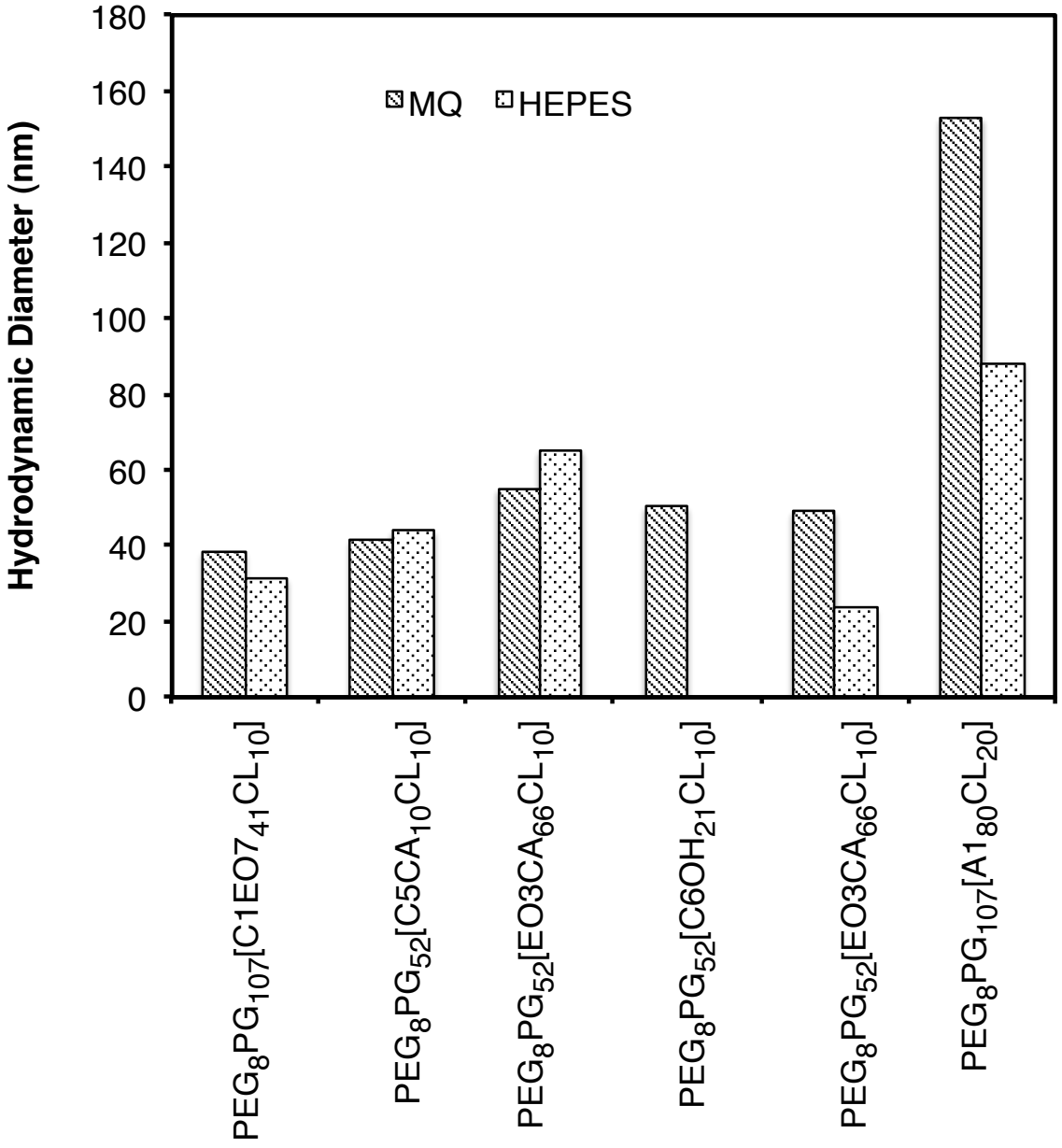

Figure 25 Hydrodynamic diameters of PPGL crosslinked nanoparticles in MQ and in HEPES buffer pH 7.4 at 1mg/mL particle concentration.

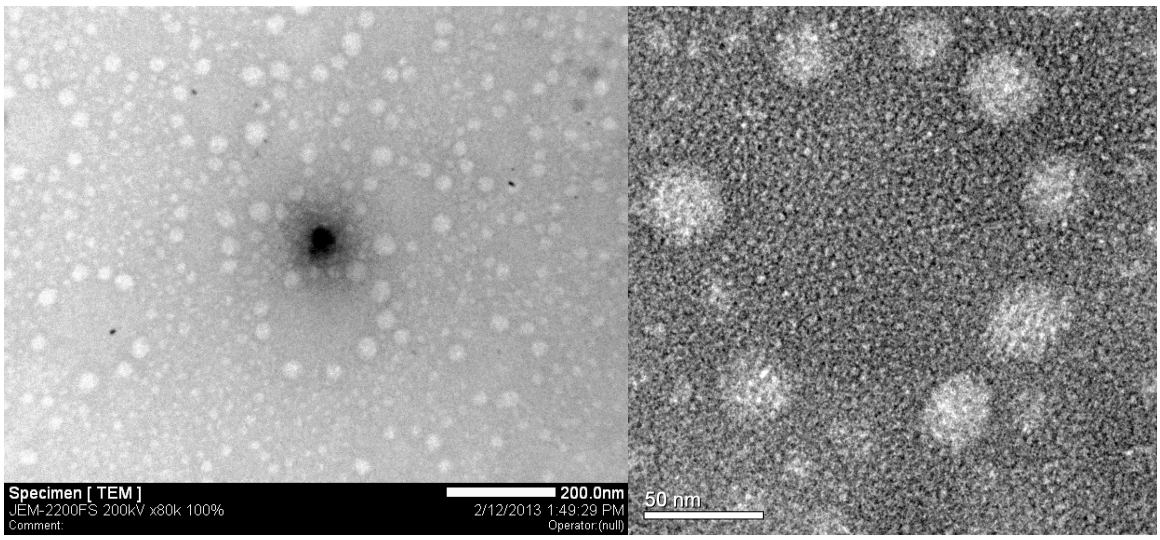

Figure 26 TEM micrographs of $PEG_8PG_{107}[C1EO7_{41}CL_{10}]$. Left scale bar is 200 nm High resolution TEM (right, scale bar is 50 nm). Black spot on the left micrograph is a burn on the camera lens.

The second part of the project was to test the interactions of the functionalized nanoparticles with a cell membrane mimic.[178] The lipid bilayer was formed with 1,2-diphytanoyl-*sn*-glycero-3-phosphocholine (DPhPC) in between a Teflon partition with a 200 µm aperture **(Figure 27)**. Nanoparticles were added at different concentrations in both sides of the chamber that was filled with an electrolyte solution 1M KCl in 20 mM HEPES pH 7.4, and the current conductance was measured. The conductance amplitude with duration of 1-150 ms is a single spike and it is considered induced current. Integral conductance is achieved by events of duration longer than 150 ms.

The pegylated and the hydroxylated particle presented single spike current but only at relatively high concentrations (300 µg/ ml). The carboxylated nanoparticles caused induced current spiked initially at concentrations of 50 µg/ml but cause integral conductance at longer run times. The aminated particle only caused integral current conductance at very low concentrations (5 µg/ml) and the membrane was not resealed

at prolonged times. At higher concentrations, the amine particles destroyed the lipid bilayer **(Figure 28)**.

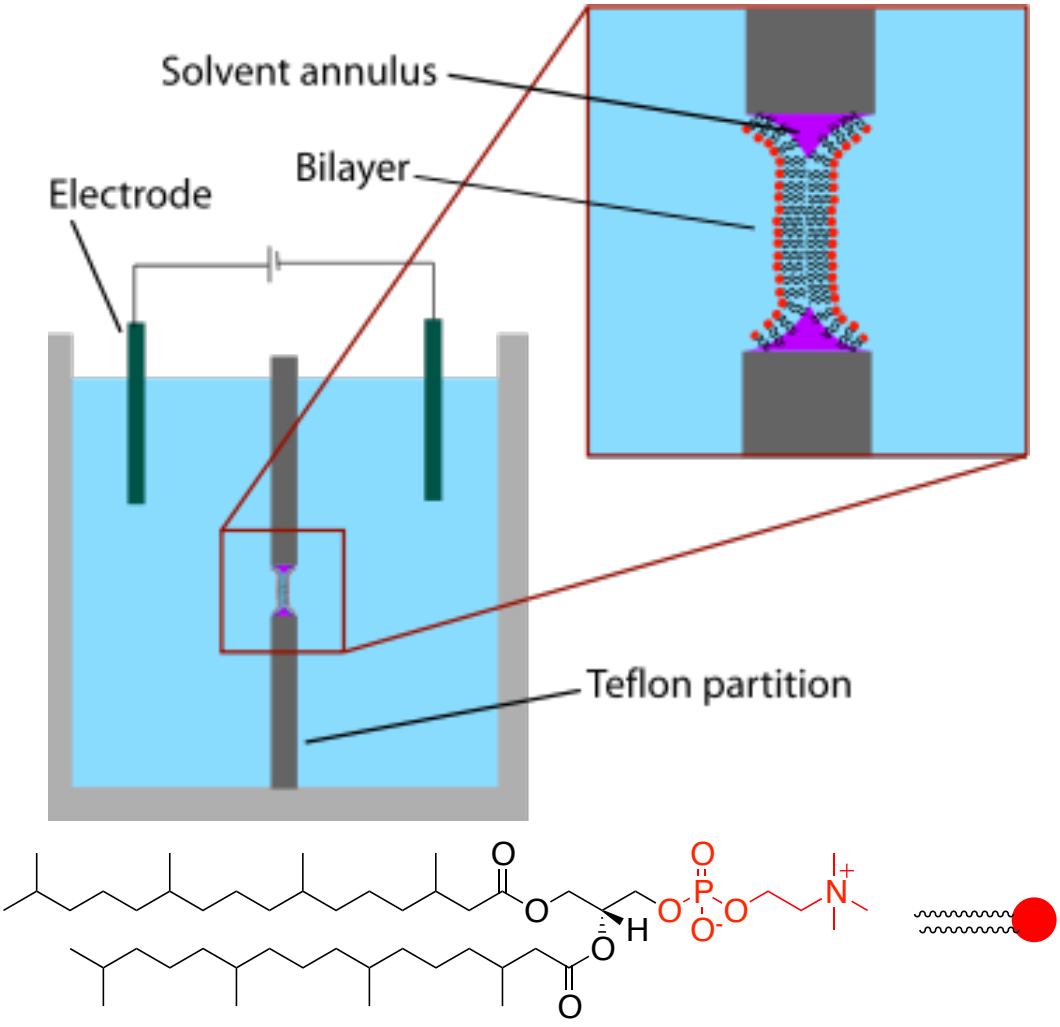

Figure 27 Schematic representation of Biomimetic lipid membrane (BLM) experimental setup.

The nanoparticles form pores in the membrane that in the case of pegylated and hydroxylated particles the membrane is able to reseal itself. The formed pores allow the nanoparticles to diffuse through the membrane. This indicates that the particles would not enter the cell via endocytosis.[179] According to Foster et al. particles of neutral charge such pegylated particulate material is taken up at a lesser extent than charged

particles.[174] Charged particles like amines and carboxylic acids show integral conductance, which means they are passing through the cell membrane more readily than uncharged particles that only show single spike conductance.

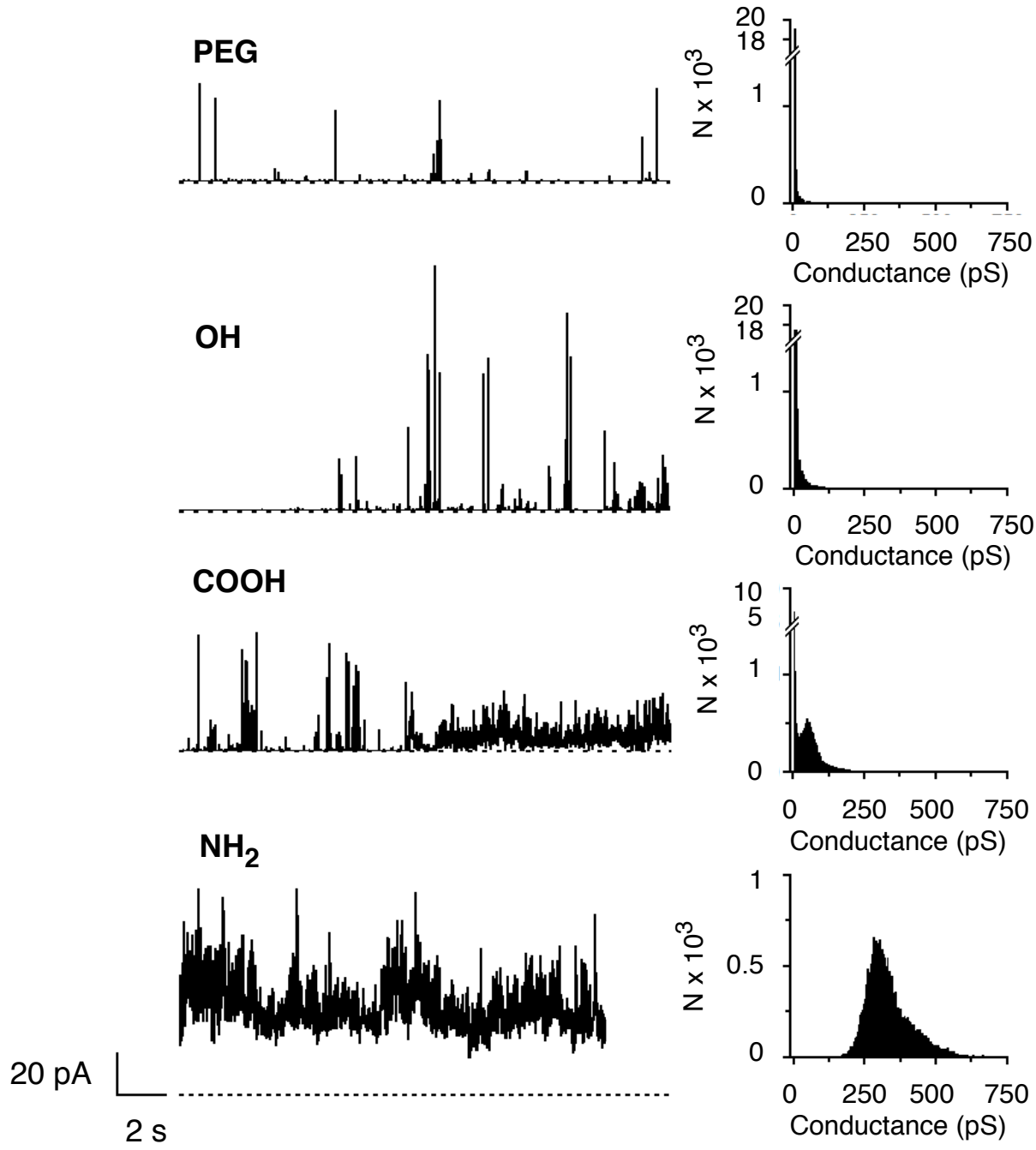

Figure 28 Current traces induced by the interactions of PGL nanoparticles with BLM. BLM were suspended between symmetric solutions of 1 M KCl, 20 mM Hepes pH 7.4 and a transmembrane potential of 100 mV was applied. Nanoparticles were added to the both sides of the membrane. At the right side of the figure, histograms of conductances corresponding to the recorded traces are presented. Dotted lines indicate zero current.

Conclusion

We prepared poly(propargyl glycolide) functionalized crosslinked nanoparticles. In our first example we introduced a reductively cleavable crosslinker to obtain a dual stimuli material. This nanoparticle is degraded in the presence of DTT a reducing agent similar to thioredoxin and glutathione that are ubiquitous in mammalian cells. Secondly, we modified the surface of the particles with different functional groups to test the interactions of the nanoparticles with a cell membrane mimic. We found that particles bearing carboxylic acids and amines are transported through the membrane more readily than pegylated and hydroxylated particles. Biodegradable crosslinked nanoparticles have great potential of use in drug delivery, knowing how to introduce them into the cell and how to aid drug release are two of the most important issues to be solved today. We have attempted to shed some light into these important factors.

Experimental

General Toluene was dried with sodium and benzophenone and freshly distilled. Dialysis was performed using regenerated cellulose membranes Spectra/Por 5 12,000-14,000 Da MWCO (Spectrum Laboratories Inc.) in water/acetone mixtures. Characterization Nuclear Magnetic Resonance (NMR) was performed in 500 MHz or 300 MHz Varian spectrometers. FTIR spectra were taken in a Mattson Galaxy series FTIR 3000. TEM (Transmission electron microscopy) was performed using a JEOL 2200FS 200 kV emission TEM on copper grids (300 mesh Carbon type B, Ted Pella Inc). TEM samples were negatively stained with 1% aqueous uranyl acetate.

Synthesis of 6-azidohexan-1-ol 6-chlorohexa-1-ol (6.2 g, 45 mmol, 1 eq.) was added to a 500 mL round bottom flask and dissolved in 340 mL of acetone/water 6:1 mixture. Sodium azide (7.3 g, 110 mmol, 2.5 eq.) was added. The mixture was refluxed at 64-68 $^{\circ}$C for 2 days. The reaction mixture was extracted with 150 mL of diethyl ether three times. The combined ethereal layers were washed with 50 mL of brines twice. Then the organic layer was dried with $MgSO_4$, filtered and condensed. The starting materials was distilled off at 80 $^{\circ}$C under vacuum leaving behind 4.7g of pure product. (72%) ^{1}H NMR $CDCl_3$ δ (ppm) 3.61-3.57 (t, 2H, CH_2—OH), 3.25-3.20 (t, 2H, CH_2—N_3), 1.68 (br, 1H, O—H), 1.60-1.51 (m, 4H, CH_2), 1.38-1.33 (m, 4H, CH_2); ^{13}C NMR CDCl3 δ (ppm) 62.6, 51.3, 32.4, 28.7, 26.4, 25.2

Synthesis of 19-azido-2,5,8,11,14,17-hexaoxanonadecane (C1EO6)

In a 250 mL round bottom flask, poly(ethylene glycol) monomethyl ether with a molecular weight of 350 g/mol (4.95 g, 14 mmol) was dissolved in 100 mL of freshly distilled pyridine. The reaction vessel was cooled to 0 $^{\circ}$C. *Para*-toluenesulfonyl chloride (6.98 g, 36 mmol, 2.5 eq.) was added. The mixture was stirred overnight under nitrogen at rt. 1 M HCl was added to the reaction and extracted with ethyl acetate (3 x 50 mL). The organic layer was washed with aliquots of 1M HCl until the pH was 1 indicating removal of pyridine. The organic layer was dried over $MgSO_4$, filtered and solvent was removed under vacuum. The tosylated PEG material was used without further purification. (1.97g, 4 mmol, 26%)

The PEG tosylate (1.97 g, 4 mmol) and sodium azide (0.63 g, 9.7 mmol, 2.5 eq) were combined and dissolved in 1:1 acetone water mixture and refluxed at 80 ^{o}C under nitrogen for 12 hours. The reaction mixture was extracted with diethyl ether (3 x 50 mL). The organic layer was dried over $MgSO_4$, filtered and solvent was removed under vacuum. (0.92 g, 60%) ^{1}H NMR $CDCl_3$ δ (ppm) 3.66-3.57 (m, 20H, O—CH_2—CH_2—O), 3.52-3.48 (m, 2H, CH_2—N3), 3.37-3.31 (m, 5H, CH_2—O, CH_3—O); ^{13}C NMR CDCl3 δ (ppm) 71.8, 70.63, 70.63 70.59, 70.52, 70.49, 70.46, 70.43, 69.96, 58.98, 58.91, 50.63; FTIR cm^{-1} (KBr Pellet) 2872, 2106, 1453, 1289, 1111, 851

Synthesis of 6-azidohexanoic acid Chromium trioxide (12.5 g, 125 mmol, 5 eq.) was dissolved in 20 mL of deionized water and cooled in an ice bath. Concentrated sulfuric acid (10 mL, 187 mmol) was added to CrO_3 dropwise while stirring. In a 250 mL round bottom flask, 6-chlorohexan-1-ol (3.5 g, 25 mmol) was dissolved in 10 mL acetone and cooled in an ice bath. The chromic acid solution was transferred to an addition funnel and added dropwise to the solution of 6- chlorohexan-1-ol. The reaction was stirred for 2 days at room temperature. Isopropanol (50 ml) was added to the mixture to remove excess chromic acid 20 g of $NaHCO_3$ were added to precipitate the chromium salts. Pentane and ethyl acetate were added and the mixture was filtered using vacuum. Aqueous HCl (10%) was added to acidify the filtrate. The aqueous layer was extracted with ethyl acetate (3 x 100 mL). The combined organic layers were washed with brine (2

x 50 mL). The organic layers were dried over $MgSO_4$ and filtered, and then the solvent was removed. The crude mixture was distilled under vacuum at 125 ^{o}C (2.09 g, 53%). The 6-chlorohexanoic acid (0.7 g, 4.4 mmol) was dissolved in DMF (10 mL). Sodium azide (0.72 g, 110 mmol, 2.5 eq.) was added and the mixture was stirred at 80 ^{o}C under nitrogen for 16 hours. The reaction vessel was allowed to cool, 50 mL of deionized water and 20 mL of 2 M HCl were added. The aqueous mixture was extracted with diethyl ether (3 x 100 mL). The combined organic layers were washed with brines (2 x 50 mL). The ethereal solution was dried over $MgSO_4$ and the solvent was removed in vacuum. The product was used without further purification. (91%); ^{1}H NMR $CDCl_3$ δ (ppm) 3.26-3.24 (t, 2H, CH_2—N_3), 2.36-2.33 (t, 2H, CH_2—COOH), 1.67-1.58 (m, 4H, CH_2), 1.44-1.39 (m, 2H, CH_2); ^{13}C NMR $CDCl_3$ δ (ppm) 179.8, 51.15, 33.79, 28.49, 26.11, 24.1; FTIR cm^{-1} 3041 br, 2942, 2869, 2098, 1680, 1392, 1284

2-(2-(2-(2-azidoethoxy)ethoxy)ethoxy)ethanol (EO3OH) was synthesized by Vogel (unpublished).

Synthesis of 1-azido-13-oxo-3,6,9,12-tetraoxahexadecan-16-oic acid[180] EO3OH (5 g, 22.9 mmol) was dissolved in 20 mL of pyridine. DMAP (0.55 g, 4.5 mmol, 0.2 eq.) and succinic anhydride (2.3 g, 22.9 mmol) were added. The reaction was stirred overnight under nitrogen at room temperature. To acidify the reaction, 20 mL of 2M HCl were added and the mixture was stirred for one hour. Dichloromethane (100 mL) was added. The organic layer was washed with 2 M HCl thoroughly and then with deionized water.

The mixture was dried over $MgSO_4$, filtered and solvent removed under vacuum. (73%); ^1H NMR $CDCl_3$ δ (ppm) 4.25-4.23 (t, 2H, $CH_2—N_3$), 3.67-3.62 (m, 14H, $O—CH_2—CH_2—O$), 3.37-3.35 (t, 2H, $CH_2—OCO$), 2.64-2.63 (t, 4H, $CO—CH_2—CH_2—COOH$); ^{13}C NMR $CDCl_3$ δ (ppm) 176, 172, 70.76, 70.58, 70.55, 70.42, 69.97, 69.95, 63.84, 50.63, 29.18, 28.97

Synthesis of 3-azido-1-aminopropane procedure by Carboni et Al.[181]

Synthesis of 1,5-diazidopentane This molecule was synthesized using a procedure by Vogel.[14]

Synthesis of 1,2-bis(2-azidoethyl)disulfide[182] In a 500 mL round bottom flask 2-hydroxyethyl disulfide (10 g, 60 mmol) was dissolved in 20 mL THF and cooled to 0 °C in an ice-water bath. Pulverized sodium hydroxide (12.9 g, 320 mmol, 5 eq.) was added to the vessel and stirred. A solution of para-toluenesulfonic acid (37 g, 194 mmol, 3 eq.) in 175 mL THF was added dropwise using an addition funnel. The reaction was stirred under nitrogen at room temperature for 12 hours. Iced water was added to the reaction to separate layers. The water layer was extracted with diethyl ether (3x 100 mL). The combined organic layers were dried over $MgSO_4$, filtered and solvent was removed under vacuum. The material was used without further purification (26 g, 94%).
The bistosylate (3.1 g 6.8 mmol) was dissolved in 30 mL acetone. Sodium azide (1.77 g 27 mmol, 4 eq) in 10 mL water was added. The mixture was refluxed at 80 °C under nitrogen overnight. The acetone was removed and the mixture was extracted with

CH_2Cl_2, dried over $MgSO_4$ and filtered. The crude was purified by column chromatography with 4% ethyl acetate in hexanes. (1.17 g, 84%) ^{1}H NMR $CDCl_3$ δ (ppm) 3.59-3.57 (t, 4H, CH2—N3), 2.86-2.84 (t, 4H, CH2—S); ^{13}C NMR CDCl3 δ (ppm) 49.9, 37.6; FTIR 2259 cm^{-1}

General click chemistry procedure A Schlenk flask was loaded with 40-60 mg of polymer, the desired mol % of azide ligand according to moles of alkyne in the polymer, 24 mol% of sodium ascorbate and the mixture was dissolved in DMF. The mixture was degassed by 3-4 freeze-pump-thaw cycles and backfilled with nitrogen gas. A 0.1 M solution of $CuCl_2 \cdot 2H_2O$ in DMF was added after degassing. The reaction mixture was stirred at room temperature overnight. After reaction, the mixture was filtered and the solids removed. Amberlite IRC-748 ion exchange resin beads were added to the filtrate to remove copper, the mixture was aged for 8 hours. After gravity filtration of the beads, DMF was removed in vacuo. The polymer film was dissolved in 3:1 water/acetone and was dialyzed in a 12- 14 kDa MWCO dialysis bag for 2-3 days. After dialysis solvents were removed under vacuum.

General cross-linking procedure for clicked PPGL nanoparticles A solution of clicked PPGL in acetone (10 mg/ml) was dripped into ice-cold MQ water to 1mg/mL of clicked polymer, containing sodium ascorbate (1 eq. relative to remaining alkynes) and $CuCl_2 \cdot 2H_2O$ (0.5 eq. relative to remaining alkynes). The solution was stirred for 10 minutes. A solution of cross-linker (0.5 eq. relative to remaining alkynes) in acetone

(1mg/ml) was added dropwise. The mixture was stirred for 48 hours under nitrogen. The solution was dialyzed for two days against 4:1 acetone water mixture in a 12-14 kDa MWCO regenerated cellulose dialysis bag. The solvent was removed and the residue dissolved in DMF. Copper ions were removed using ion exchange resin beads. After the beads were removed, DMF was removed under vacuum. The residue was suspended in MQ water to 10 mg/mL

Chapter 4: Reductively degradable clicked poly(propargyl glycolide) for siRNA delivery

Introduction

Fast degradation of PPGL is required for prompt release of nucleic acids. Due to the polyester backbone, PPGL is hydrolytically degradable, but preliminary data suggest that it degrades on the timescale of days. The interior of cells is a highly reducing environment[183-185] that can degrade molecules or macromolecules that contain reductively labile groups such as disulfide bonds. If disulfide bonds are introduced into the polyester backbone of PPGL, the biodegradability of PPGL within cells should be enhanced.

Polymers that contain disulfide bonds are readily biodegradable under reductive conditions, and have the potential to deliver gene vectors or other therapeutic agents.[67, 184-189] The driving force for release is the enhanced biodegradability provided by the disulfide linkage, which is cleaved under the cell's reductive environment. Some polymers have been synthesized with disulfide segments, and then cleaved with thiols. For example, Tsarevski and Matyjaszewski synthesized a disulfide initiator from bis-2-hydroxyethyl disulfide and 2-bromoisobutyric acid, and then used ATRP to synthesize linear and degradable polymethacrylates with internal disulfide bonds. The polymer degradation was studied by cleaving the disulfide bonds with tributyl phosphine.[190]

Davis and coworkers[58] used RAFT to synthesize a biodegradable hyperbranched PDMAEMA, with bis-2-hydroxyethyl disulfide as the initiator and a

disulfide containing cross-linking agent. DNA binding was assessed for the polymer, and DNA was completely bound at a 1:1 N/P ratio. In another report, the pendant amines of poly(lysine) were extended, placing disulfide bonds in the branches, and an ammonium tosylate at the terminus[188] **(Scheme 13)**. Presumably, the ammonium salt bound DNA electrostatically. Upon treatment with dithiothreitol (DTT), the disulfide bonds were cleaved and the nucleic acid released. The authors found that luciferase activity was higher when transfection was carried out with the modified poly(lysine) than the unmodified poly(lysine).

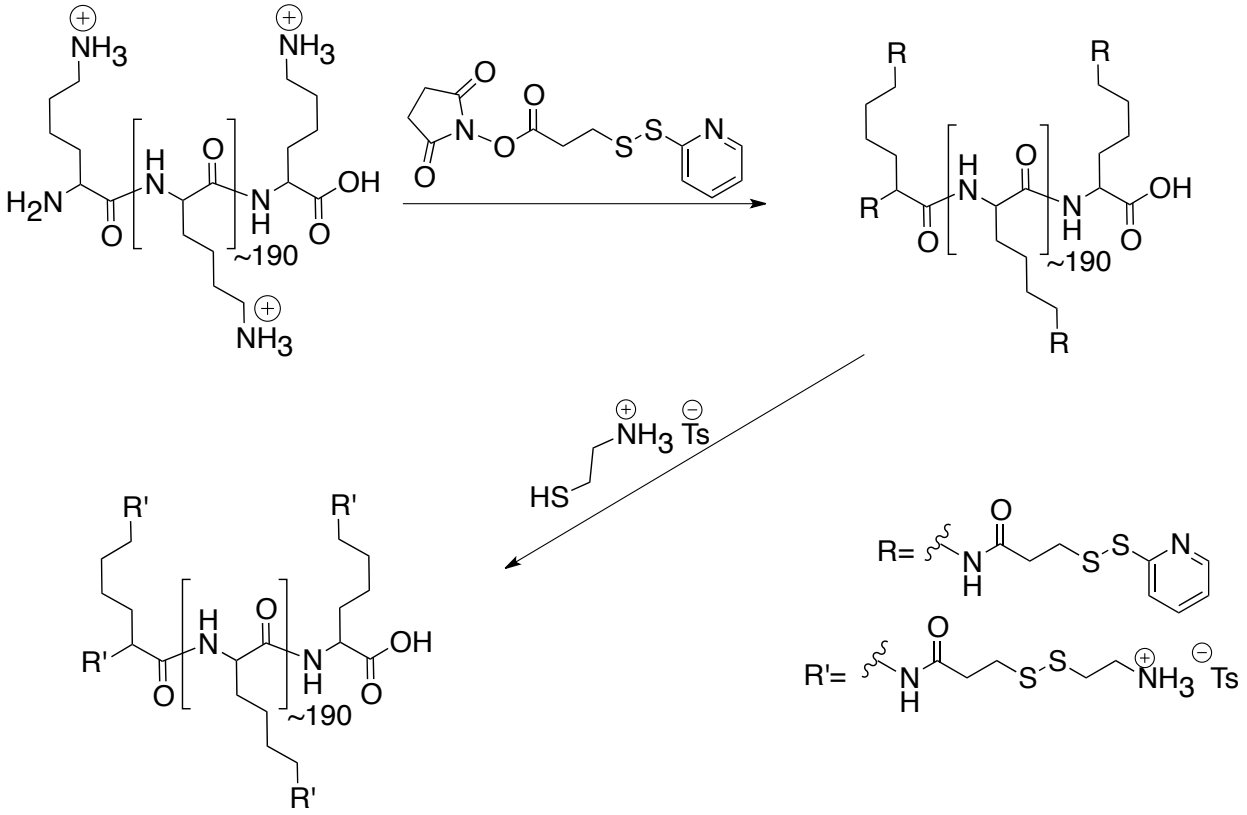

Scheme 13 Poly(lysine) derivative with degradable disulfide bonds for gene therapy

Cleavable disulfide bonds have also been used to covalently bind siRNA or DNA to a polymeric vehicle by activating the nucleic acid with a crosslinker such as N-

succinimidyl-3-(2-pyridyldithio) propionate (SPDP) and then reacting it with a thiol-terminated polymer.[66, 191, 192] For example, an amine terminated siRNA was conjugated to SPDP and then bound to sulfhydryl-PEG which was then electrostatically bound to PEI and the conjugate self-assembled into micelles. When transfected into a human prostate carcinoma cell line, there was evidence of silencing of vascular endothelial growth factor (VEGF) production.[191] Similarly, Wolff and coworkers used a disulfide bond to conjugate siRNA to poly(aminobutyl vinyl ether) grafted with PEG and N-acetylgalactosamine, a ligand that targets hepatocytes.[192] Expression of apolipoprotein B (apoB) was silenced by apoB-1 siRNA in mice. Lastly in another example, siRNA was covalently bound through a disulfide bond to make a pH and redox sensitive polyconjugate fabricated from PLL, and dimethyl maleic anhydride masked melittin (DMMAn-Mel), an endosomolytic peptide.[66] The polyconjugate showed gene knockdown of luciferase protein expression in Neuro2A-eGFPLuc cells without affecting the viability of the cells.

Polymers that contain multiple disulfide bonds along the backbone are uncommon, and only a handful of examples are found in the literature. One example is the ring opening polymerization of 1,2-dithiane[193] **(Figure 29)** which produces a polycatenane architecture which can be degraded photochemically. Linear aromatic disulfide polymers have been derived from 4,4'-oxybis(benzenethiol)[194] from macrocyclic monomers, and by oxidation of 4,4'-oxybis(benzenethiol)[195] However, the

previous examples are not suitable as biomaterials. An example of a suitable biomaterial in this category is poly(disulfide amines) in the work of Christensen and Kim.[184, 185]

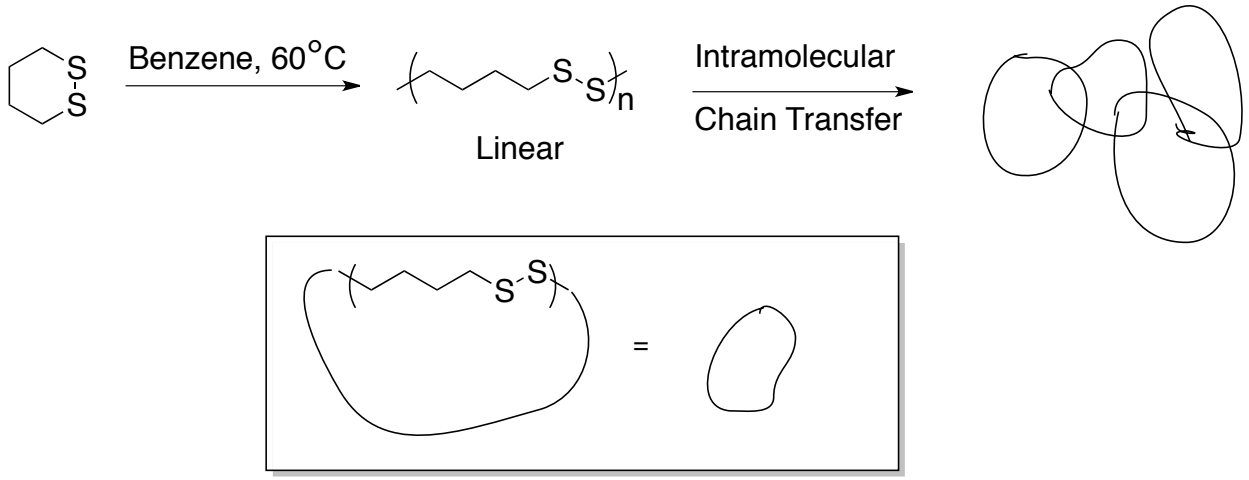

Figure 29 Ring opening polymerization of 1,2-dithiane to form polycatenanes.

Polymers with one disulfide linkage in the polymer backbone are more common. Usually, the disulfide bond is cleaved to obtain a thiol functional group[191] as in the case of the preparation of thiol functionalized poly(ethylene glycol)-*block*-polyesters.[196] Also, polymers containing thiol or disulfide sidechains have been used as crosslinking sites.[67, 187]

The objective of this project is the synthesis and characterization of poly lactide derived polymers that are potential delivery vectors for siRNA in order to activate the RNAi machinery. Herein, the synthesis and characterization of a polymer derived from PLA and designed for siRNA delivery are described.

Results and Discussion

Ideally, the polymers for gene silencing should bind high concentrations of RNA and release it soon after entering the cell. Triggered release of the nucleic acid cargo can be by a change in the environment, such as a change in pH or redox.

In an attempt to synthesize effective delivery agents, Vogel synthesized amphiphilic poly(ethylene glycol-*block*-propargyl glycolide)s, and used click chemistry to attach short PEGs, alkylamines, alkyls, and fluorescent dyes to the polymers. While alkylamines bind electrostatically to nucleic acids, short PEG segments were expected to decrease immunogenicity,[64] increase polymer solubility, and increase blood circulation,[67] and adding *n*-alkyl chains increased the binding affinity of the polymer for the nucleic acid.

The polymers bound nucleic acids and the polymer/nucleic acid conjugate effectively entered cells, but no knockdown of GFP was detected. The lack of silencing was thought to be due to irreversible RNA binding, or slow release of siRNA may deliver a nucleic acid concentration too low to effect gene silencing. The obvious solution is to synthesize polymers that exhibit good binding, enter cells, and release a high concentration of siRNA to trigger silencing. In this work, we focused on solutions to the binding and release problem. We hypothesized that modified polyPGL vehicles with cleavable disulfide bonds in the polymer backbone would enhance its degradation rate in the reductive cell environment. Cleavage of the disulfide bond should destabilize the polymer-siRNA conjugate and enhance siRNA release.

Poly(propargyl glycolide)s with internal disulfide bonds PG_5SSPG_5

We used a two-step route to poly(propargyl glycolide) polymers with disulfides inserted into the polymer backbone. As shown in **Scheme 14**, ring opening polymerization of propargyl glycolide was initiated with 2-hydroxyethyl disulfide and catalyzed by DMAP, placing a single disulfide in the center of the polymer chain. Such polymerizations are often run at room temperature, however, PGL has limited solubility in chloroform and therefore, the polymerization was run at 60°C. The monomer to initiator ratio was set to 10, which provides on average, two PGL segments of $X_n = 5$ (10 acetylene groups per segment) for subsequent click chemistry. The resulting oligomer was denoted as PG_5SSPG_5, two poly(PGL) segments, each with a degree of polymerization of 5 (PG_5), and connected by 2-hydroxyethyl disulfide (SS).

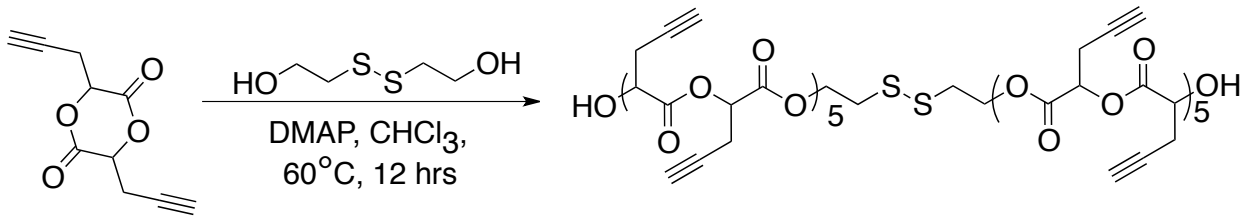

Scheme 14 Synthesis of PG_5-SS-PG_5 oligomers

The oligomer molecular weights were confirmed by ^{1}H NMR. Comparing the integrated signals from the terminal methines at each chain end to signals from the methylenes of the initiator (-$CH_2C\mathbf{H}_2O$-, 4.4 ppm) allows calculation of X_n. (The C$\mathbf{H}_2$-S-

S-C**H**$_2$ methylene signals and the propargyl glycolide methylenes overlapped and could not be used to calculate X_n.) **(Figure 30 top).**

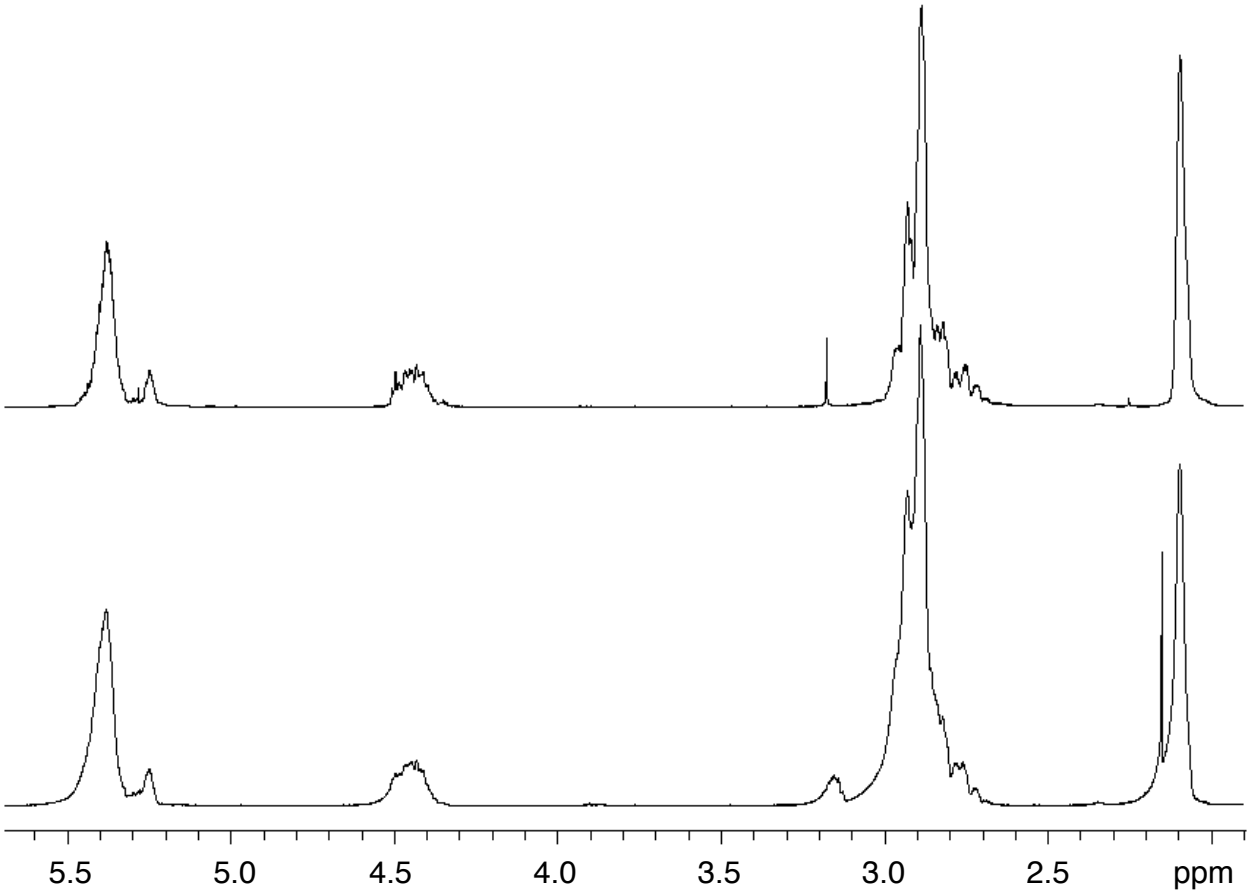

Figure 30 ^{1}H NMR spectra for PG_5SSPG_5 (Top) and thiol terminated PGSSPG (Bottom)

Table 6 shows data from four replications of the oligomer synthesis. The number average molecular weights (M_n) were obtained from ^{1}H NMR and Gel Permeation Chromatography (GPC). Also, the oligomers have narrow molecular weight distributions, and the molecular weights of PG_5SSPG_5 were comparable to the targeted degree of polymerization.

Table 6 GPC and NMR data for PG_5SSPG_5

	GPC			NMR	
Entry	M_n **x** 10^{-3}	**PDI**	**DP**	M_n **x** 10^{-3}	X_n
1	2.5	1.0	13	1.9	10
2	3.78	1.32	20	1.98	10
3	3.19	1.17	16	1.69	9
4	2.97	1.19	15	1.94	10

Replicates of synthesis of PGSSPG DMAP/bis(2-hydroxyethyl)disulfide/PGL 1:1:10 60 °C $CHCl_3$ 12 h.

The disulfide oligomers (PG_5SSPG_5) were extended by capping the hydroxyl end groups with 3-mercaptopropanoic acid using EDC and DMP, and then oxidizing the chain ends to form disulfides. **(Figure 30, Bottom, Scheme 15).** Several oxidation methods were tested[197-200] including MnO_2,[201] I_2 in an oxygen atmosphere[202] and hydrogen peroxide.[67] As shown in **(Table 7)**, these attempts to extend the oligomers by oxidation gave modest increases in M_n, ~ 3× with MnO_2. Hydrogen peroxide caused degradation of the polymer and was unsuitable for thiol oxidation. Overlapping signals prevented direct determination of M_n by ^1H NMR, and therefore M_n was estimated by GPC.

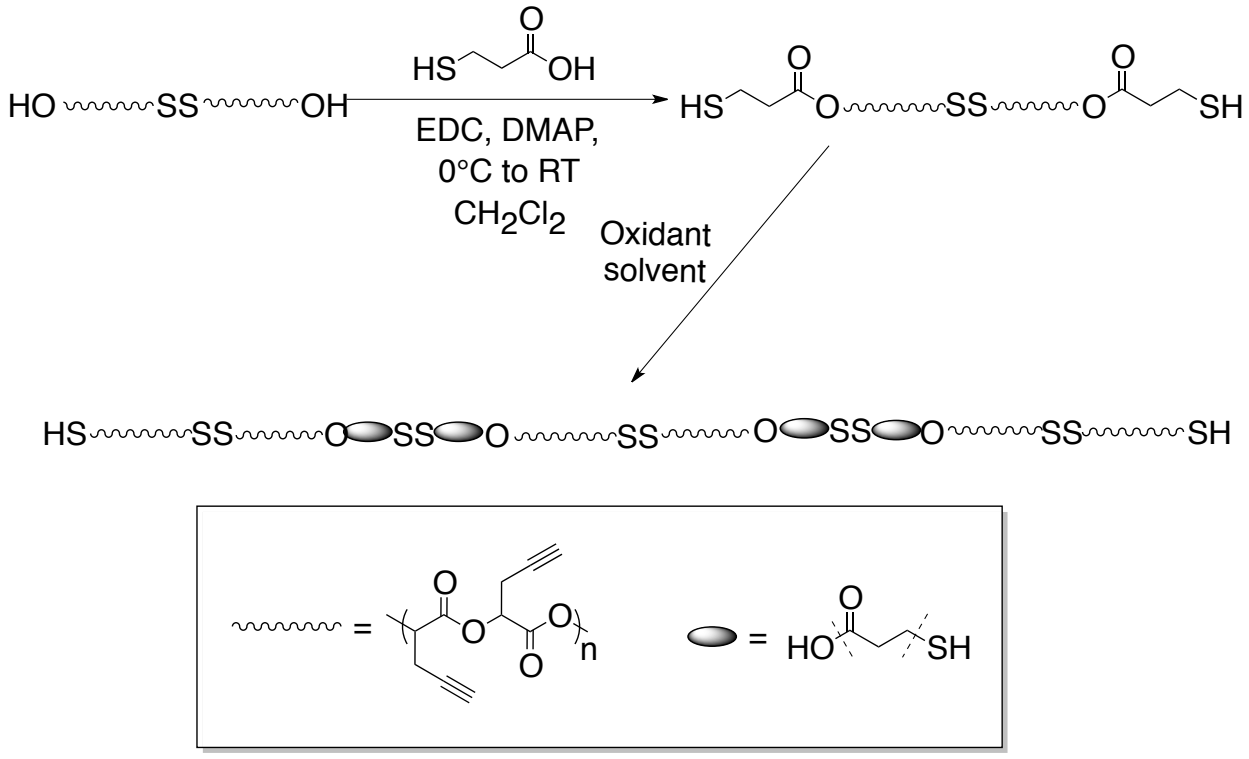

Scheme 15 Thiol terminated oligomer and chain extension by oxidation of the thiol groups to disulfide bonds.

Table 7 GPC data for chain extended thiols

Entry[a]	Starting material[b]			Chain extended		
		M_nx10^{-3}	PDI	Oxidant	M_nx10^{-3}	PDI
6	$HSPG_5SSPG_5SH$ **3**	1.7	1.16	MnO_2[c]	5.2	1.46
7	$HSPG_5SSPG_5SH$ **1**	2.5	1.07	I_2/O_2[d]	4.0	1.11
8	$PEG_8PG_{45}SH$ **5**	20.6	1.26	H_2O_2[e]	6.8	1.21

[a] Entry number refers to product. [b] Thiol modified starting material. [c] MnO_2 (1 equivalent) in CH_2Cl_2, RT overnight. [d] Iodine (3 equivalents) under O_2 in THF 12 hrs. [e] H_2O_2 30% solution in THF RT, overnight.

Reductive degradation of PG_5SSPG_5

Due to their polyester backbone, polylactides degrade under hydrolytic conditions and the resulting reduction in molecular weight is expected to accelerate the release of bound nucleic acids. However, amorphous polylactides degrade in the body on the timescale of days and months for crystalline polylactides. Disulfide bonds are labile under the reductive environment of the cell, mainly due to glutathione and thioredoxin,[67, 185, 188, 203] and inserting disulfide moieties in a polylactide backbone should accelerate the polymer degradation rate, *in vitro* or *in vivo*.

Since the degradation kinetics will depend on the functional groups added to the parent PGSSPG polymer, we focused on the degradation of PGSSPG. We used dithiothreitol (DTT),[203] which is commonly used in lieu of glutathione or thioredoxin, common thiols found in cells. The reductive degradation of PGSSPG was performed using four molar equivalents of DTT in d^6-DMSO at 37°C, (PGSSPG is insoluble in water), and tracked by ^{1}H NMR. However, it was difficult to track the degradation of PG-SS-PG due to a great signal overlap. We used PLLA-SS-PLLA to avoid signal overlapping **(Figure 31).** We treated PLLA-SS-PLLA under identical reductive degradation conditions. Using PLLA-SS-PLLA instead of PG-SS-PG facilitated the tracking of degradation products.

The ^{1}H NMR spectra of PLLA-SS-PLLA show minimal overlap of the signals, and the signals were assigned by comparison to spectra of the pure materials in d^6-DMSO.

We used a generic ^{1}H NMR arrayed experiment of 120 sets each with 16 transients taking 2.4 minutes per transient. Through this arrayed experiment, we found that the intensity of the signal from the methylene adjacent to the disulfide bond, centered at 3.0 ppm, decreased with the reaction time, while a new signal assigned to the methylene adjacent to the thiol group from the product (2.74 ppm) increased in intensity with reaction time. The reaction was evident by the first spectrum acquired in the experiment, indicating that the reaction proceeds immediately. The peak intensities can be correlated to conversion of starting material to product. The two signals correlated proportionally to appear and disappear respectively by 1.4 hours **(Figure 32)**. This time range is comparable to the previous degradation experiment using PG-SS-PG being under two hours.

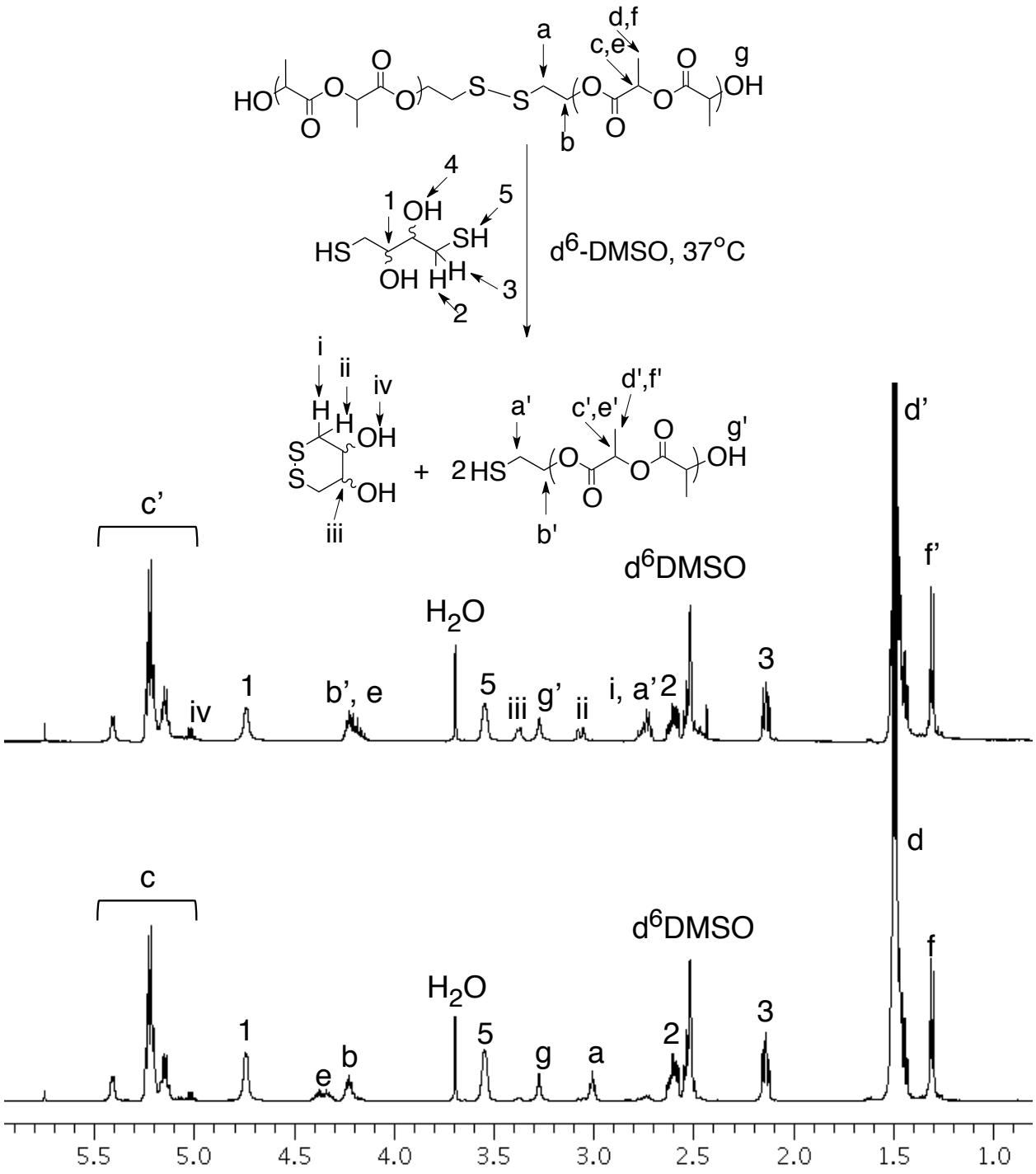

Figure 31 Reductive degradation of PLLA-SS-PLLA in the presence of DTT. Initial ^{1}H NMR after adding DTT to PLLA-SS-PLLA (bottom). Final ^{1}H NMR after 1.4 hrs of reaction at 37°C in d^{6}-DMSO (top). The inset is the reaction scheme for the degradation reaction.

The NMR experiment was performed in DMSO; this does not correlate accurately with what would happen physiologically. The reaction mechanism for this reduction requires proton exchange events. The reaction may be affected by the absence of water. The DMSO used in the experiment contained a small amount of water still making proton exchange possible.

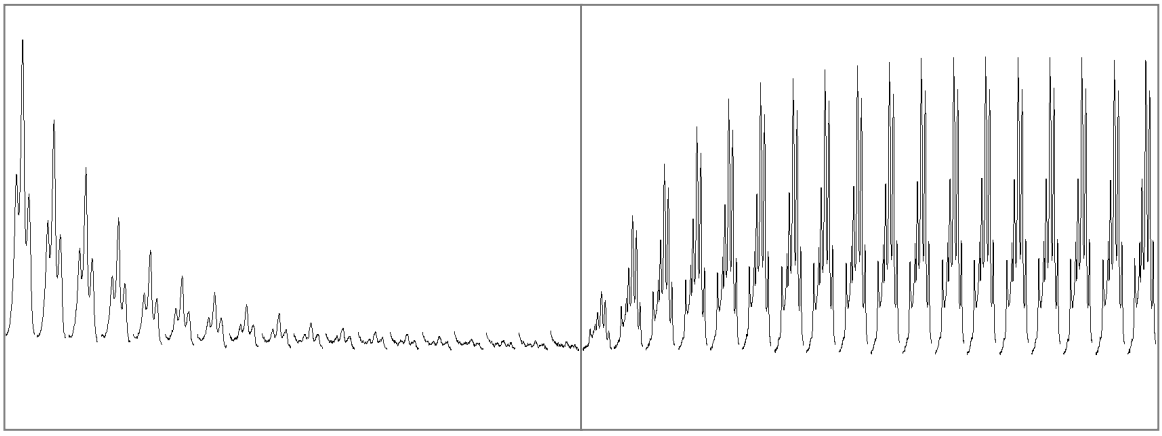

Figure 32 ^{1}H NMR peak signals from the reductive degradation of PLLA-SS-PLLA by DTT exchange in d^{6}-DMSO at 37°C. The peak intensity of the proton signal at 3.0 ppm decreased (left) and peak intensity of the signal at 2.74 ppm increased (right).

Clicked PG_5SSPG_5

A polymer-based vehicle for delivering DNA or siRNA requires charged groups to bind nucleic acids, solubility in aqueous environments, cell transfection, and DNA or siRNA release. The reaction of azides with pendant alkynes in PG_5SSPG_5, "click chemistry", provides a rapid and facile route to modify polymers with such characteristics **(Scheme 16).** Generally, click reaction conditions are mild, quantitative, and tolerant to a broad range of functional groups, enabling the synthesis of many

compositions from a single polymer. While many azides could be used for modifying PG_5SSPG_5, the three azides shown in **Figure 33** are the focus of this study. A12 has both a primary and a secondary amine, separated by three methylenes, to promote strong binding to nucleic acids at physiological pH. C1EO4 provides solubility in aqueous solutions and shields the hydrophobic backbone of PG_5SSPG_5, and Chol(S) has been suggested to increase aid transfection efficiency.[65, 204]

Using the click reaction, PG_5SSPG_5 was modified with one or more azides. The compositions of clicked polymers are denoted by the azide(s) used in the reaction, and the mole fraction of ligands appended to the polymer. For example, $PG_5SSPG_5[A12_{100}]$ indicates that all 20 sites on PG_5SSPG_5 were modified with the A12 azide. In reactions designed to add azides to a portion of the polymer, the azide was the limiting reagent and the conversion was monitored by ^1H NMR using the triazole proton signal and comparing it to the remainder alkyne protons.

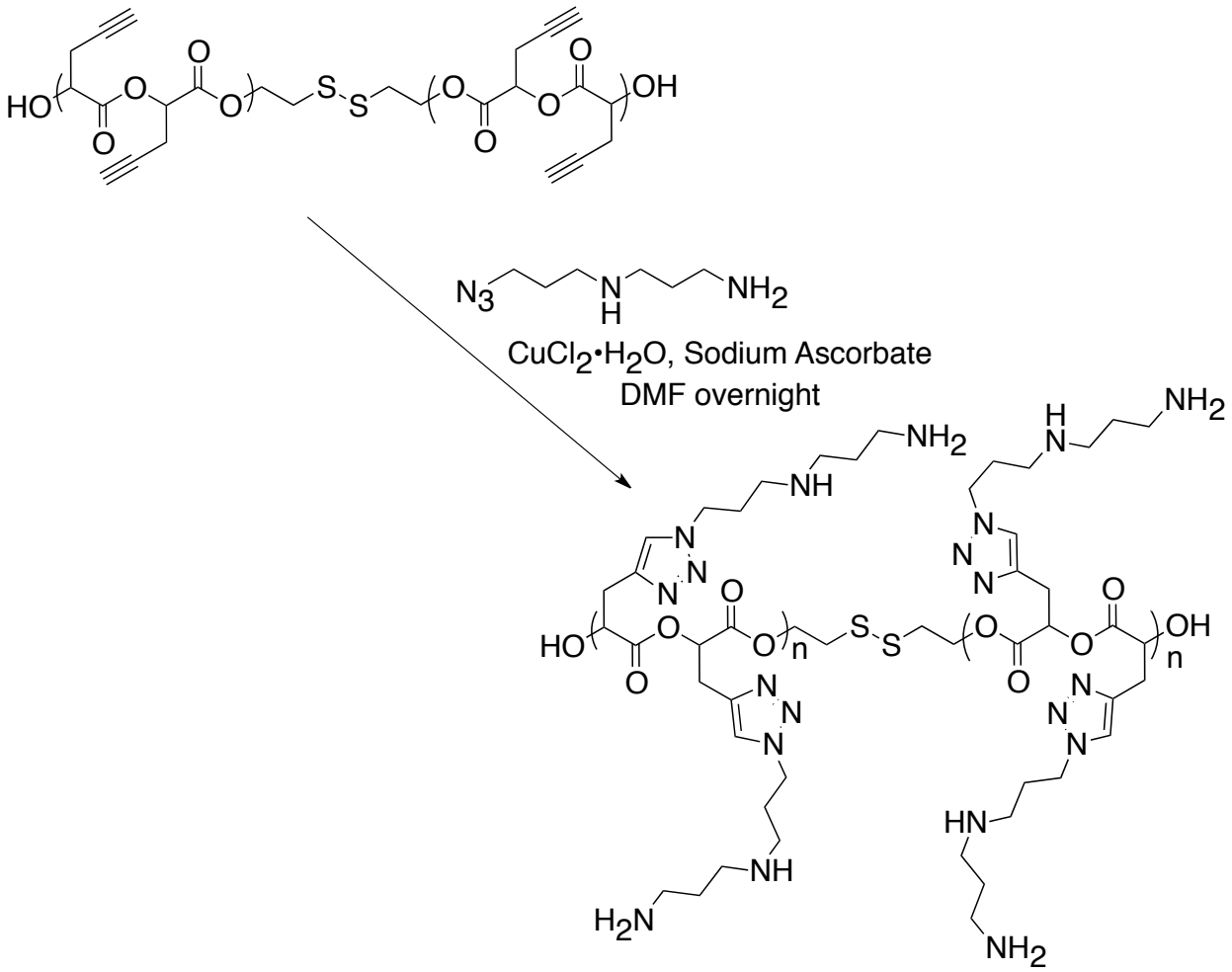

Scheme 16 Reaction of diamine ligand A12 and PG_5SSPG_5 via Cu(I) catalyzed click chemistry

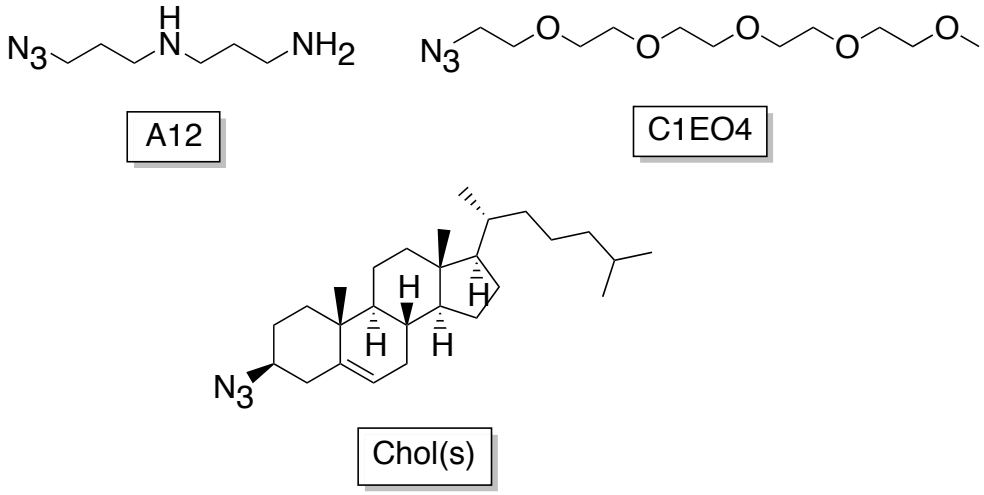

Figure 33 Azide ligands used to tune clicked polymer properties

Quantification of amines in polymers

The click reaction is normally assumed to be quantitative. However, in the case of two or more azides it's difficult to determine the ratio between the two. Quantifying the amino groups that are grafted to the polymer chain is important, in order to determine the necessary percentage of amines for binding to the nucleic acid and accurate N/P ratios. Methods have been developed for quantifying amines in proteins such as BSA (bovine serum albumin) [205-208] and these methods have been adapted to quantify amines in polymers and polymeric nanoparticles.[66, 209] Most methods rely on conjugation of a protein or polymer with a chromophore, followed by measuring the absorbance of the conjugate. Due to steric factors, TNBS (2,4,6-trinitrobenzensulfonic acid) only conjugates to free primary amines, and simplifies the assay for the A12 ligand. The TNBS assay is performed under mild basic conditions; pH 8.5 in sodium bicarbonate buffer at 37°C, and it can be adapted to a 96-well cell plate. We used free A12 as our standards and treated with TNBS, we generated a calibration curve for

determining the amount of amine ligand present in the polymer. The absorbance of the TNBS adducts were linear from 0 to 16 μL, and all polymer conjugates fell within the concentration range of the calibration curve. However, since the molecular weight for this polymer system is undetermined, it is difficult to determine the molar amine content with accuracy. We could however calculate the moles of amine per µg of polymer using the absorbance and the concentration of amine obtained from the slope of the calibration curve.

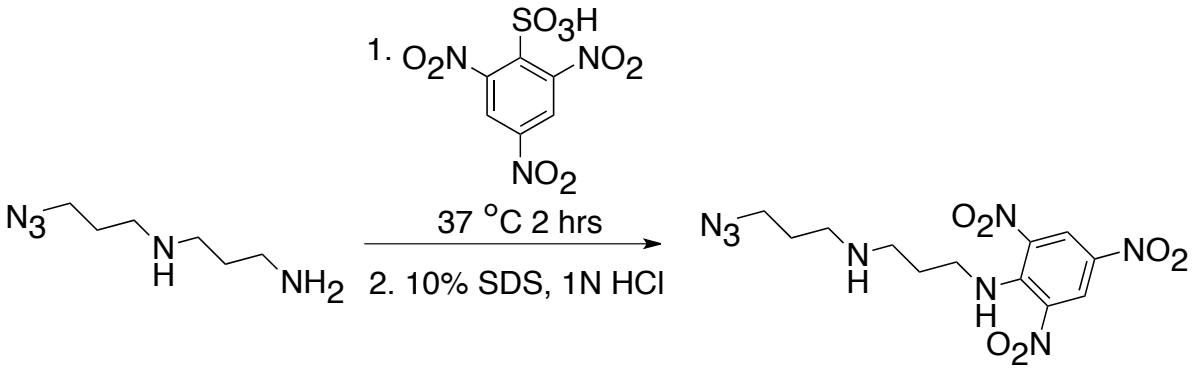

Scheme 17 Reaction of TNBS with the A12 ligand. TNBS only reacts with the primary amine in the ligand.

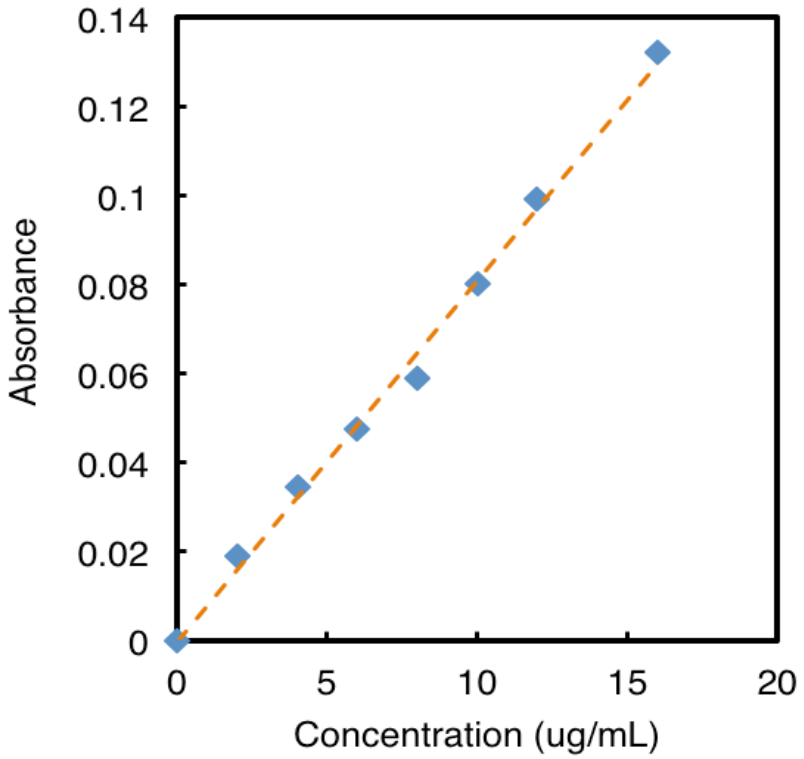

Figure 34 Calibration curve generated from A12 standards (0 to 16 µg/mL). Samples were treated with 0.1% TNBS, 1N HCl and 10% SDS incubated for 2 hours at 37 °C.

Table 8 TNBS amine quantification assay

Absorbance	µg/mL	Mol amine	Composition
0.020	2.48	$7.9x10^{-10}$	$PG_5SSPG_5[A12_{80}]$
0.068	8.36	$2.6x10^{-9}$	$PG_5SSPG_5[A12_{100}]$
0.016	1.95	$6.2x10^{-10}$	$PG_5SSPG_5[A12_{80}C1EO4_{15}Ch(S)_5]$
0.0039	0.50	$1.6x10^{-10}$	$PG_5SSPG_5[A12_{80}ChS_{20}]$
0.095	11.6	$3.7x10^{-9}$	$PG_5SSPG_5[A1_{50}]$

Treated with 0.1% TNBS, 1N HCl and 10% SDS was incubated for 2 hrs at 37 °C

Fluorescently tagged PGSSPG

Confocal microscopy was used to detect transfection of GFP mutant cells by the polymer vector and the gene knockdown efficiency. To determine whether the polymer delivered nucleic acids to the cell, siRNA tagged with a red fluorescent chromophore (Dy547-siRNA), and the polymer was tagged with a blue fluorescent chromophore **(Figure 35).** Blue fluorescent carbodiimide, 7-dimethylaminocoumarinacetic acid (DMACA) was coupled to the hydroxy termini of PG_5-SS-PG_5 **(Scheme 18)**. The polymer was dialyzed against ultra pure water (MilliQ) extensively to ensure that no free dye remained in the polymer. Afterward, the polymer was submitted to click conditions to append A12 diamine; the reaction was performed in the dark to avoid bleaching of the dye **(Figure 36)**. The dye concentration in the polymers was unchanged, 0.0172 M before click reaction and 0.0179 M after dialysis. (The DMACA concentration was calculated from the Beer-Lambert law, $A = \varepsilon cl$, using the known molar absorbance of DMACA (22,000) at l_{max} (394 nm).

We used confocal microscopy to track the blue fluorescent nanoparticles conjugated with red fluorescent Dy547-siRNA in green fluorescent cells **(Figure 37)**. We observed that the polyconjugates were internalized into the green fluorescent cells. After 24 hours, the cells were still fluorescing and healthy. We also observed a few healthy but non-fluorescent cells. This indicates that there was some silencing of GFP. However, the majority of the cells were still green and even though some silencing occurred, it was insignificant. This could mean that a higher concentration of siRNA needs to be delivered in order to obtain a significant silencing response.

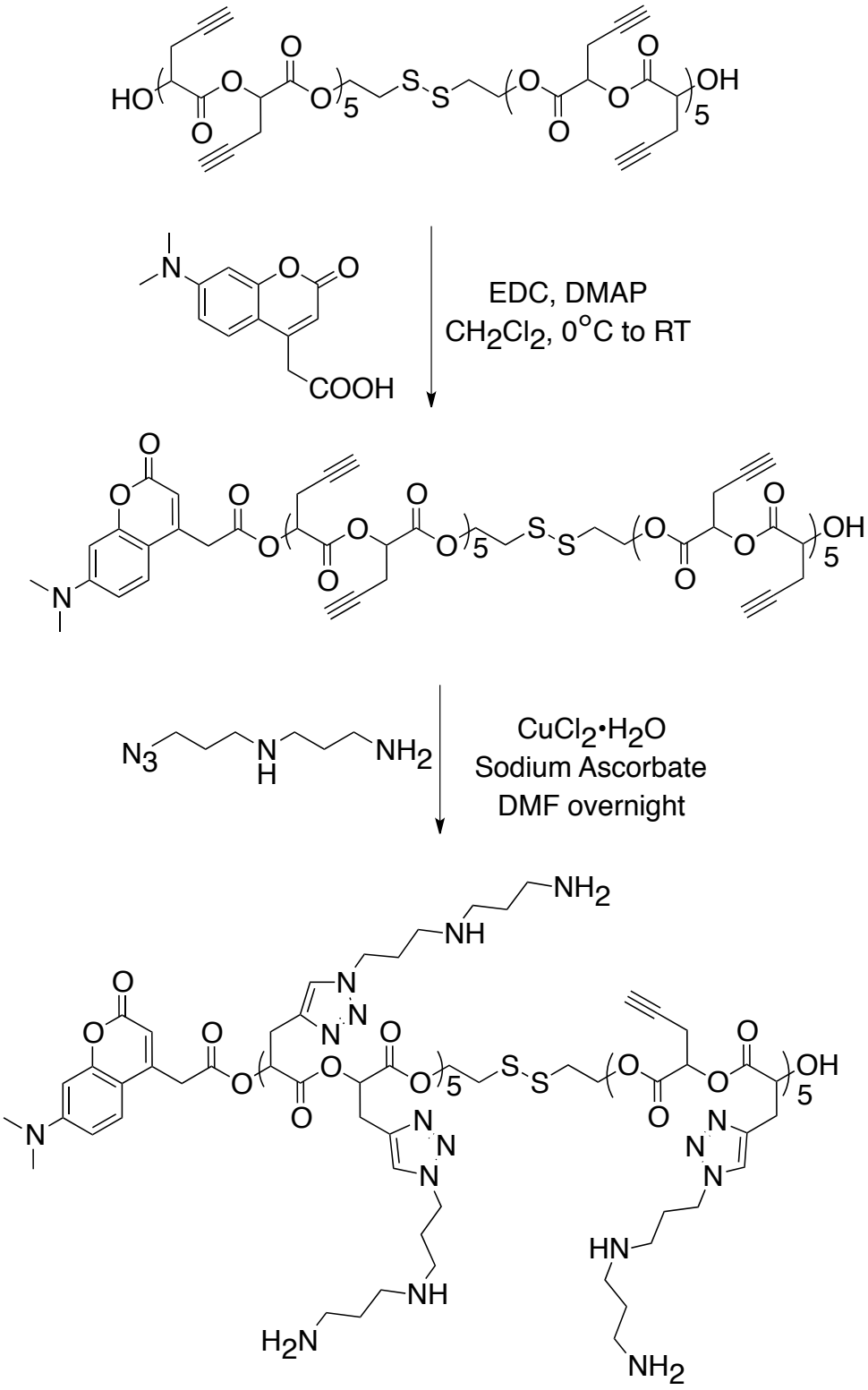

Scheme 18 Synthesis of polymers with blue fluorescence tags

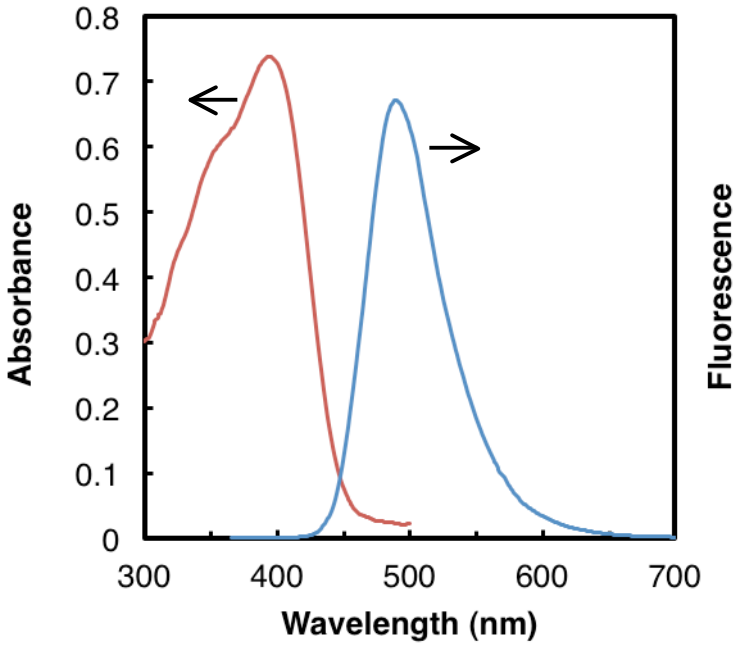

Figure 35 Absorbance and emission spectra of DMACA-tagged clicked polymers.

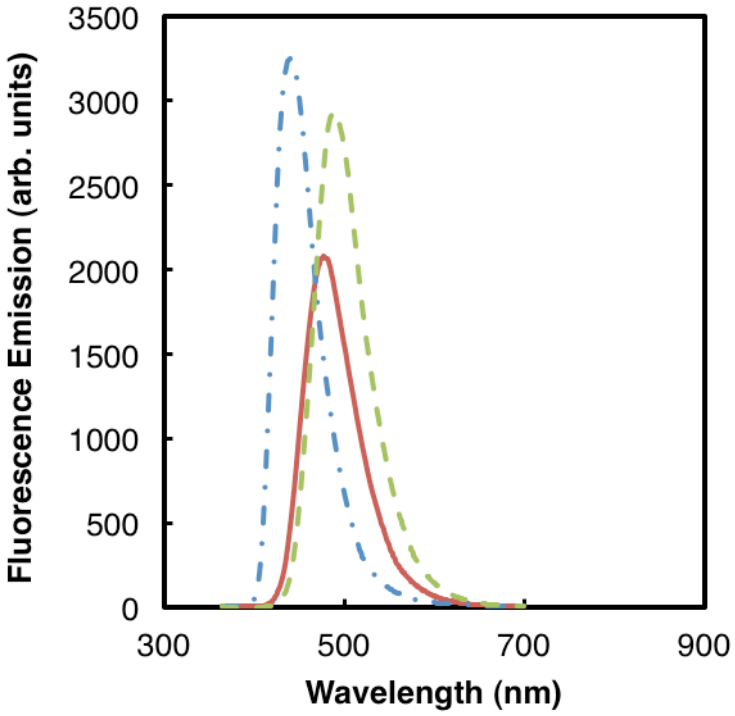

Figure 36 Fluorescence spectra excited at 360 nm of DMACA blue fluorescent PGSSPG before and after click reaction. Polymer before click (– · –) Polymer after click (– –) DMACA and amine ligand without polymer (——)

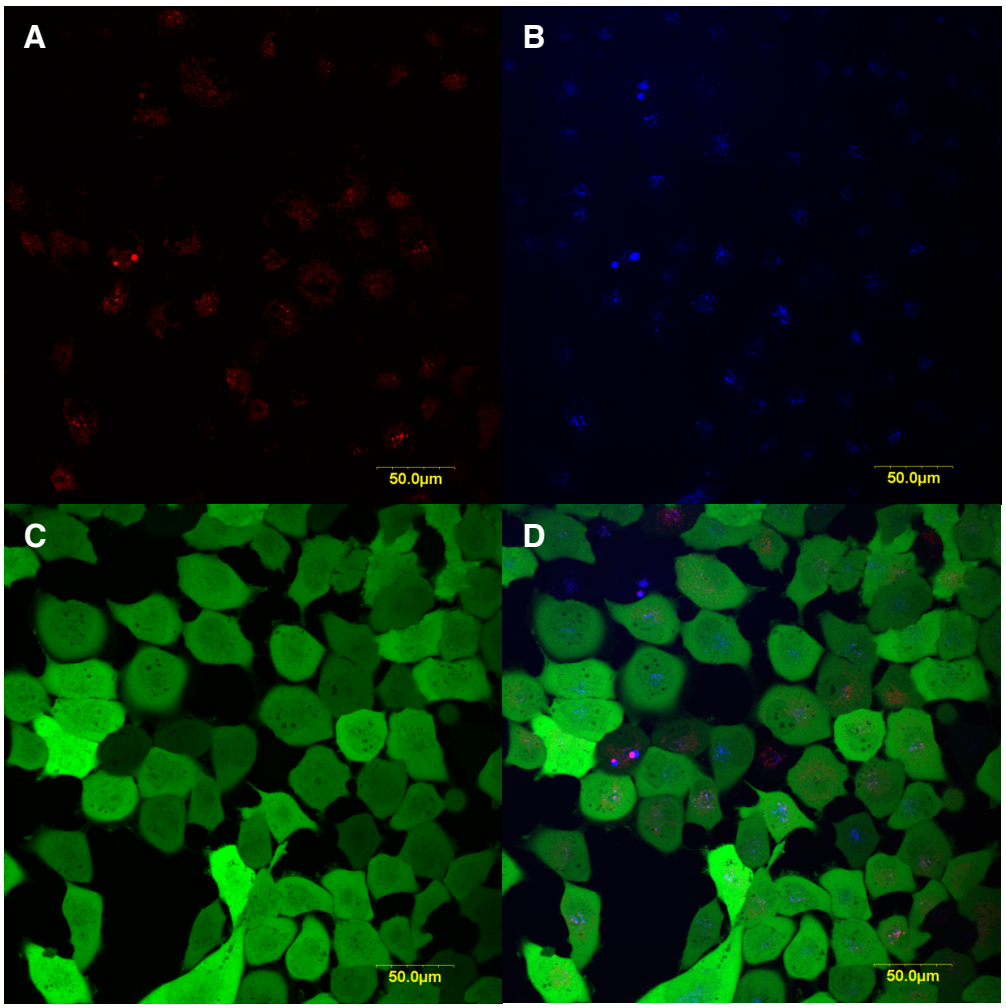

Figure 37 Confocal microscopy pictures of DMACA tagged nanoparticles in GFP cells. Red fluorescent siRNA (A), Blue nanoparticles (B), GFP cells (C) and overlay of previous three (D) 24hrs after transfection and 40X magnification

Polyconjugate Binding and Silencing of GFP

The binding capabilities of each polymer composition were evaluated using dsDNA (double stranded DNA). dsDNA and siRNA have comparable binding characteristics, but dsDNA is much less costly. Solutions of the polymer in MilliQ water were combined with 200 nM dsDNA, incubated for 15 minutes, and then resolved in 0.8% agarose gels. The gels were developed using SYBR gold nucleic acid dye, and the fluorescence intensities of unbound dsDNA were quantified from gel images and

normalized to the intensity of naked dsDNA (no polymer) signal. The data **(Figure 15)** were then fit to a modified Hill equation[210] using Origin and Excel software.

$$f = \frac{[NP]^n}{K_d{}^n + [NP]^n} \qquad \text{Hill equation}$$

In our modified version of the Hill equation we know the concentration of dsDNA and the concentration of nanoparticle [NP], and the fraction bound of the polymer to dsDNA (*f*) is calculated from the fluorescence measured after the binding gel is resolved and stained. The binding affinity, K_d, measures the extent of binding within a fixed time interval, and therefore, K_d is not a true equilibrium constant. K_d can also be defined as the polymer concentration needed to bind 50% of the nucleic acid. A low K_d value indicates rapid (and presumably more stable) binding and "n" is a binding cooperativity index; n=1 binding cooperativity exists. When a macromolecule has multiple binding sites, the binding at one site increases the binding affinity at a different site. If the binding of one site is lowered by another site, then there is negative cooperativity. Non-cooperative macromolecules have independent binding from site to site.[210-212]

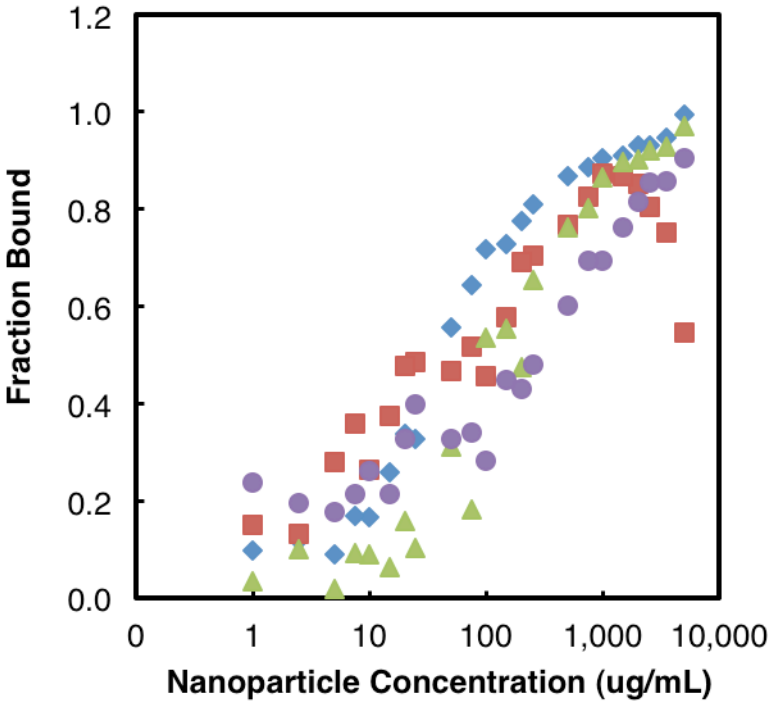

Figure 38 Binding of PG_5SSPG_5 clicked polymers to dsDNA. $PG_5SSPG_5[A12_{100}]$ ◆ $PG_5SSPG_5[A12_{80}]$DMACA ■ $PG_5SSPG_5[A12_{80}]$ ▲ $PG_5SSPG_5[A12_{80}Chol(S)_{20}]$DMACA ●

Binding affinities for four polymers are shown in **Table 9**. $PG_5SSPG_5[A12_{100}]$, with amine groups installed at each alkynyl group, had the lowest K_d which makes it the best binder. The blue fluorescent tag; DMACA interferes with the fluorescence signal used to measure the binding affinity, therefore, $PG_5SSPG_5[A12_{80}]$ was synthesized without DMACA so that the binding affinity can be calculated confidently, yet, the binding affinity still had a high error for the K_d value. $PG_5SSPG_5[A12_{80}]$ had a higher K_d than $PG_5SSPG_5[A12_{80}]$DMACA, this can be ignored since the fluorescent signal increases due to the DMACA and makes the binding appear to be lower.

Table 9 Binding affinity values for the clicked polymers

Polymer	K_d	n
$PG_5SSPG_5[A12_{100}]$	46 ± 2.7	0.88 ± 0.04
$PG_5SSPG_5[A12_{80}]$	151 ± 14.3	0.92 ± 0.07
$PG_5SSPG_5[A12_{80}]$DMACA	48 ± 6.3	0.48 ± 0.04
$PG_5SSPG_5[A12_{80}Chol(S)_{20}]$DMACA	1780 ± 436	0.4 ± 0.04

Samples were incubated for 15 min with 200 nM dsDNA. Gel images were quantified and normalized to naked dsDNA.

Using Dynamic Light Scattering (DLS) and Zeta potential measurements, we tried to complement the binding gel data. Dynamic light scattering helps us determine the size of particles in solution and zeta potential is a measurement of the charge on surface of the particles. siRNA is negatively charged and the particles range from slightly negatively charged to positively charged. The phospates in the siRNA backbone will bind electrostatically with the amines grafted to the PPGL. First, the zeta potential and size of 100nM siRNA was measured. Then, aliquots of nanoparticle solution were added **(Figure 39)**. The zeta potential and size were measured after every aliquot addition. From this titration experiment, we can obtain a curve that will allow us to calculate the point at where the siRNA and particles are at a N/P ratio of 1. At N/P=1 the particles are neutral this is important for transfection and release. Positive or negative particles are more difficult to transfect as has been shown in McCormick's work.[213]

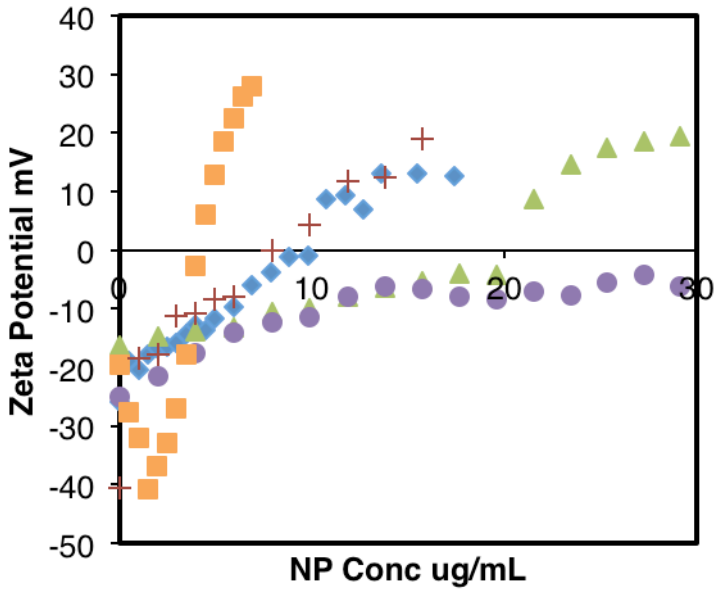

Figure 39 ζ Potential curves of siRNA titrated with aliquots of clicked polymers. $PG_5SSPG_5[A12_{100}]$ ◆, $PG_5SSPG_5[A12_{80}]$ ▲, $PG_5SSPG_5[A12_{80}Chol(S)_{20}]DMACA$ ●, Lipofectamine LF2K ■, LPEI +

The zeta potential data allows us to approximate amounts to where the N/P=1.0. **Table 10** summarizes the concentrations where the polyconjugates have a zeta potential as close to 0 mV as possible thus having neutral surface charge and N/P=1. All polymers presented a sigmoidal curve from negative to positive ζ with increasing polymer concentration. The only polymer that fell from this trend was $PG_5SSPG_5[A12_{80}Chol(S)_{20}]DMACA$, it is not understood as to why that was the case, however it can just mean that very high concentrations of polymer are needed to reach N/P=1. This particle contains cholesterol ligands, which may hinder the binding therefore needing a high concentration of polymer.

Table 10 Zeta potential and size for near neutral polyconjugates with siRNA

Polymer	Concentration (μg/mL)	ζ potential (mV)	R_h (nm)
$PG_5SSPG_5[A12_{100}]$	9.8	-0.987	23
$PG_5SSPG_5[A12_{80}]$	19.6	-4.1	52
$PG_5SSPG_5[A12_{80}Chol(S)_{20}]C$	27.2	-4.23	192
LPEI	7.9	0.05	111
Lipofectamine 2000 LF2K	3.9	-2.8	264

Measurements were done in MQ water in a Malvern NanoZS

With this data in mind, we attempted silencing experiments using the concentrations of nanoparticle necessary to neutralize the siRNA for $PG_5SSPG_5[A12_{100}]$. Unfortunately, our hypothesis was proven wrong. There was no silencing achieved using the small nanoparticle concentrations listed in table 5 **(Figure 40)**. For good measure, the silencing experiment was performed using a concentration range close to the neutral concentration.

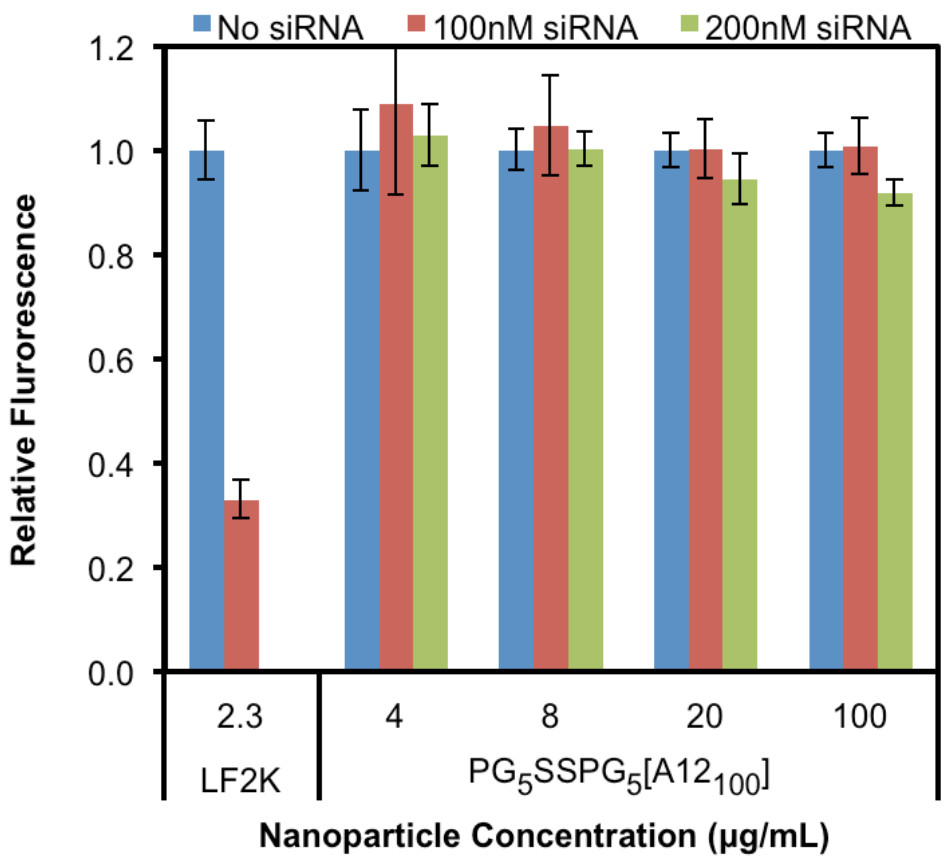

Figure 40 Quantification of silencing response of $PG_5SSPG_5[A12_{100}]$ in H1299 GFP cells. The polyconjugates were bound 30 min prior to treatment for 24 hours.

Conclusion

The synthesis of disulfide containing polymers was described. The polymers were further modified to contain a thiol end cap so the polymer chain can be extended by a condensation polymerization by oxidizing the thiol groups to disulfide linkages. PGSSPG was also modified via click chemistry with different azide ligands in order to obtain polymers suitable as nucleic acid delivery vectors. Unfortunately gene silencing hasn't yet been achieved satisfactorily and other alternatives ought to be explored. Also further characterization is in order, so better understanding of these polymers and their properties can be achieved.

Experimental

General All reagents were purchased from Aldrich or Alfa Aesar, and were ACS reagent grade. Chloroform was dried over phosphorous pentoxide, dichloromethane was dried over CaH_2 and THF was dried over sodium and benzophenone. DMAP was purified by sublimation at 35-40^{o}C. bis-(2-hydroxyethyl)disulfide was distilled under vacuum. All glassware was oven-dried.

Characterization Nuclear Magnetic Resonance (NMR) was performed in 500 MHz or 300 MHz Varian spectrometers. FTIR spectra were taken in a Mattson Galaxy series FTIR 3000. Absorbance for 96-well plates was measured in Molecular Devices SpectraMax M5^{e} plate reader with SoftMax Pro software.

Synthesis of poly(propargyl glycolide) with disulfide initiator (PGSSPG)[73] An oven dried Schlenk flask was charged with propargyl glycolide (PGL) and DMAP, the flask was evacuated for at least two hours, then bis-(2-hydroxyethyl)disulfide initiator solution (0.11M in $CHCl_3$) [M]/[I] 10:1 was added, the monomer concentration was adjusted to 0.5 M by adding dry chloroform. The reaction mixture was degassed by 3 freeze-pump-thaw cycles, then backfilled with nitrogen gas. The flask was immersed in an oil bath at 60 ^{o}C and was stirred for 12 hrs. After polymerization, the solvent was removed and the white stringy solid was redissolved in THF and dialyzed against THF/Water 3:1 in a 1000 MWCO cellulose membrane. The polymer was then dried under vacuum. ^{1}H NMR

($CDCl_3$): δ5.47-5.35 (br, 8H) 5.26-5.22 (br, 1H) 4.52-4.36 (m, 3H) 3.04-2.84 (br m, 20H) 2.83-2.72 (m, 2H) 2.12-2.03 (br, 10H)

Synthesis of thiol terminated PPGL (HSPGSSPGSH) In a 20 ml vial PGSSPG (0.14 g) was dissolved in anhydrous dichloromethane, DMAP (2.7 mg) and EDC (42 mg) were added to the polymer, the mixture was purged with N_2. In a round bottom flask, 3-mercaptopropionic acid (23 mg) was added and dissolved with 10 ml dichloromethane; it was purged with N_2 and cooled to 0 ^{o}C. The polymer mixture was added via syringe slowly. The mixture was stirred at 0 ^{o}C for 2hrs and the warmed up to room temperature and stirred overnight. The reaction mixture was washed twice with 0.5M HCl and twice with saturated $NaHCO_3$. It was dried over $MgSO_4$. The solvent was removed the material was redissolved in THF and dialyzed against THF:water 3:1 in a 1000 MWCO dialysis tubing (See appendix for NMR).

Condensation of HSPG-SS-PGSH In a Schlenk flask (157 mg, 7.3 x 10^{-5}mol) of HSPGSSPGSH was dissolved in anhydrous THF and I_2 was added (55 mg, 0.2 mmol, 3 mol equiv.). The reaction mixture was saturated with oxygen for 1hr, then the mixture was stirred at room temperature overnight. The mixture was washed with 5% aqueous $Na_2S_2O_3$ to remove remaining iodine. The mixture was heated gently to separate the layers. The organic layer was dried over magnesium sulfate, filtered and solvent was removed. The polymer was redissolved in THF dialyzed against 1:1 THF/water mixture

with 5% $Na_2S_2O_3$ in a 3500 MWCO tubing. After dialysis the sample was dried under vacuum (See appendix for NMR).

Fluorescently tagged PGSSPG DMACA (0.11 mmol, 27 mg) was dissolved in 10 mL dichloromethane, was cooled to 0°C and purged with N_2. In a vial PGSSPG (0.11mmol) EDC (0.11mmol) and DMAP (10 mol %) were mixed and dissolved in 10 ml dichloromethane and purged with N_2. The polymer mixture was transferred slowly via syringe to the acid solution. It was allowed to stir at 0°C for two hours and then for 12 hrs at room temperature. The reaction mixture was washed with 0.5 M HCl twice then with saturated $NaHCO_3$ twice. It was dried over $MgSO_4$, filtered and solvent was removed under reduced pressure. The tagged polymer was dialyzed against THF/H_2O 3:1 in 1000 MWCO tubing for one day in the dark. The sample was dried under vacuum (See appendix for NMR).

Synthesis of 1-azido-3-aminopropane[181] 3-chloropropyl-1-amine hydrochloride (10 g, 77 mmol) and sodium azide (7.5 g, 115 mmol) were added in a round bottom flask and dissolved in 65 ml of deionized water. The mixture was stirred under nitrogen at 80°C overnight. After reaction, the mixture was concentrated and cooled to 0°C. To the cooled mixture, diethyl ether (50ml) and KOH were added (6g) and stirred until dissolved. The reaction mixture was extracted with diethyl ether, dried over $MgSO_4$, solvent was removed under reduced pressure. The product was purified by vacuum

bulb-to-bulb transfer, a clear liquid with ammonia odor was obtained (75% yield). ^{1}H NMR ($CDCl_3$, 300 MHz) δ: 3.25 (t, 2H, *J*= 6.83 Hz), 2.67 (t, 2H, *J*= 6.83 Hz), 1.60 (t, 2H,), 1.24 (br, 2H) ^{13}C NMR ($CDCl_3$, 75 MHz) δ: 48.35, 39.03, 32.15

Synthesis of N-(3-bromopropyl)-1,3-diaminopropane dihydrochloride[181] 1-azido-3-aminopropane (4.2 g, 42 mmol) was treated with 63 ml of 1M HCl in diethyl ether. The mixture was allowed to stir and then the solvent was removed and dried under vacuum. The hydrochloride salt was dissolved in anhydrous dichloromethane and purged with nitrogen. In a Schlenk flask, triethyl silane (6.9g, 59 mmol) and allyl bromide (7 g, 59 mmol) were degassed by 3 cycles of freeze-pump-thaw. Concurrently, a 3-neck round bottom flask fitted with an addition funnel, nitrogen inlet and rubber septum was purged with nitrogen and then cooled to -78°C. Boron trichloride (6.9 g, 59 mmol, 59 mL, 1M solution in dichloromethane) was added via cannula. The triethyl silane and allyl bromide solution was transferred to the BCl_3 solution via cannula and allowed to stir for 5 minutes to make the dichloroborane in situ. The newly formed dichloroborane was added via cannula to the hydrochloride salt solution. Nitrogen gas evolved almost immediately. The reaction mixture was stirred at room temperature for 9-12 hrs. Then it was quenched with 20 mL of methanol and stirred for 15 min, after a white precipitate was formed, 150 mL of diethyl ether were added. The white precipitate was filtered and washed with aliquots of diethyl ether (75% yield). ^{1}H NMR (D_2O, 500 MHz) δ: 3.41 (t, 2H), 3.11 (t, 2H), 3.04 (t, 2H), 2.97 (t, 2H), 2.16-2.10 (m, 2H), 2.0-1.92 (m, 2H)

Synthesis of N-(3-azidopropyl)-1,3-diaminopropane[181] N-(3-bromopropyl)-1,3-diaminopropane dihydrochloride (8.5 g, 31.7 mmol) and sodium azide (8.45 g, 130 mmol) were dissolved in 85 ml of deionized water. The reaction mixture was allowed to stir under nitrogen at 80°C overnight. The mixture was cooled to 0°C and Sodium hydroxide (4 g, 100 mmol) was added. After all sodium hydroxide was dissolved, the water was removed almost completely; the mixture was suspended in dichloromethane and triturated. The solid was filtered out and washed with aliquots of dichloromethane. The solution was dried over $MgSO_4$, and the solvent removed under removed pressure. The liquid was vacuum distilled (b.p. 72°C 128 mtorr) (60% yield). ^{1}H NMR ($CDCl_3$, 300 MHz) δ: 3.35-3.25 (t, 2H), 2.74-2.68 (t, 2H), 2.67-2.58 (dd, 4H), 1.76-1.64 (pent, 2H), 1.62-1.51 (pent, 2H), 1.15 (br, 3H)

Cholesteryl Iodide (R) Modified procedure from Posner et al[214] ^{1}H NMR ($CDCl_3$) 5.31 (t, 1H), 4.02 (m, 1H), 2.91 (t, 1H), 2.69-2.60 (dq, 1H) 2.32-1.03 (m, 24H), 1.02 (s, 3H), 0.97 (m, 2H), 0.89 (d, 3H), 0.84 (dd, 6H), 0.65 (s, 3H).

Cholesteryl Azide (S) Cholesteryl iodide (1.03 g, 2 mmol) were combined with sodium azide (0.65 g, 4 mmol) and dissolved in 10 ml DMF. The reaction mixture was stirred at 80°C overnight. The solvent was removed under high vacuum. The solid was redissolved in diethyl ether and washed with water, sodium metabisulfite ($Na_2S_2O_3$) and NaCl. The organic layer was dried over $MgSO_4$. The solid was recrystallized from absolute ethanol (60 % yield). ^{1}H NMR (CDCl3) δ: 5.38 (t, 1H), 3.86 (t, 1H), 2.54-2.45

(m, 1H), 2.21-2.13 (1H), 2.04-2.02 (2H), 1.86-1.02 (24H), 0.99 (s, 3H), 0.90 (d, 3H), 0.85 (dd, 6H), 0.66 (s, 3H) ^{13}C NMR ($CDCl_3$) 138.08, 123.17, 58.28, 56.7, 56.1, 49.9, 42.3, 39.7, 39.5, 37.1, 36.2, 36.0, 35.8, 33.6, 31.82, 31.79, 28.2, 28.0, 26.1, 24.26, 23.8, 22.8, 22.5, 20.7, 18.9, 18.7, 11.8 FTIR 2080 cm^{-1} (N_3)

Standard click chemistry procedure A Schlenk flask was loaded with 40-60 mg of polymer, with the desired mol % of azide ligand according to moles of alkyne in the polymer, 24 mol% of sodium ascorbate and the mixture was dissolved in DMF. The mixture was degassed by 3-4 freeze-pump-thaw cycles and backfilled with nitrogen gas. A 0.1 M solution of $CuCl_2 \cdot 2H_2O$ (8 mol %) in DMF was added after degassing. The reaction mixture was stirred at room temperature overnight. After reaction, the mixture was filtered and the solids removed. Amberlite IRC-748 ion exchange resin beads were added to the filtrate to remove copper, the mixture was aged for 8 hours. After gravity filtration of the beads, DMF was removed in vacuo. The polymer film was dissolved in 3:1 water/acetone and was dialyzed in a 12- 14 kDa MWCO dialysis bag for 2-3 days. After dialysis solvents were removed under vacuum.

TNBS assay for quantification of amines was adapted to a 96-well plate. 50 µl of polymer 200 µg/ml in 0.1M $NaHCO_3$ buffer pH 8.5 was loaded into a well and 25 µl of freshly prepared 0.1% TNBS in $NaHCO_3$ buffer were loaded and mixed in a shaker for 3 minutes. The plate was incubated for 2 hours at 37 ^{o}C. After incubation 25 µl of 10% SDS and 25 µl of 1N HCl were added to each treated well and blanks, the plates was

mixed in shaker again followed by immediate measurement. Standard solutions of A12 were prepared from 2-16 μg/ml in $NaHCO_3$ buffer. The absorbance was measured at 335 nm.

siRNA titration using ζ potential A Malvern zetasizer NanoZS was used for all titration experiments. A 100 nM solution of siRNA was added to a disposable cuvette and the dipcell was fixed. The ζ potential and hydrodynamic radiuses were measured. 5 μL of 1mg/ml polymer solution in milliQ water were added to the cuvette and mixed. After each aliquot addition of polymer solution the ζ potential and hydrodynamic radius were measured. The titration was stopped once the curve seemed to plateau. A plot of polymer concentration vs. ζ potential was generated using Microsoft Excel.

Chapter 5: Functionalized Silica Nanoparticles for siRNA Delivery

Introduction

Delivery of siRNA still remains a challenge for effective and safe therapeutic goals. Delivery vehicles are divided into two main categories; viral vehicles and non-viral vehicles. Non-viral vehicles like liposomes and cationic polymers are amongst the most widely used. Recently, inorganic nanoparticles have started to be explored as gene vectors. Mesoporous silica has properties that would make it advantageous for delivering large molecules; they have large surface area, tunable pore sizes, high loading, and an easily modifiable surface.[215, 216] It has also been suggested that mesoporous silica is biocompatible and bioresorbable.[217] Mesoporous silica nanoparticles (MSNs) can deliver siRNA successfully.[215, 216, 218-224] The surface of silica is unable to bind nucleic acids since both are negatively charged. Therefore, the modification of silica nanoparticles (SiNPs) surface is necessary to allow nucleic acid binding. Soo-Won Seo[225] and Hongchen Gu[215, 221] modified the surface of SiNPs with PEI to bind siRNA. PDMAEMA was used to modify MSNs by Oupicky.[218]

Cationized dextran was used as an siRNA delivery vehicle. Frechet modified dextran with spermine[226] and De Smedt copolymerized a dextran functionalized methacrylate and an amine containing methacrylate.[227] Crosslinked Dextran-PEI composites were made by Gupta.[228] Dextran, the homopolymer of glucose was used because of its biocompatibility, biodegradability and its FDA approval.[229, 230] Huang

used dextran stabilized magnetic iron nanoparticles, the dextran was amine functionalized to introduce hyaluronic acid moieties.[231] The amino dextran functionalized nanoparticles were tested for binding and silencing efficiency in our lab. They were successful delivery vehicles; we also tested commercially available amino functionalized iron nanoparticles, which in turn did not show any silencing efficiency. This result led us to believe that dextran aided the silencing response.

This chapter pertains to the synthesis of silica nanoparticles functionalized with dextran and amine groups and their use as siRNA delivery vehicles. We attempted to silence Human lung carcinoma cells that expressed EGFP.

Results and Discussion

Synthesis of dextran containing silica nanoparticles

We synthesized dextran functionalized silica nanoparticles (SiNPs) by condensing tetraethoxy silane under basic conditions using a method similar to Stöber's.[232] Dextran was suspended in solution during the condensation, thus encapsulating dextran within the silica matrix. In order to introduce amine groups we capped the silica surface using 3-aminopropyltriethoxysilane (APTES).

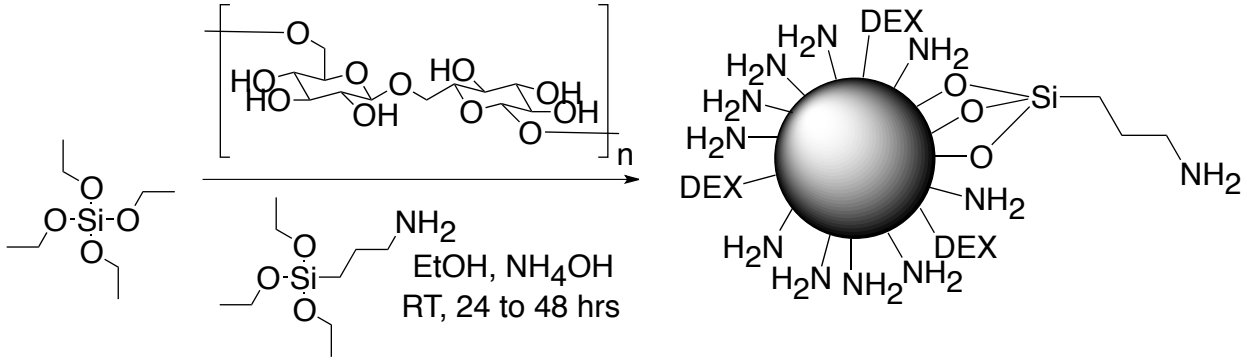

Scheme 19 Synthesis of silica nanoparticles containing dextran and amino groups.

Stöber's method calls for alcoholic solvents, we used ethanol in our experiments. However, dextran is a water-soluble polymer and it does not dissolve well in alcoholic solvents. Therefore, dextran was added to the reaction dissolved in a small amount of water. In our initial experiments, dextran was dissolved in 5 mL of water to 150 mL of ethanol. Right away the dextran seemed to precipitate. In order to circumvent dextran precipitation, we added greater amounts of water 60 and 90 mL into the same amount to ethanol (150 mL).

Using the mentioned amounts of water, dextran was apparently completely dissolved. However, the concentration of TEOS was changed. The different reaction methods **(Table 11)** also resulted in different particle morphologies as shown in TEM **(Figure 41)**. All samples presented large particles ~ 250 nm in diameter. The sample made with 5 mL of water contained globular silica, the samples made with 60 mL of water presented 100 nm silica particles and the samples made with 90 mL of water had particles ~20 nm in diameter which were the major component. The materials made using 60 mL of water were the most active silencers, thus this method was explored in more depth.

Table 11 Differences between nanoparticle synthesis methods.

	Method α	**Method β**	**Method γ**
Ethanol vol. (mL)	150	150	150
Water vol. (mL)	5	60	90
NH_4OH vol. (mL)	10	10	10
[TEOS] (M)	0.06	0.01	0.0096
APTES addn. (min)	30	10	15

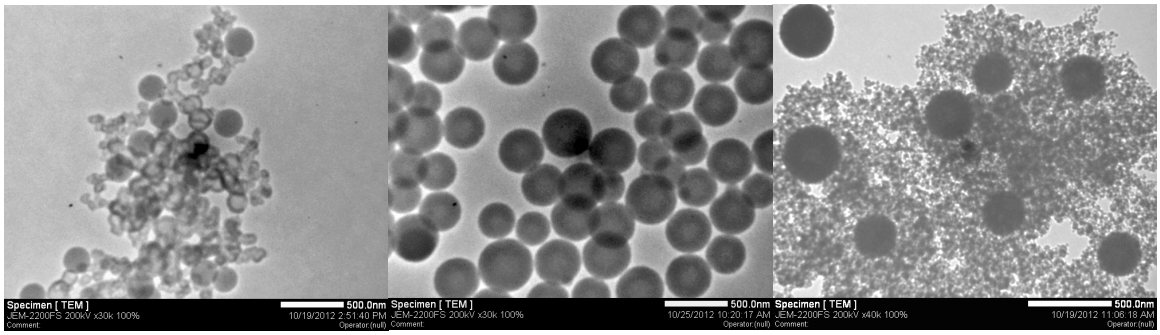

Figure 41 Dextran containing SiNPs obtained with different water contents 5 mL (left), 60 mL (middle) and 90 mL (right) (Scale bar 500 nm).

We synthesized nanoparticles with varying amounts of amine content in the presence or absence of a constant amount of dextran (0.1 mol %). We used 0.5-99% mole percent of APTES relative to TEOS. The SiNPs containing dextran presented a bimodal distribution **(Figure 42)**. Independently of amine content, the particles had the same size for both distributions in different frequencies. The SiNPs with 40% APTES were mostly monomodal with the presence of 100 nm particles almost null. There was no apparent trend on the frequency of 100 nm particles throughout the samples. We placed APTES under the same reaction conditions in the absence of TEOS and dextran **(Figure 43)**. The resulting materials were 100 nm particles. With the previous experiment we verified that the 100 nm particles in the dextran containing SINPs were formed by self-condensation of APTES. Others have tried to control nanoparticle size and distribution by using longer chain alkoxy groups (i.e. pentyl, butyl),[232] the nature of the alcoholic solvent,[232, 233] and the rate of addition of the tetraethoxy silane.[234] In our case, the appearance of the second population of particles could be due to slight changes in the rate of APTES addition. Faster addition of APTES would cause faster

reaction with itself slower addition would most likely reduce the amount of the second population.

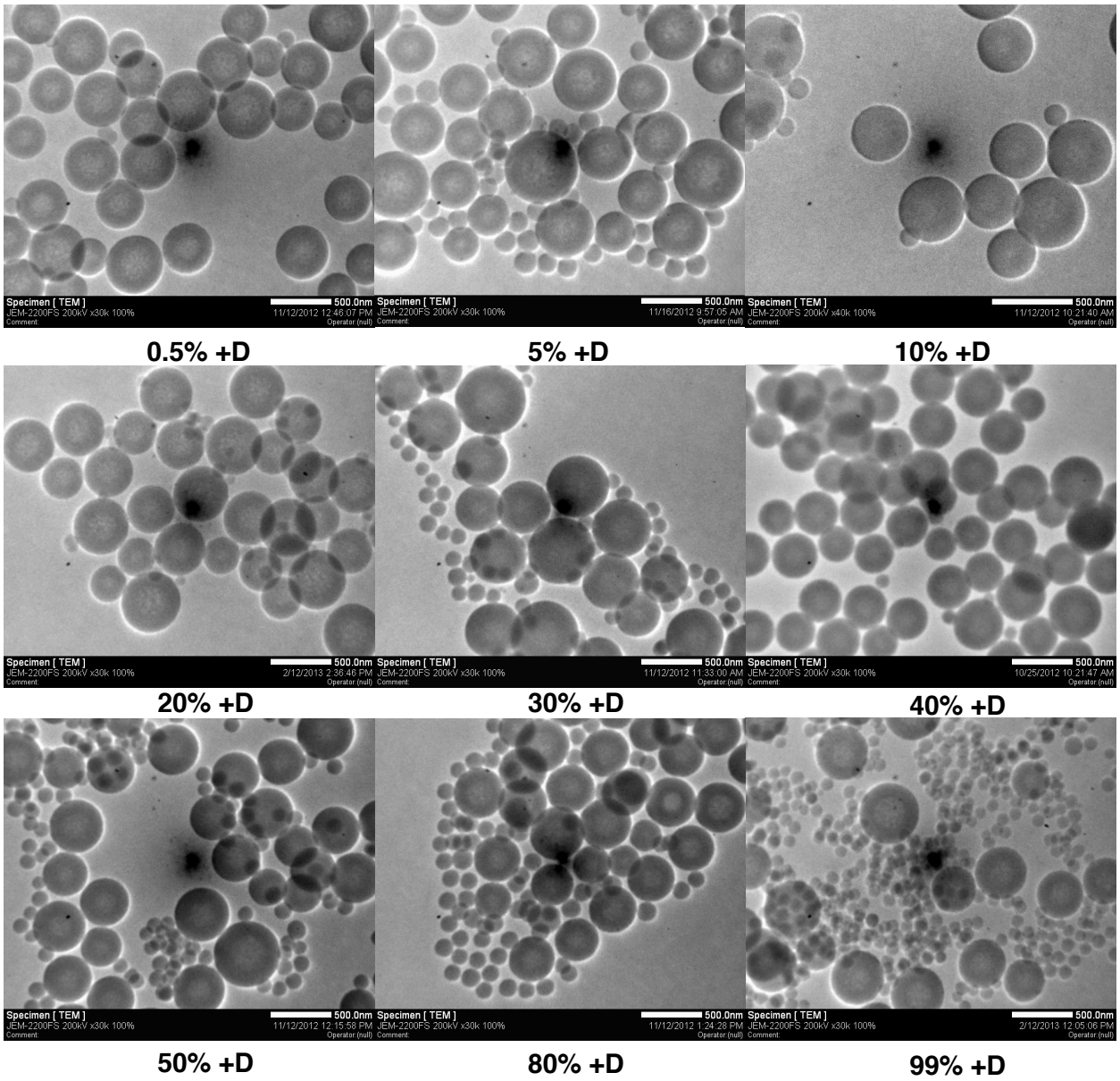

Figure 42 Transmission electron micrographs of dextran containing silica nanoparticles. The percentage refers to APTES content and +D refers to dextran. Scale bar is 500 nm.

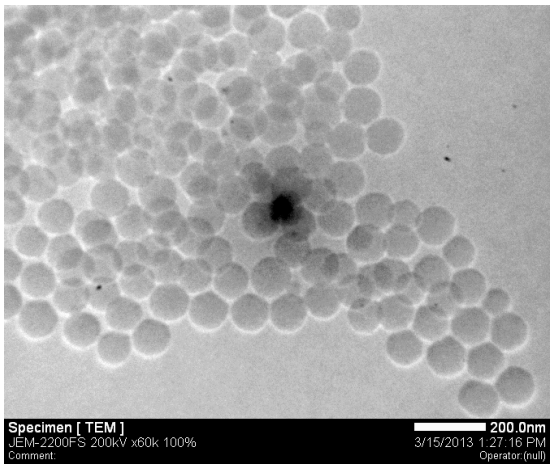

Figure 43 Silicon nanoparticles made by self-condensation of APTES (scale bar 200 nm).

We synthesized SiNPs without dextran using 0.5-99 mole percent of APTES relative to TEOS. **(Figure 44)** All the nanoparticles were bellow 100 nm but in a broad distribution 20-100 nm. Again throughout the series there was no significant difference in the particle size with increasing APTES content. This indicates that under our reaction conditions the mole percentage of the capping organosilane does not affect particle size.

The particles were tested for zeta potential in two different media, MQ water and HEPES buffer pH 7.4 **(Figure 45)**. A general trend was apparent for both types of nanoparticles. Except for the 0.5% amine all SiNPs had positive zeta potential and it increased with increasing APTES content. The zeta potential of the –D SiNPs was higher than the zeta potential of the +D SiNPs in HEPES. This can be explained due to the size distribution of the particles. The smaller size of –D SiNPs would bear more charge density on the surface assuming the same amount of grafting. The zeta potential in HEPES buffer was higher than in MQ water which is counter intuitive given that the pH of MQ water is more acidic (pH=6). One would assume that all the amines are

protonated at pH 6, and the particles would have higher repulsion. HEPES is zwitterionic buffer has a great buffering capacity which could lower the amount of protonated amines.

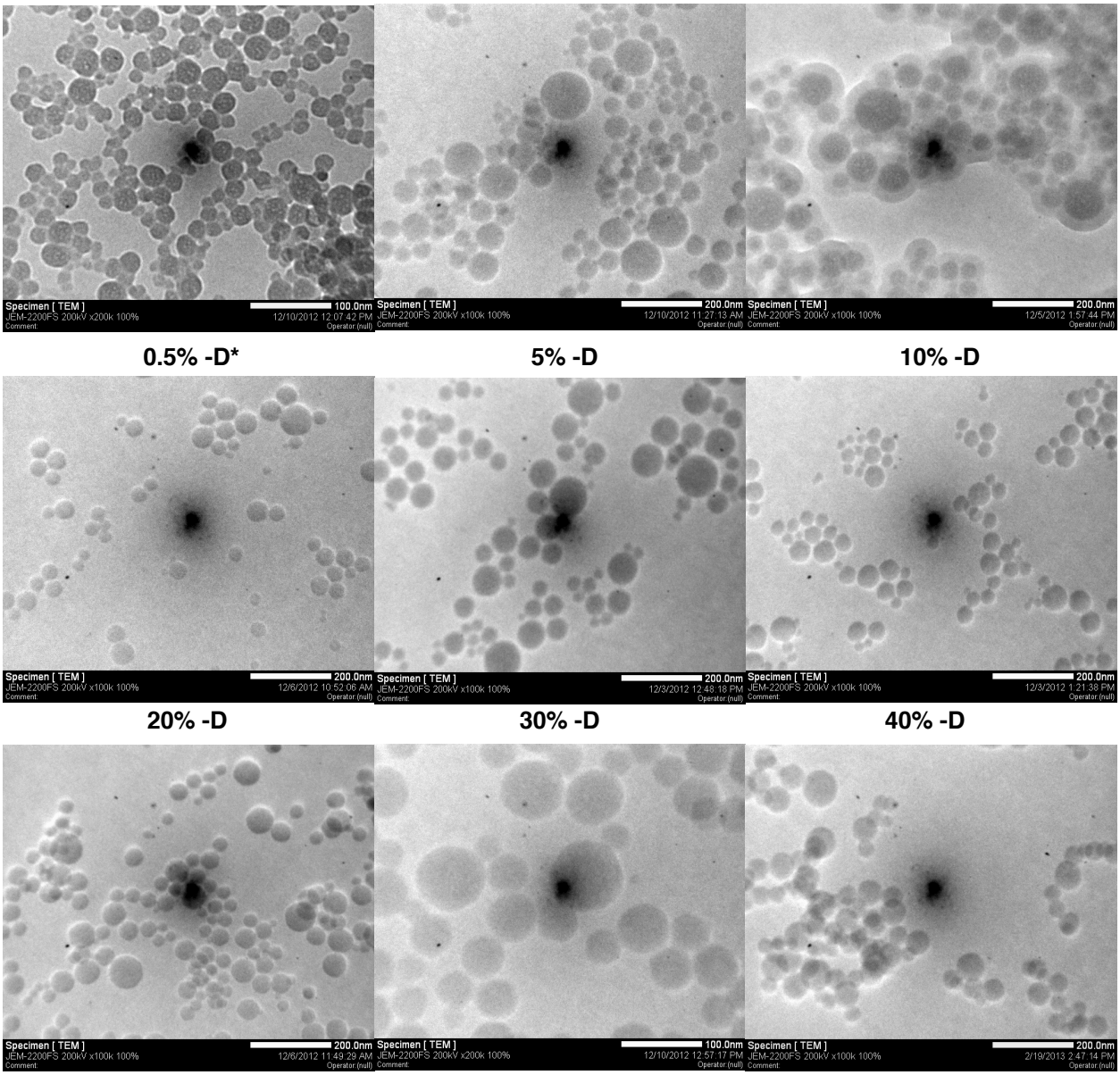

Figure 44 Transmission electron micrographs of no dextran containing silica nanoparticles. The percentage refers to APTES content and -D refers to dextran. Scale bar is 200 nm, *100nm.

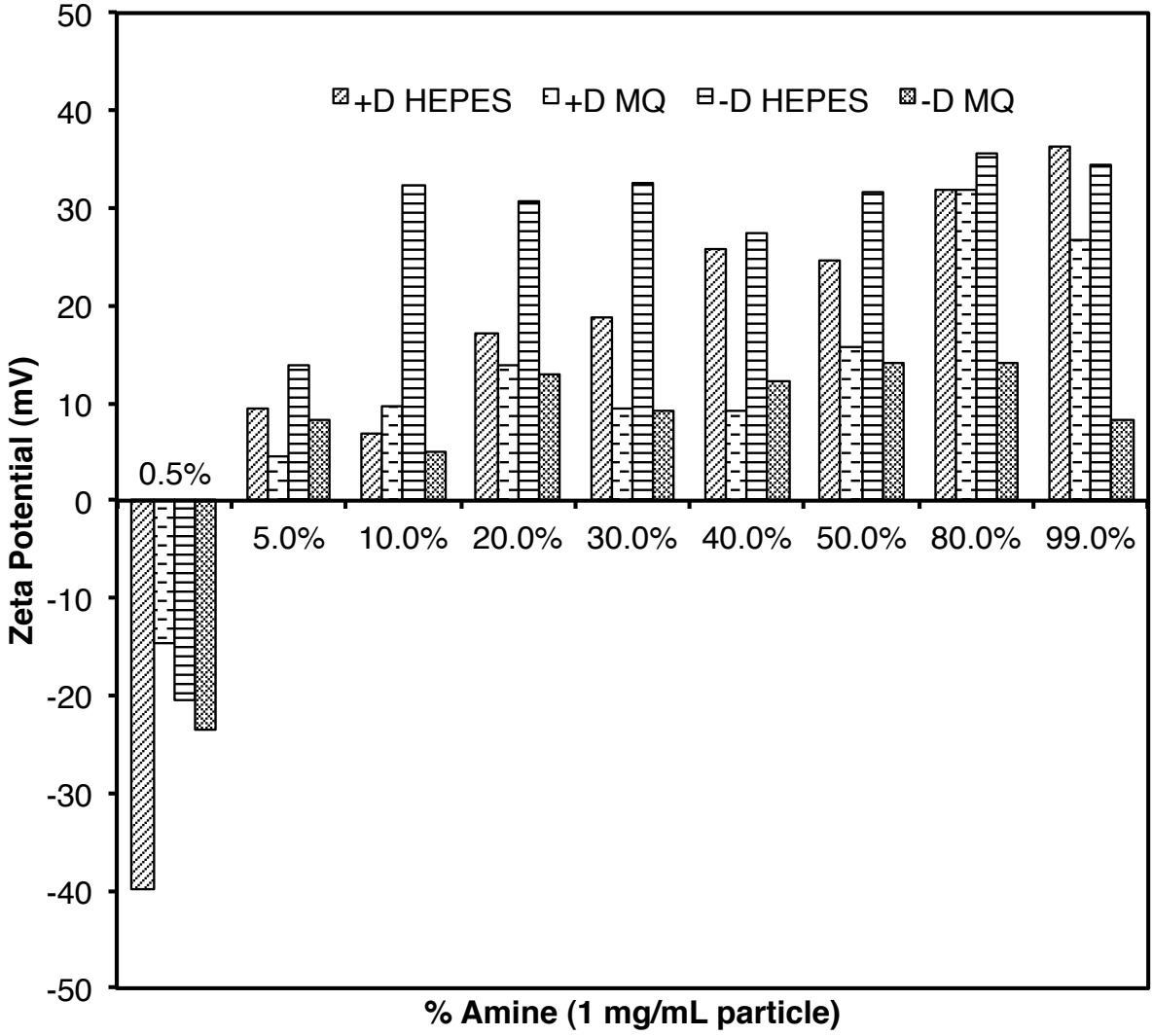

Figure 45 Zeta potential of amine modified silica nanoparticles in HEPES buffer pH 7.4 and in MQ water pH 6.

We used thermogravimetric analysis to determine the amount of grafting **(Figure 46)**. Even after drying overnight under vacuum the particles still contained a high percentage of water but it can be subtracted from the total mass after maintaining the sample isothermal at 120 ^{o}C for 30 minutes. There was no trend from TGA, we also cannot discriminate the weight loss from APTES and dextran.

Since the SiNPs presented bimodal distribution quantifying the grafting of amines on the surface of the particle is difficult. We also attempted to perform a TNBS assay using propyl amine as our standard since the use of APTES starts reacting during the assay. We can calculate the moles of amine per μg of particles but to calculate the moles of amine per particle we need the surface area of the particle and we calculated using the diameter average from TEM but this is strongly biased due to the two particle populations.

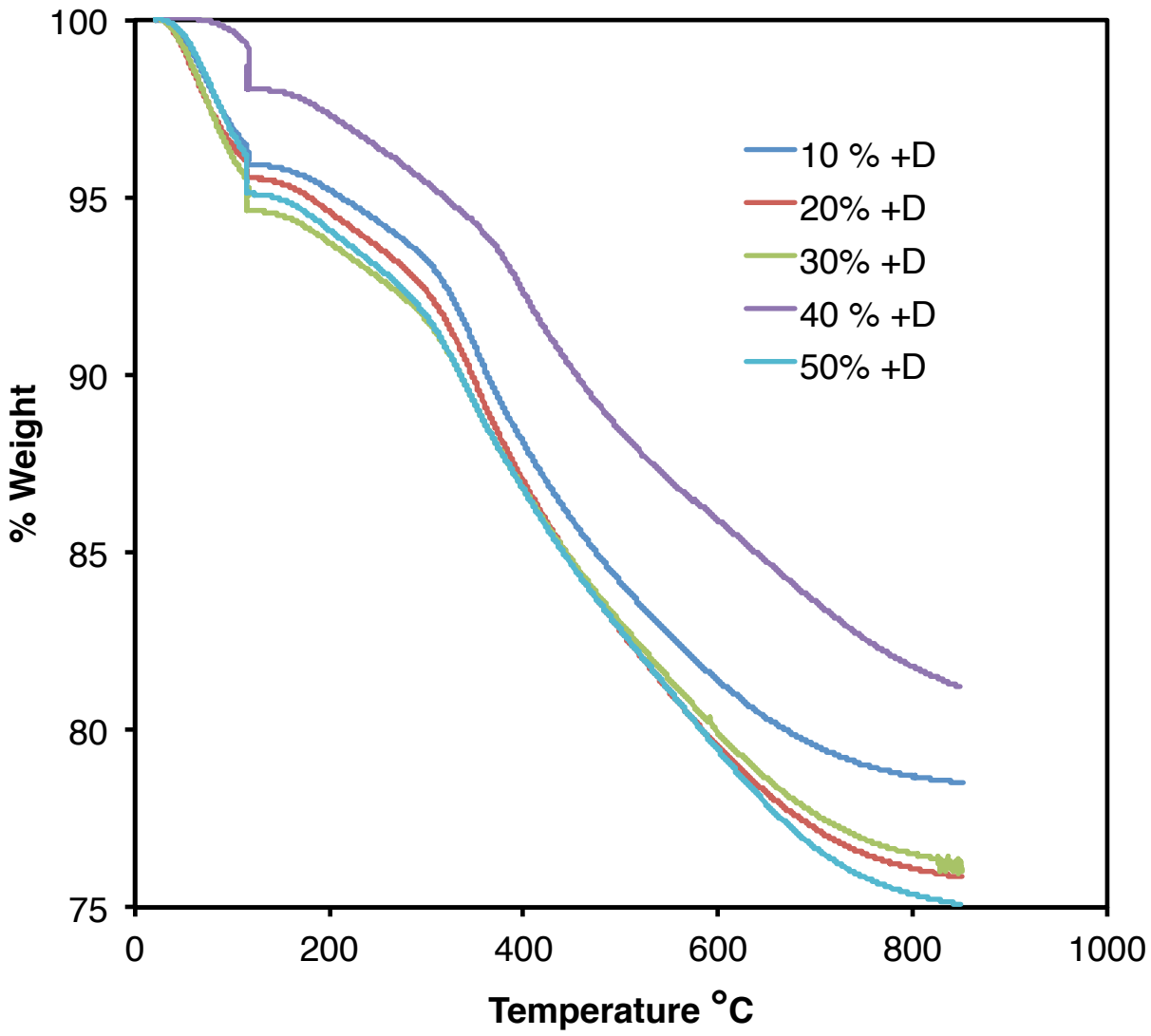

Figure 46 TGA traces of +D SiNPs.

The SiNPs contain a very small percentage of dextran, but more important than the quantification is the location of dextran within the particle it's its location. Dextran is a non-specific carbohydrate, so it cannot be quantified by assays like ELISA. The amount of dextran used is so small that using a phenol-sulfuric acid assay is inefficient and it requires large samples. We adapted a tissue staining protocol that stains carbohydrates specifically to stain samples of +D SiNPs on TEM grids. The protocol

involves digestion of the carbohydrates with periodic acid then treating it with silver nitrate and hexamethylene tetramine (methenamine). The treatment with periodic acid exposes aldehydes that are then oxidized by the silver nitrate precipitating silver crystals. **Figure 47** shows 40% +D SiNPs before and after treatment with the silver staining. Before treatment, the SiNPs have a smooth surface and after treatment the particles have a rougher granular surface that is attributed to the silver crystals. TEM permits us to use energy dispersive spectroscopy to identify the elements in the sample. The granules on the surface of the particle were confirmed to be silver.

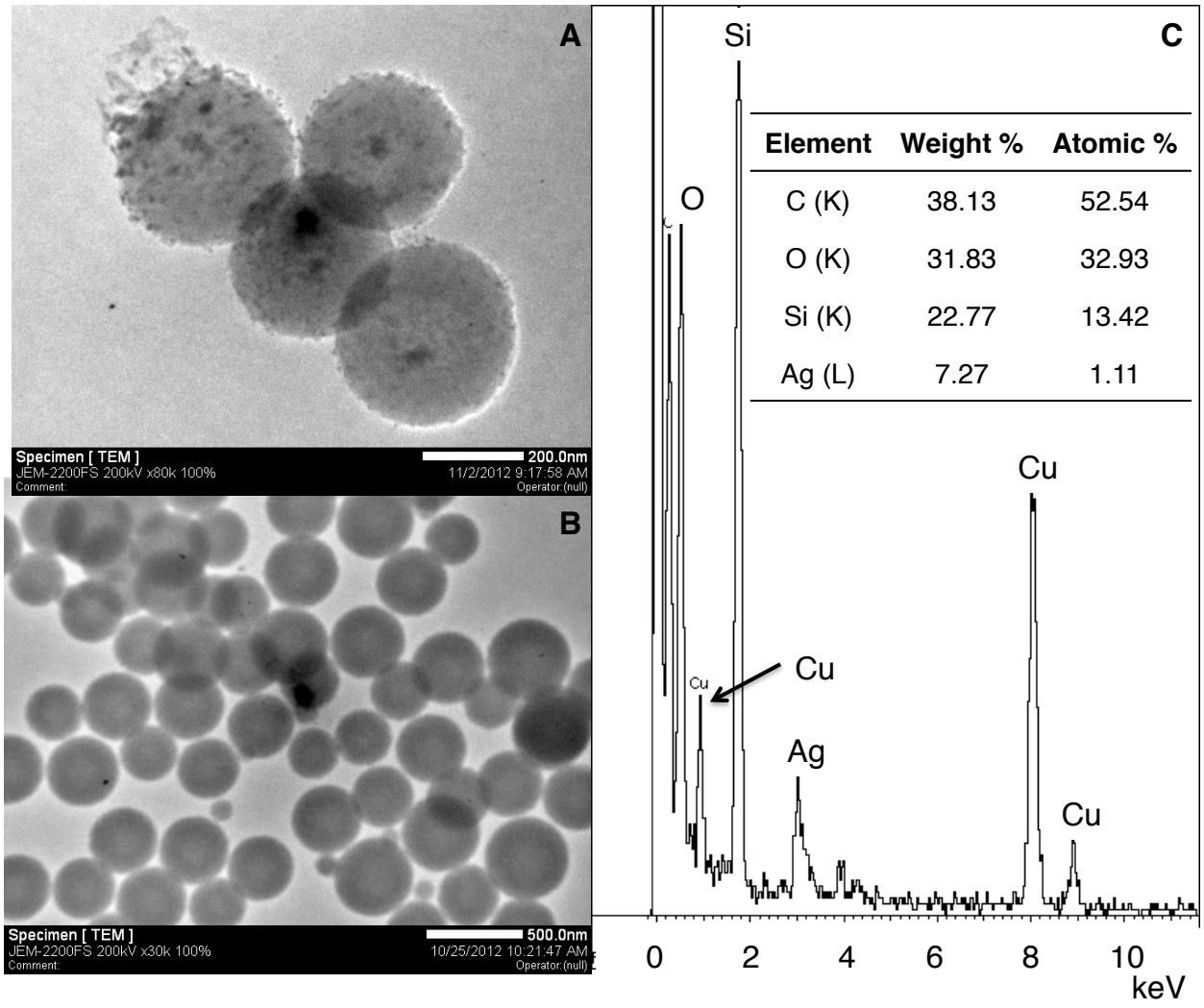

Figure 47 Localization of Dextran on the particle surface. 40% +D SiNP stained with silver methenamine (A) 40% + D SiNP without contrast staining (B) EDS plot of silver stained particles, elemental analysis inset table (Cu energy lines are derived from the copper TEM grid) (C)

Silencing efficacy of dextran containing silica nanoparticles

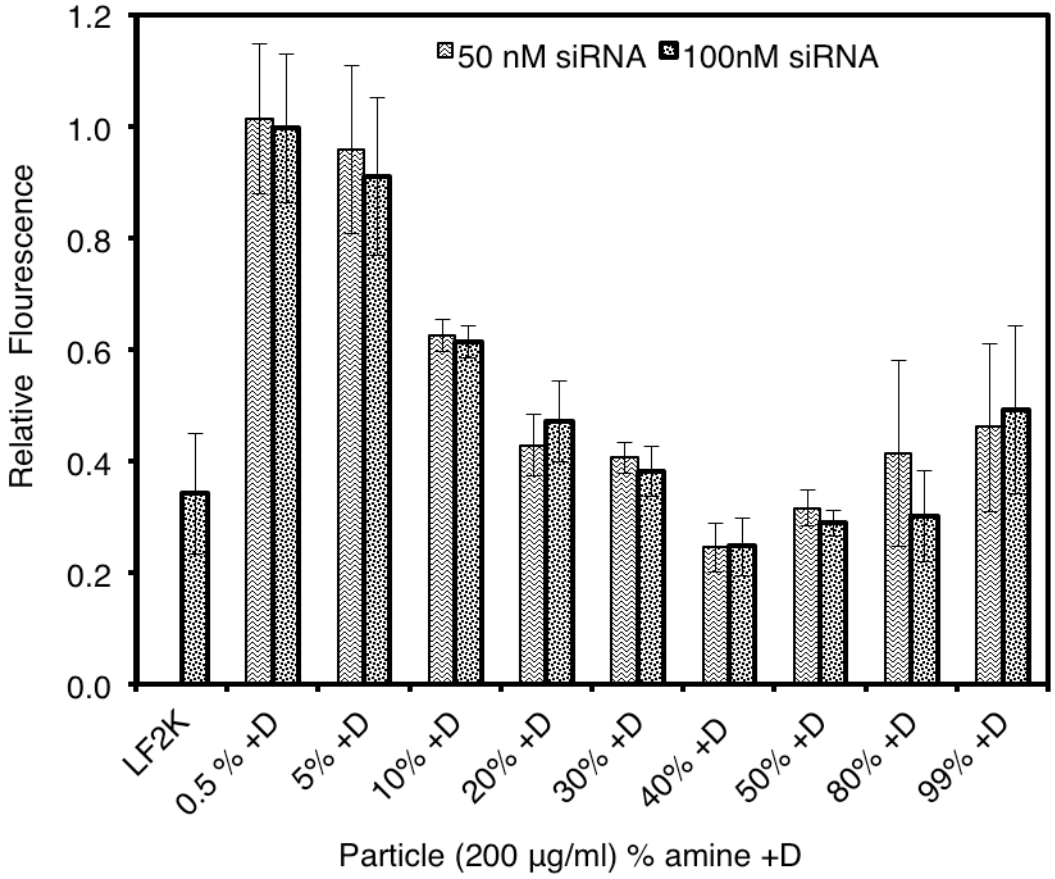

Figure 48 Silencing response of EGFP on H1299 cells after 24 hours of treatment with dextran containing (+D) silica nanoparticles with increasing mole percentages of amine (APTES). Normalized to particle only no siRNA cells.

We tested the silencing efficiency of our SiNPs using human lung carcinoma cell line H1299. This cell line expresses EGFP and we targeted this protein to obtain a visual response. The absence of green fluorescence indicates successful delivery and transfection of the targeting siRNA. The lowest content of APTES was 0.5% and at low amine concentration, there is no silencing response. The +D SiNPs start silencing EGFP at 10% APTES content. The best silencing efficiency was obtained by 40% APTES +D SiNPs with ~70-80% efficiency, which is comparable to the silencing efficacy

of Lipofectamine **(Figure 48)**. However, the +D SiNPs did not show signs of toxicity as lipofectamine does. The –D SiNPs did not show silencing efficacy but also did not show signs of toxicity **(Figure 49)**. There are two factors that may be involved in the efficacy of these delivery vehicles. One of them is size and the other one is the presence of dextran. +D SiNPs are significantly larger than the –D SiNPs. Larger nanoparticle size can bind to higher amounts of siRNA thereby making it possible to bind and deliver large amounts of siRNA into the cells. Also, containing dextran would facilitate passing of the SiNPs through the cell membrane.

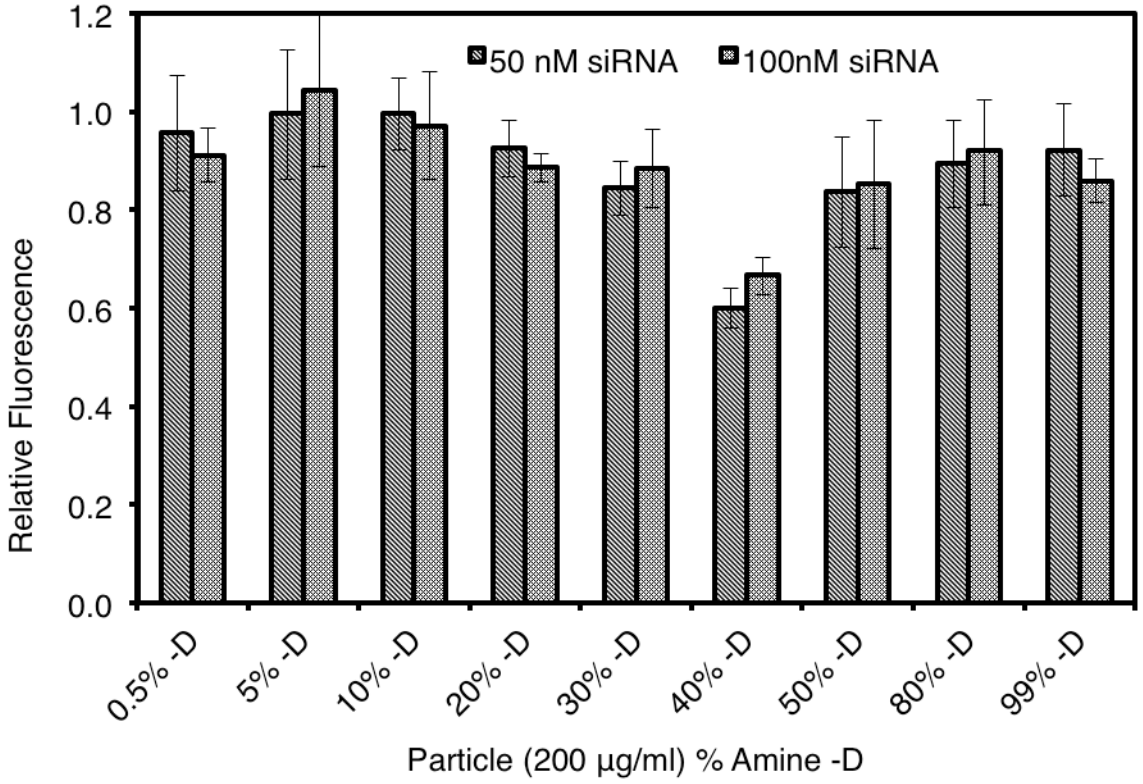

Figure 49 Silencing response of EGFP on H1299 cells after 24 hours of treatment with no dextran containing (-D) silica nanoparticles with increasing mole percentages of amine (APTES). Normalized to particle only no siRNA cells.

The bimodal distribution of the +D SiNPs begs the question on what is the fraction responsible for silencing. As mentioned before, we placed APTES under the same reaction conditions in the absence of TEOS and dextran. We confirmed that the 100 nm particles present in the +D SiNPs samples were the product of APTES self condensation. We tested this sample for silencing response and the result was negative. The 40% +D SiNPs were composed of mostly monomodal particles of 250-300 nm in diameter. This was as of yet our best silencer that lack a high population of the smaller particles. This suggests that the fraction responsible for silencing were the larger particles in the sample. We also imaged the particles inside the cells and we discovered that only the large particles are internalized and remain within the cell cytoplasm **(Figure 50)**. At this point we are unsure if the 100 nm particles are internalized at all or they are just secreted by the cells faster than the timeframe for imaging. We used the same imaging for the –D SiNPs as well and we did not find any particles insides the cell cytoplasm.

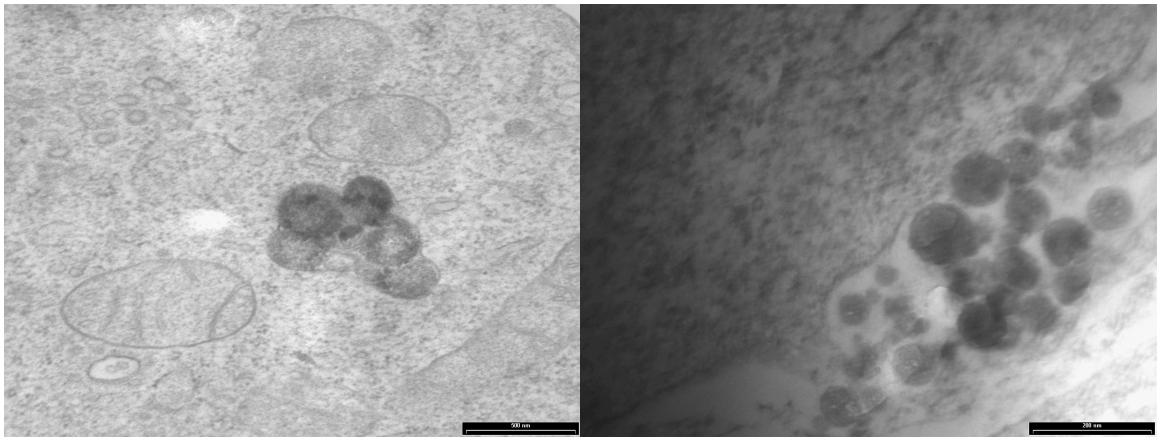

Figure 50 TEM of internalized 50 % +D SiNPs in HeLa cells (Left, scale bar 500 nm) 50 % -D SiNPs outlining the cell membrane but none found in the cell cytoplasm (Right, Scale bar 200 nm).

Although it has been suggested that optimal delivery of siRNA is mostly done using delivery vehicles under 200 nm in size. We believe that using larger particles we can pack large amounts of siRNA on the surface and in the pores and even if only a few particles are internalized we reach a high concentration of siRNA sufficient to trigger a silencing response.

Conclusion

We developed a series of amine surface modified silica nanoparticles containing dextran and in the absence of dextran as our control. We modified the surface with amines so they can bind siRNA. SiNPs containing dextran were successful delivery vehicles of siRNA that lead to the silencing of EGFP in human lung carcinoma cells. In the absence of dextran the SiNPs were unsuccessful delivery agents. We learned that dextran is important for internalization of the delivery vehicle and its cargo. However, dextran SiNPs in the absence of amines would not be able to trigger a silencing response. We have to control the size distribution of the particles so we can obtain thoroughly characterized homogeneous materials. With a material of narrow distribution we could have a better understanding of the internalization mechanism.

Experimental

General All chemicals were purchased from Aldrich and used as received. MQ water was obtained from a Millipore Synergy UV water purification system, RNAase free water was purchased from Fisher Scientific. DLS and ζ potential were measured using a Malvern zetasizer NanoZS.

Hydrodynamic radius measurements by dynamic light scattering were performed using disposable UV cuvettes (Brandtech®). The nanoparticle stock sample of 500 µL was measured at the original concentration, and then it was diluted by two-fold and measured again. After every measurement the sample was diluted by two-fold until the concentration is close to 0.05 mg/mL at which time the size will also be stabilized. TEM (Transmission electron microscopy) was performed using a JEOL 2200FS 200 kV emission TEM on copper grids (300 mesh Carbon type B, Ted Pella Inc) Nickel grids (300 mesh carbon film only) were used for silver staining samples.

Synthesis of silicon oxide nanoparticles +/- dextran

Three different synthetic methods were employed for the synthesis of +/- dextran silicon oxide nanoparticles. The methods were denominated α, β and γ. **Table 1** shows the main differences between methods.

Method α A 500 mL round bottom Schlenk flask was charged with 150 mL of absolute ethanol. Dextran 9-11 KDa (0.01 mmol, 100 mg) was dissolved in 5mL of MQ water. Tetraethoxysilane (TEOS, 10 mmol, 2.2 mL) and dextran solution were added simultaneously dropwise via syringe. Following the addition of TEOS, 10mL of NH_4OH (~30% as NH_3) were added via syringe. The mixture was stirred at room temperature for 30 minutes under nitrogen. 3-aminopropyltriethoxysilane (APTES, 20% mol, 2 mmol, 0.46 mL) was added. The reaction mixture was stirred for 24 hours at room temperature under nitrogen atmosphere. The reaction mixture was purified by pressure filtration using a regenerated cellulose membrane (Millipore, 30 KDa MWCO, 47mm diameter) at

40 PSI rinsing with MQ water three times. The filtered solid were suspended in MQ water and sonicated until well dispersed.

Method β A 500 mL round bottom Schlenk flask was charged with 150 mL of absolute ethanol and 50 mL of MQ water. Dextran 9-11 KDa (2.4×10^{-6} mol, 24 mg) was dissolved in 10mL of MQ water and added, followed by 10mL of NH_4OH (~30% as NH_3). TEOS, (2.4 mmol, 0.53 mL) was added dropwise via syringe. The mixture was stirred at room temperature for 10 minutes under nitrogen. APTES (40% mol, 9.6×10^{-4} mol, 0.46 mL) was added. The reaction mixture was stirred for 24 hours at room temperature under nitrogen atmosphere. The reaction mixture was purified by pressure filtration using a regenerated cellulose membrane (Millipore, 30 KDa MWCO, 47mm diameter) at 40 PSI rinsing with MQ water three times. The filtered solid were suspended in MQ water and sonicated until well dispersed.

Method γ A 500 mL round bottom Schlenk flask was charged with 150 mL of absolute ethanol and 80 mL of MQ water. Dextran 9-11 KDa (2.4×10^{-6} mol, 24 mg) was dissolved in 10mL of MQ water and added, followed by 10mL of NH_4OH (~30% as NH_3). TEOS, (2.4 mmol, 0.53 mL) was added dropwise via syringe. The mixture was stirred at room temperature for 15 minutes under nitrogen. APTES (40% mol, 9.6×10^{-4} mol, 0.46 mL) was added. The reaction mixture was stirred for 24 hours at room temperature under nitrogen atmosphere. The reaction mixture was purified by pressure filtration using a regenerated cellulose membrane (Millipore, 30 KDa MWCO, 47mm

diameter) at 40 PSI rinsing with MQ water three times. The filtered solid were suspended in MQ water and sonicated until well dispersed.

Silver methenamine staining for TEM

The following solutions were prepared in MQ water; 100 mL 3% hexamethylene tetramine (methenamine), 5 mL 5% silver nitrate, 0.5% periodic acid and 5% sodium borate. The silver methenamine stock solution was prepared by adding the silver nitrate solution dropwise to the methenamine solution. The solution was filtered through a 0.2 µm PTFE filter into an amber bottle. The stock solution was kept at 4 ^{o}C until used. The silver methenamine working solution was prepared by mixing 50 mL of silver methenamine stock with 5 mL of 5% sodium borate solution. A 5µL sample of silica nanoparticles was placed on a Nickel TEM grid and allowed to air dry. The sample was treated with periodic acid solution 0.5% for 30 minutes. The grid was washed three times by scooping 5µL droplets of MQ water and absorbing it with the tip of a filter paper wedge. After rinsing, a 5 µL droplet of silver methenamine working solution was placed on the grid and air dried in the dark. The grid was again rinsed three times with MQ water and air-dried.

APPENDICES

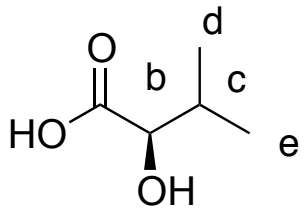

	δ ppm	Integral
a	6.64	2
b	4.16	1
c	2.17	1
d	1.08	3
e	0.93	3

Appendix 1 ^{1}H NMR of 2(R)-hydroxy-3-methylbutanoic acid in $CDCl_3$ 500 MHz

δ ppm
179.3
74.84
31.96
18.75
15.84

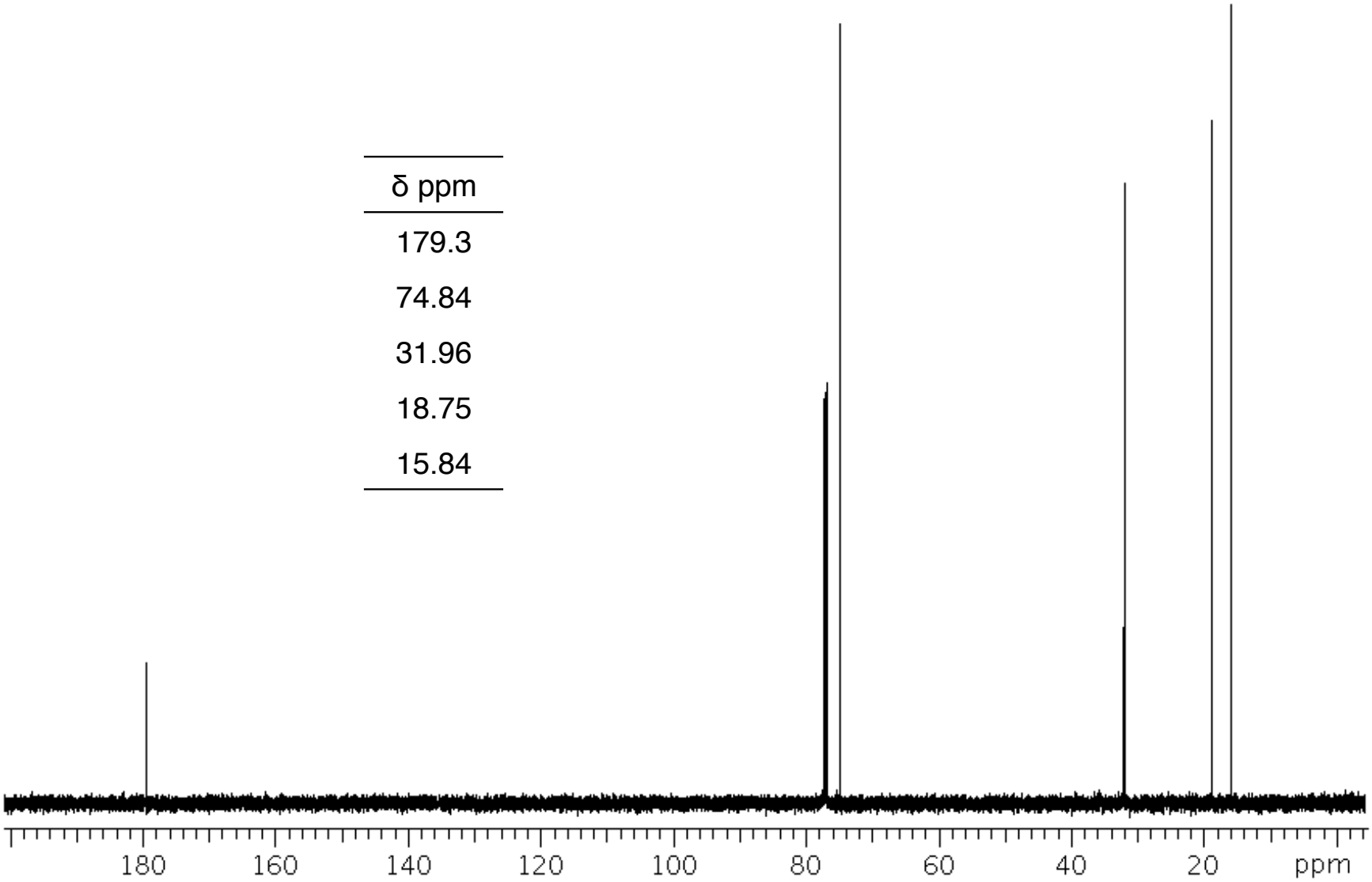

Appendix 2 ^{13}C NMR of 2(R)-hydroxy-3-methylbutanoic acid in $CDCl_3$ 125 MHz

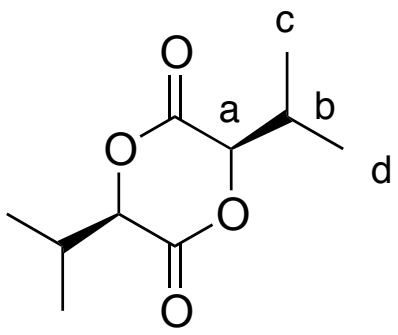

	δ ppm	integral
a	4.68	2
b	2.47	2
c	1.13	6
d	1.03	6

Appendix 3 ^{1}H NMR of D-isopropyl glycolide acid in $CDCl_3$ 500 MHz

δ ppm
166.35
79.55
29.37
18.55
15.81

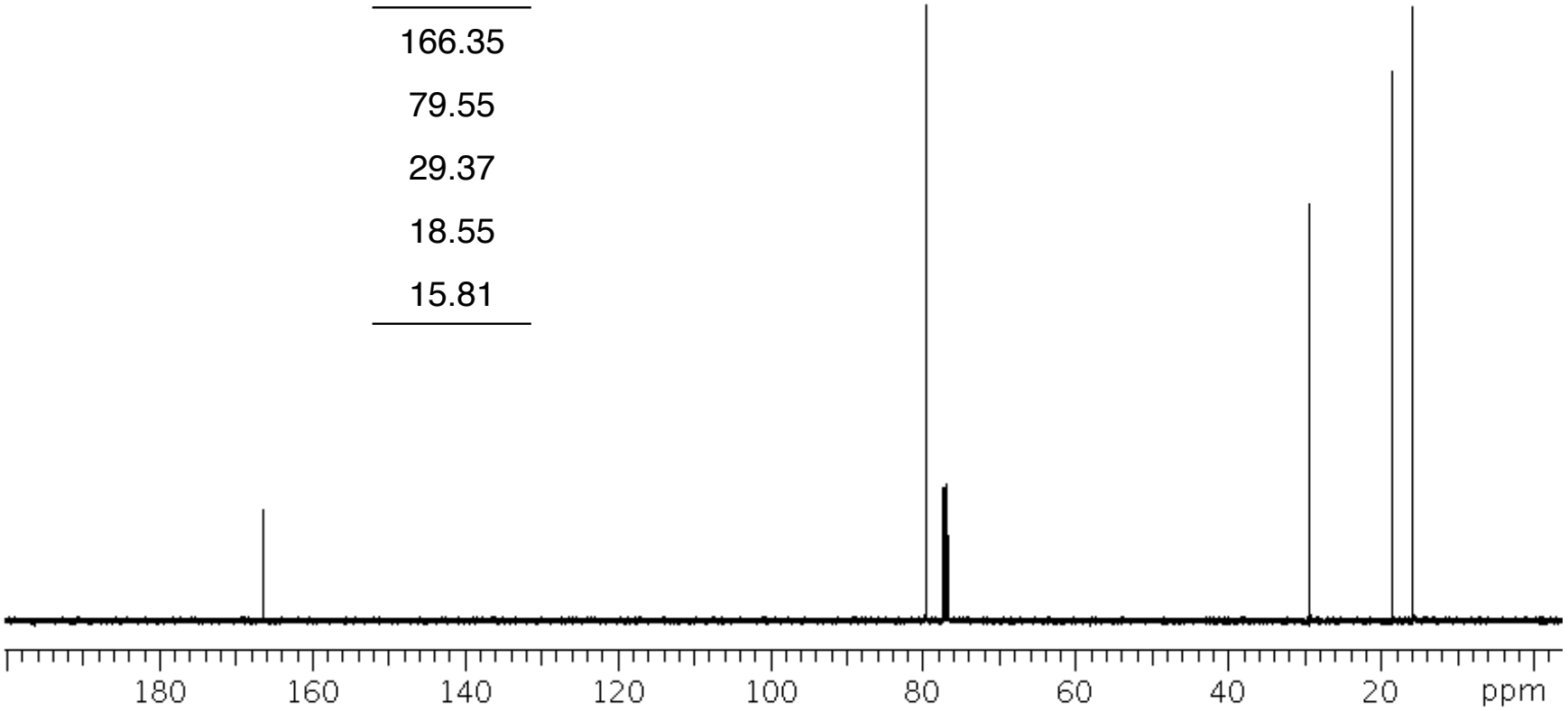

Appendix 4 ^{13}C NMR of D-isopropyl glycolide acid in $CDCl_3$ 125 MHz

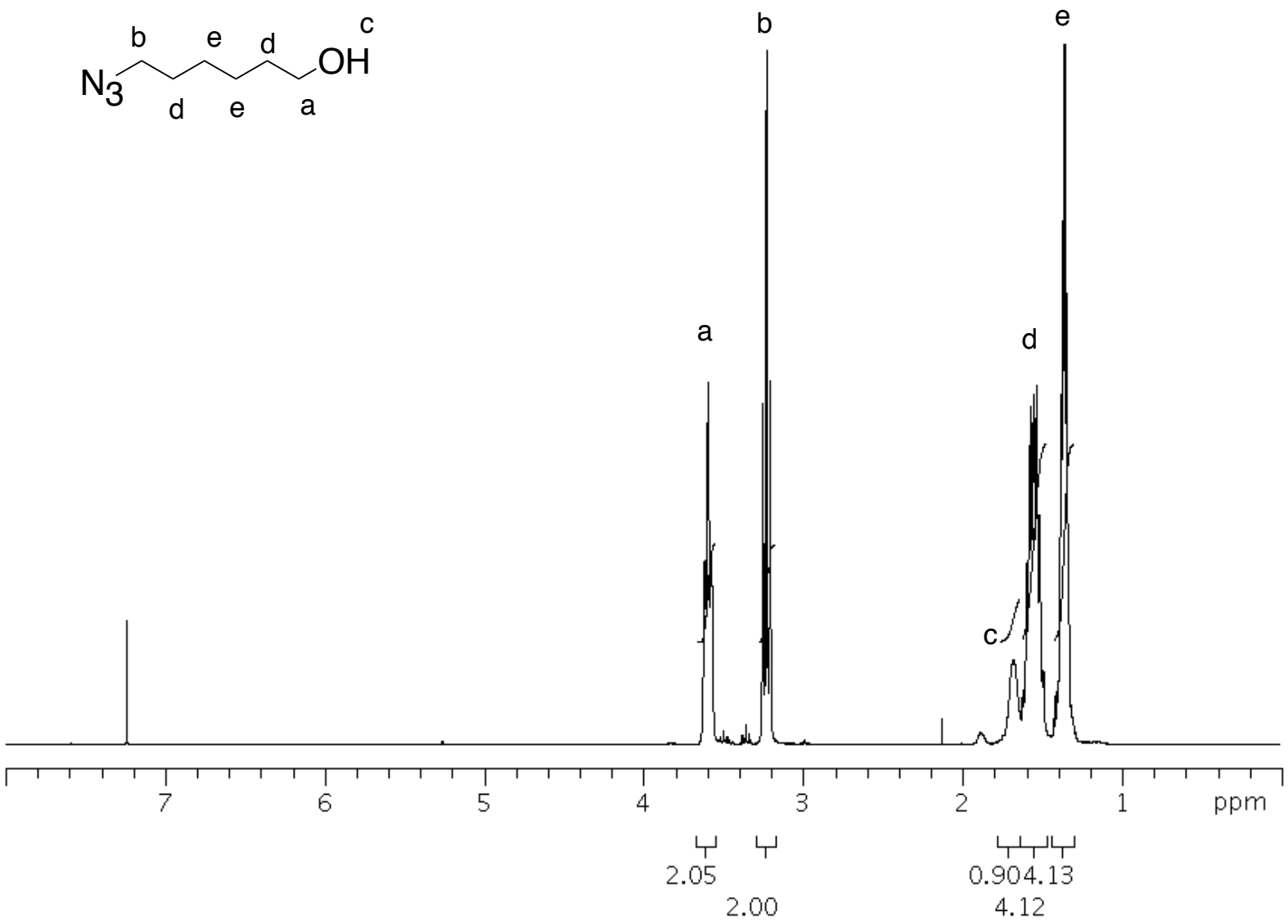

Appendix 5 ^{1}H NMR of 6-azidohexan-1-ol in $CDCl_3$ 500 MHz

δ ppm
62.61
51.30
32.44
28.72
26.43
25.24

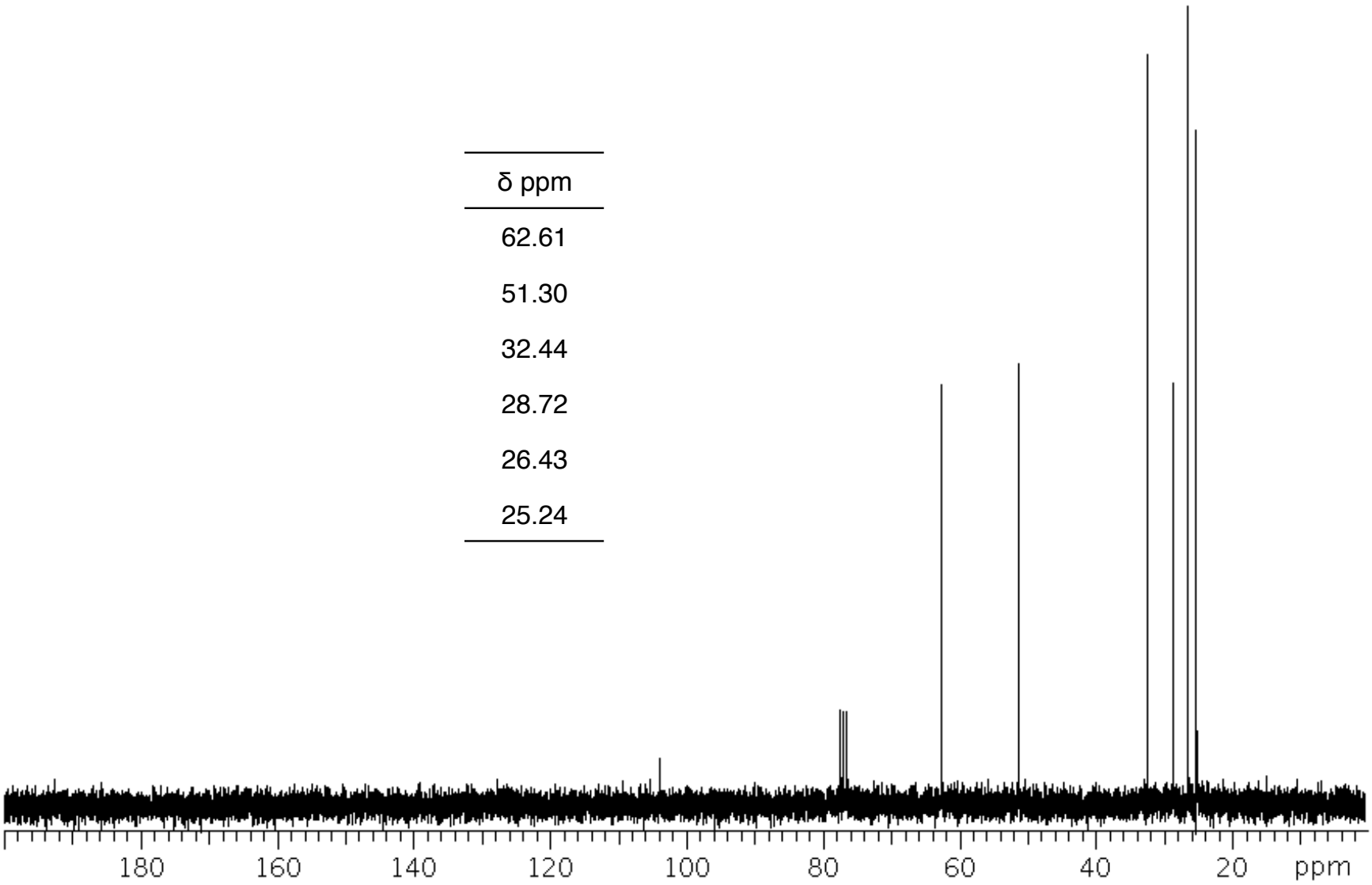

Appendix 6 ^{13}C NMR of 6-azidohexan-1-ol in $CDCl_3$ 125 MHz

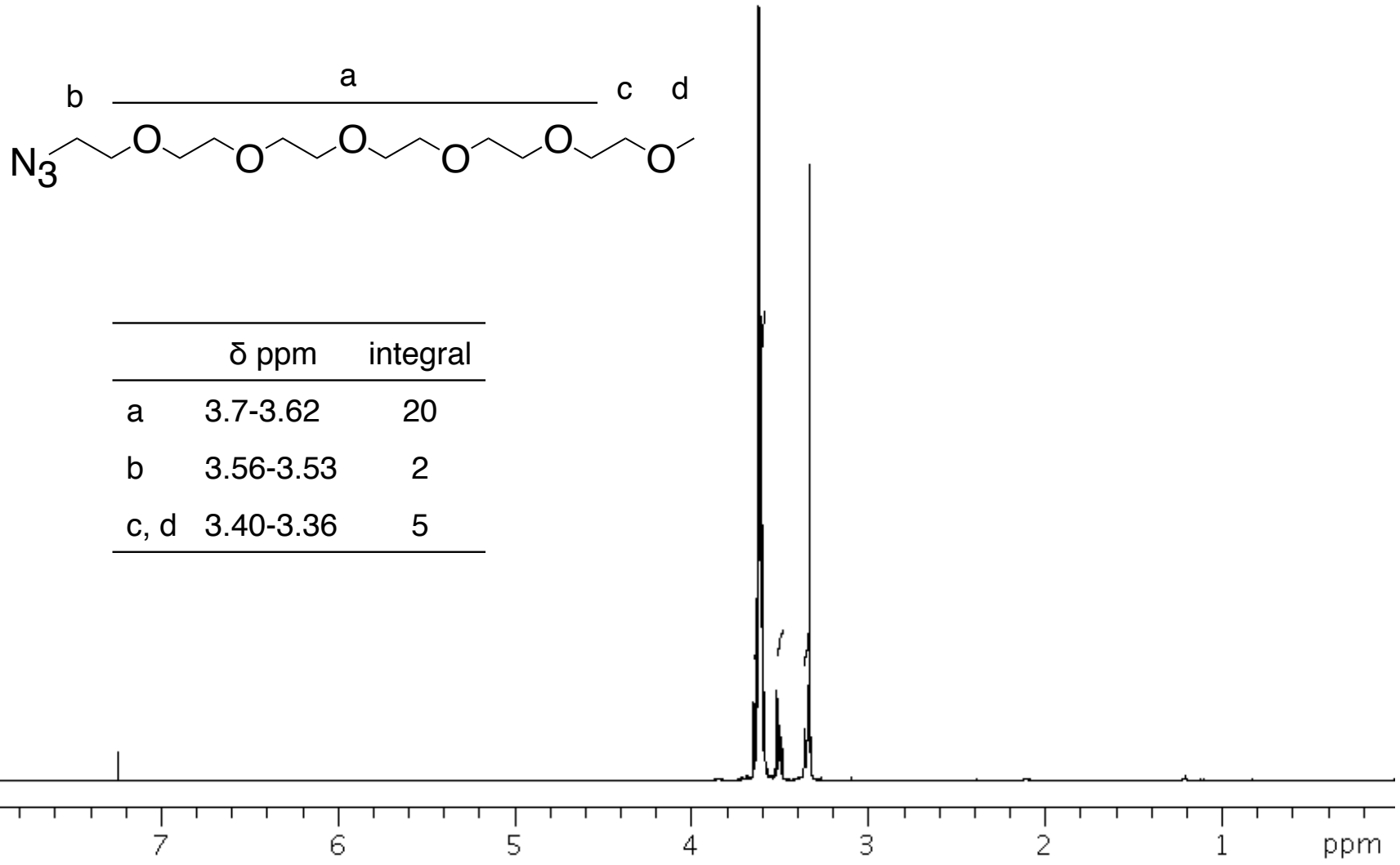

Appendix 7 ^{1}H NMR of 19-azido-2,5,8,11,14,17-hexaoxanonadecane (C1EO6) in $CDCl_3$ 500 MHz

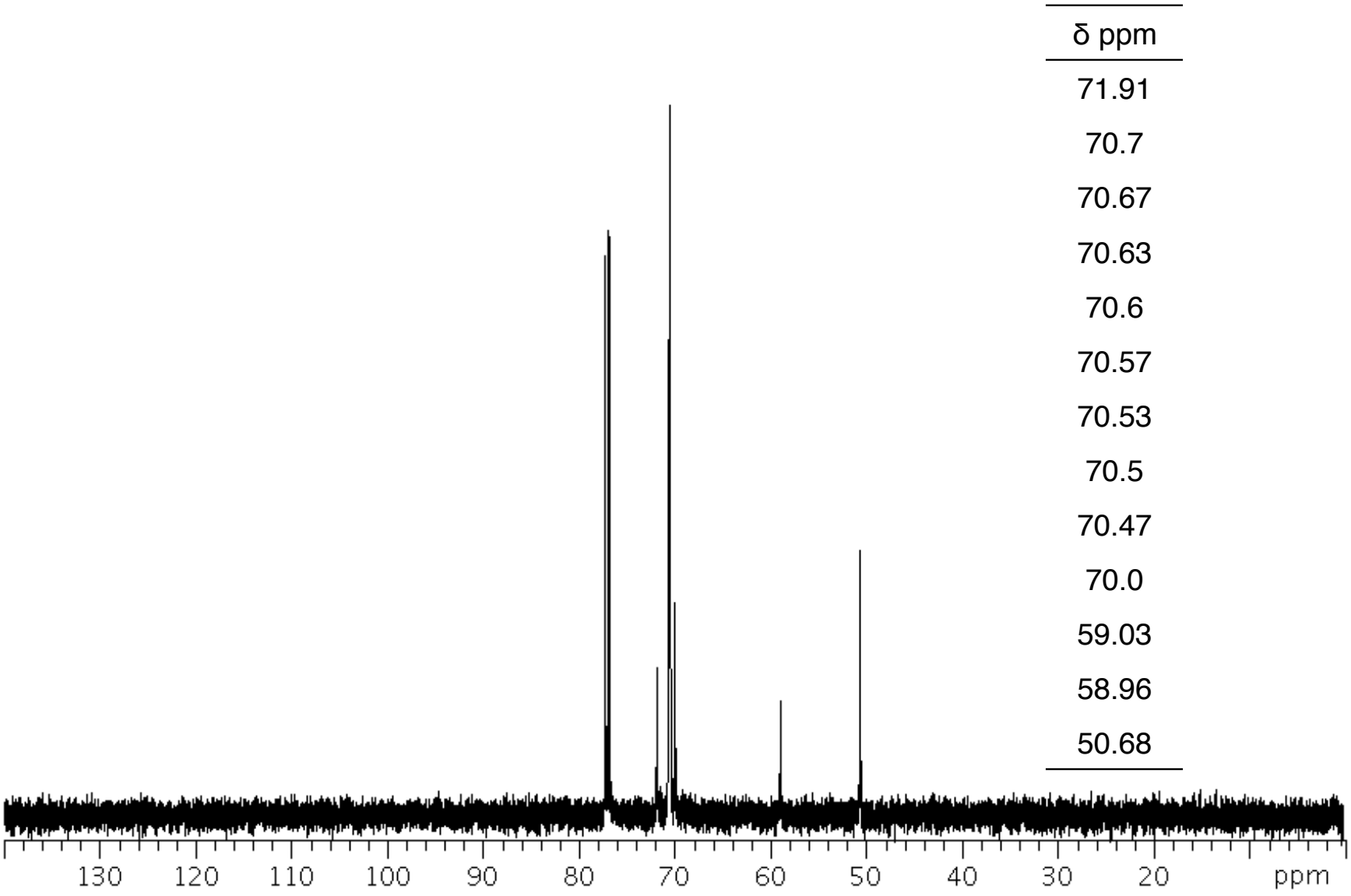

Appendix 8 ^{13}C NMR of 19-azido-2,5,8,11,14,17-hexaoxanonadecane (C1EO6) in $CDCl_3$ 125 MHz

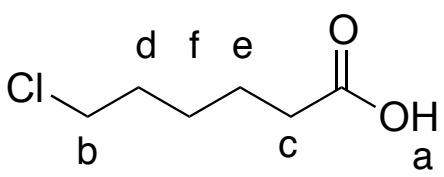

	δ ppm	integral
a	11.9	1
b	3.6-3.5	2
c	2.4-2.3	2
d	1.8-1.7	2
e	1.7-1.6	2
f	1.5-1.4	2

Appendix 9 ^{1}H NMR of 6-chlorohexanoic acid in $CDCl_3$ 500 MHz

δ ppm
180.05
44.65
33.82
32.15
26.26
23.86

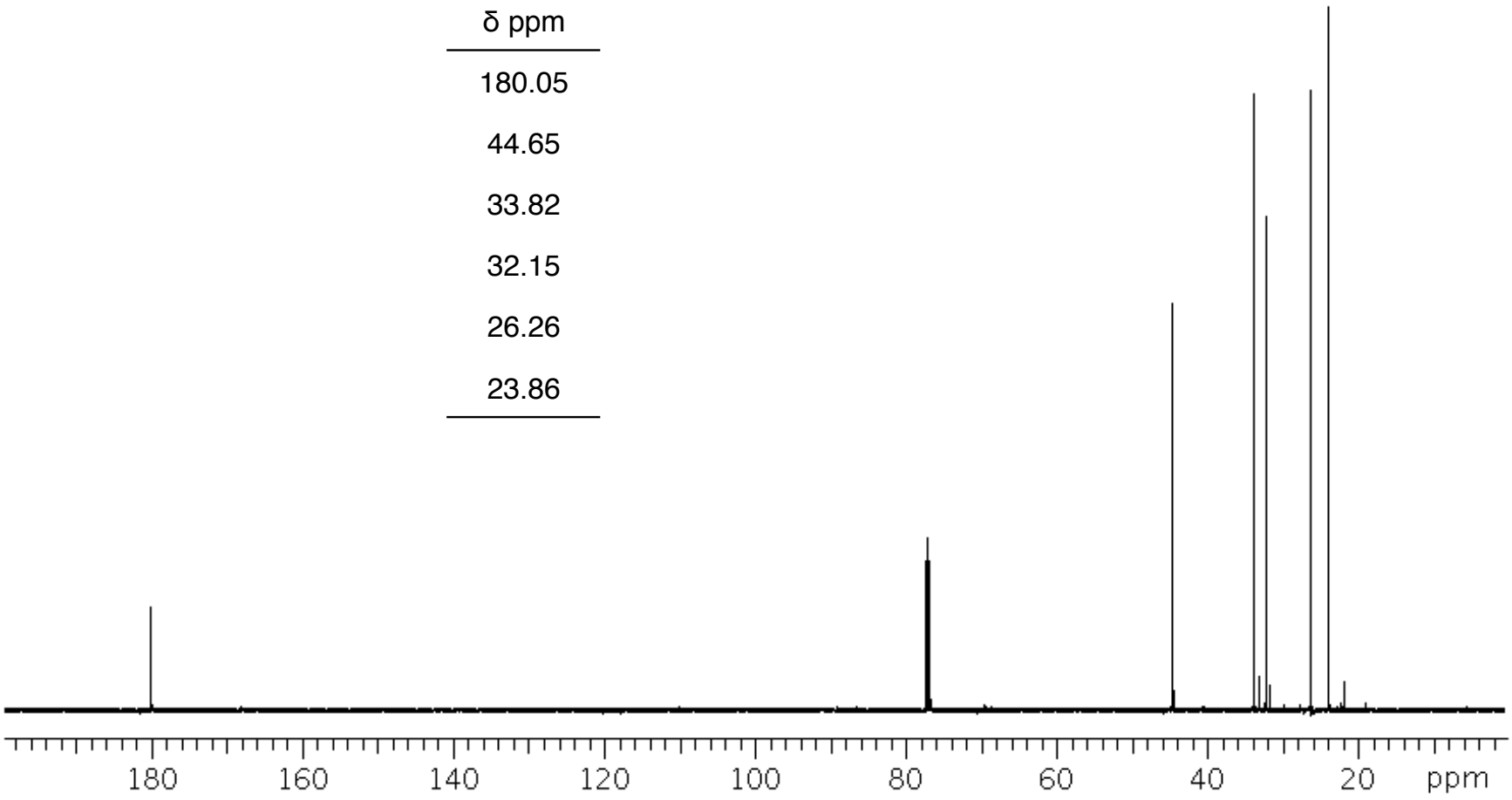

Appendix 10 ^{13}C NMR of 6-chlorohexanoic acid in $CDCl_3$ 125 MHz

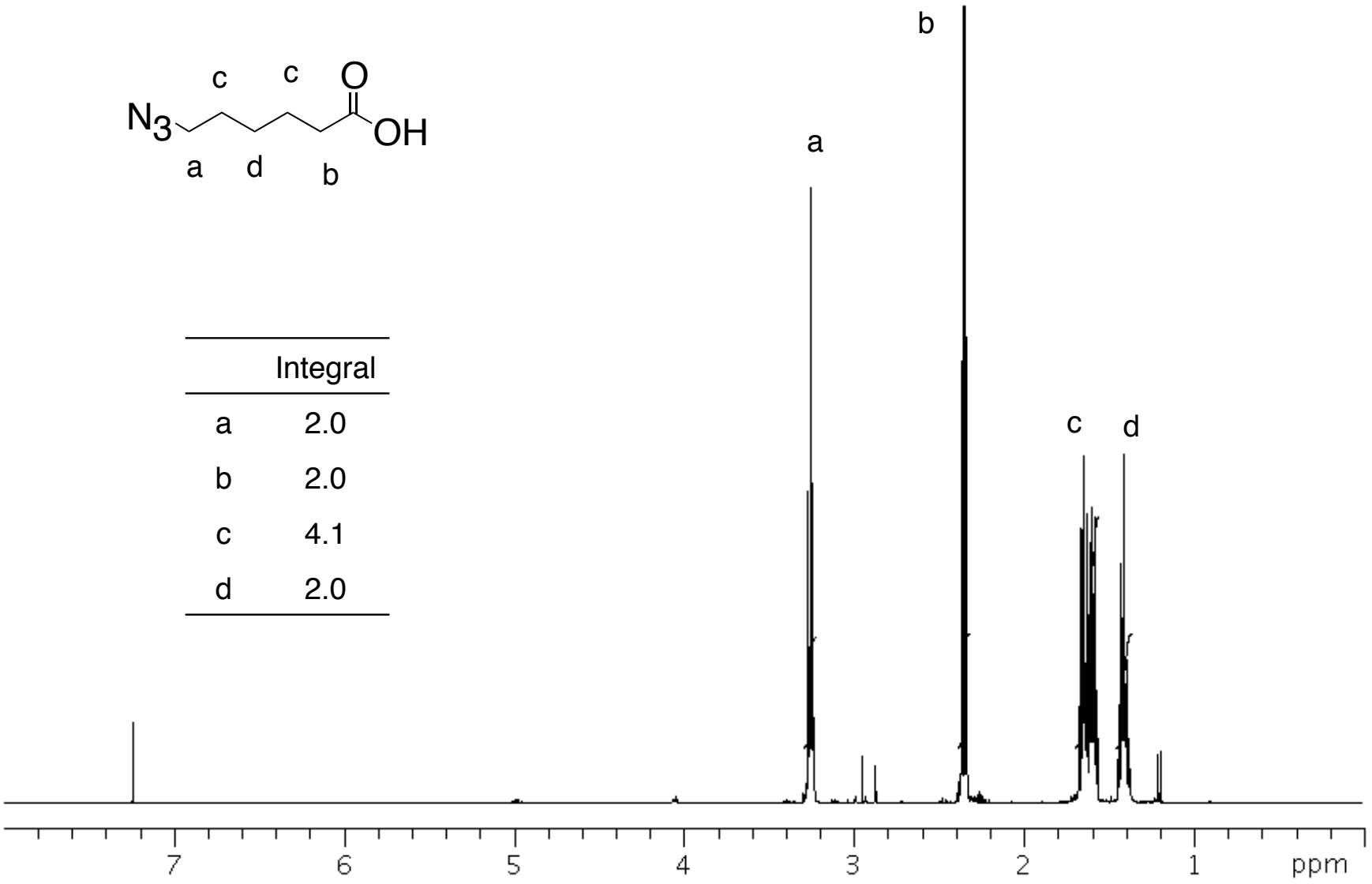

	Integral
a	2.0
b	2.0
c	4.1
d	2.0

Appendix 11 ^{1}H NMR of 6-azidohexanoic acid in $CDCl_3$ 500 MHz

δ ppm
179.83
51.18
33.8
28.51
26.13
24.1

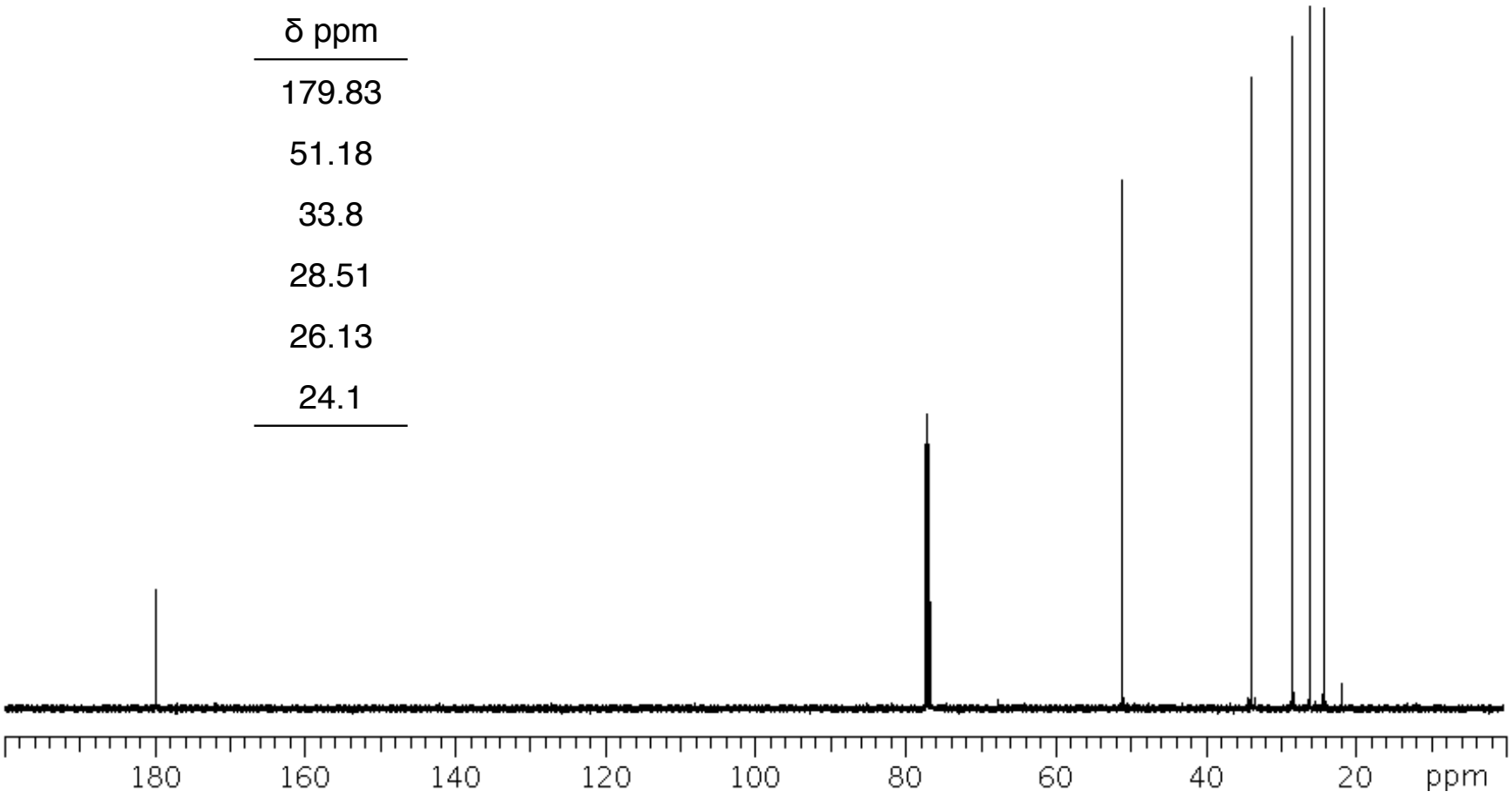

Appendix 12 ^{13}C NMR of 6-azidohexanoic acid in $CDCl_3$ 125 MHz

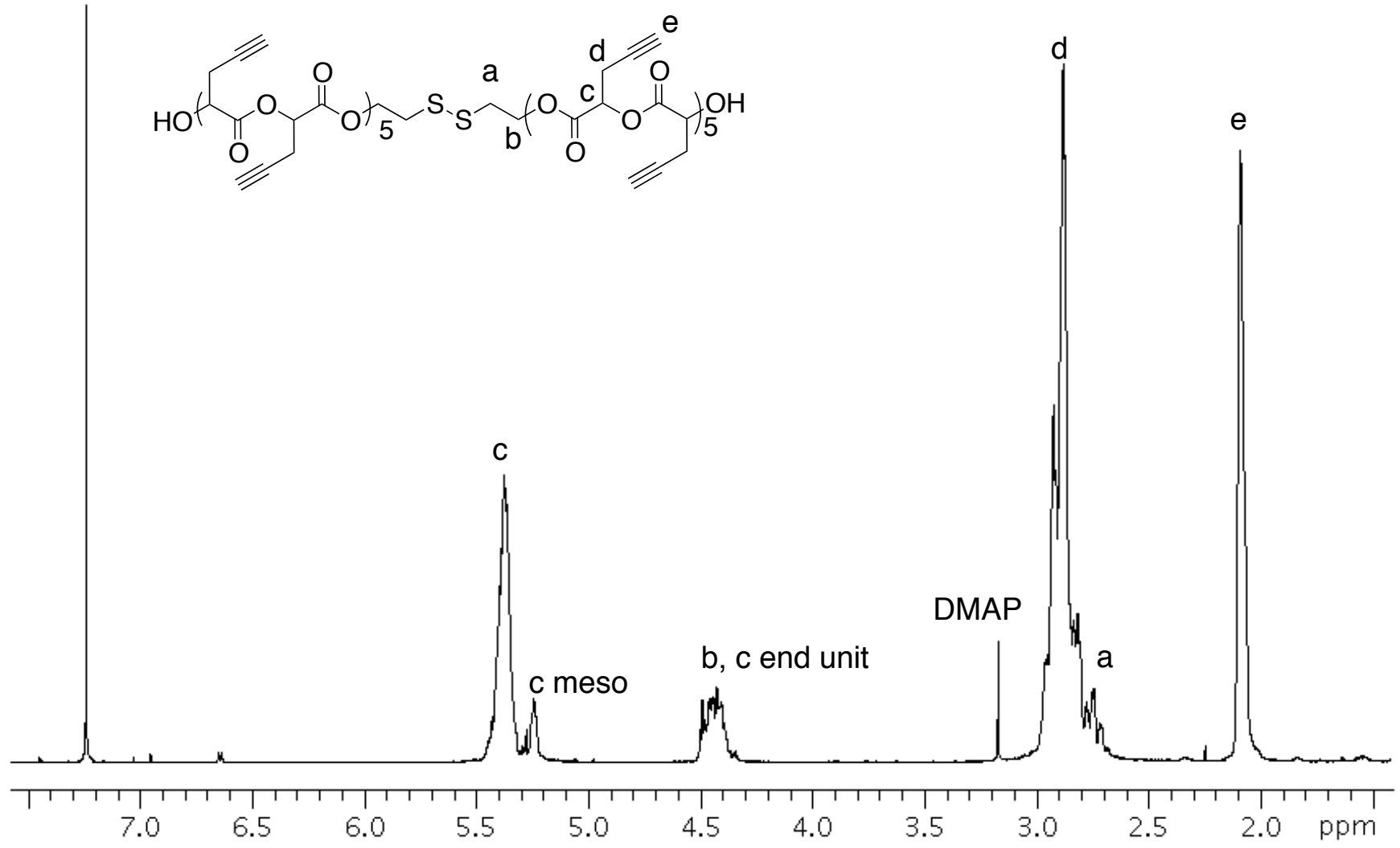

Appendix 13 ^{1}H NMR of bis[2-[poly(propargyl glycolide)]ethyl]disulfide in $CDCl_3$ in $CDCl_3$ 500 MHz

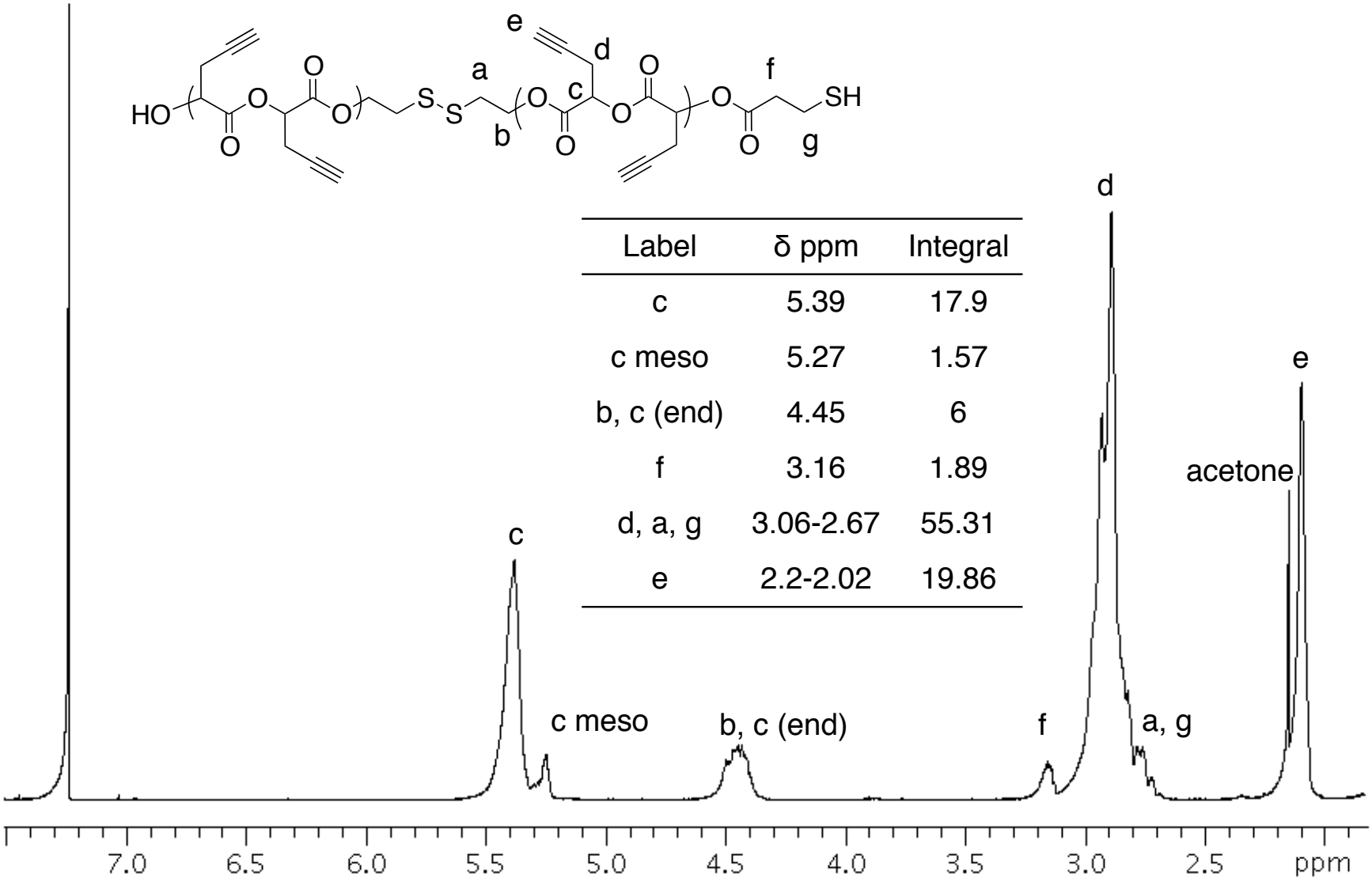

Label	δ ppm	Integral
c	5.39	17.9
c meso	5.27	1.57
b, c (end)	4.45	6
f	3.16	1.89
d, a, g	3.06-2.67	55.31
e	2.2-2.02	19.86

Appendix 14 ^{1}H NMR Asymmetric thiol modification of PG_5SSPG_5 in $CDCl_3$ 500 MHz

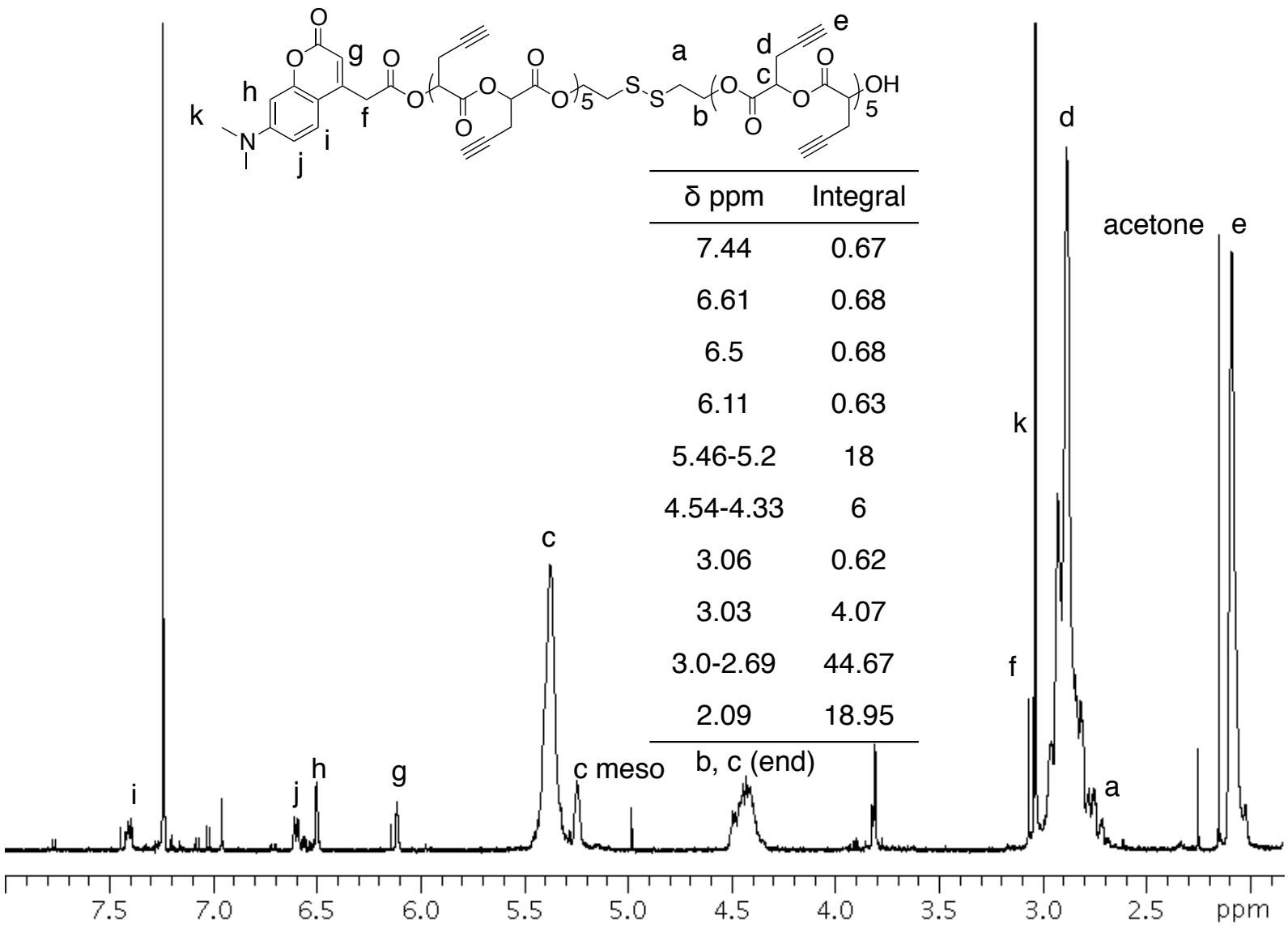

Appendix 15 ^{1}H NMR of DMACA tagged PG_5SSPG_5 in $CDCl_3$ 500 MHz

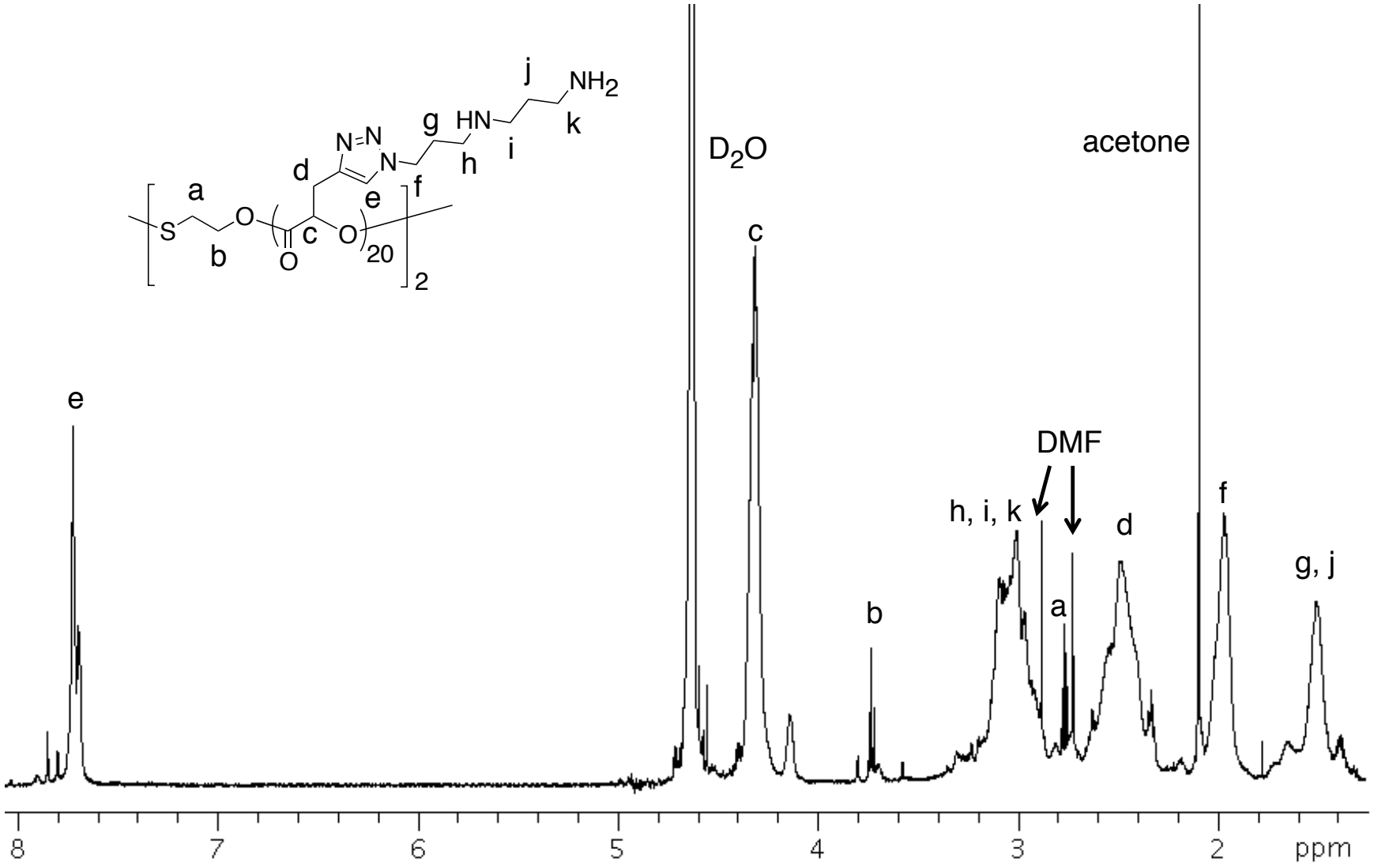

Appendix 16 ^{1}H NMR of clicked PGSSPG with 100% A12 in D_2O 500 MHz

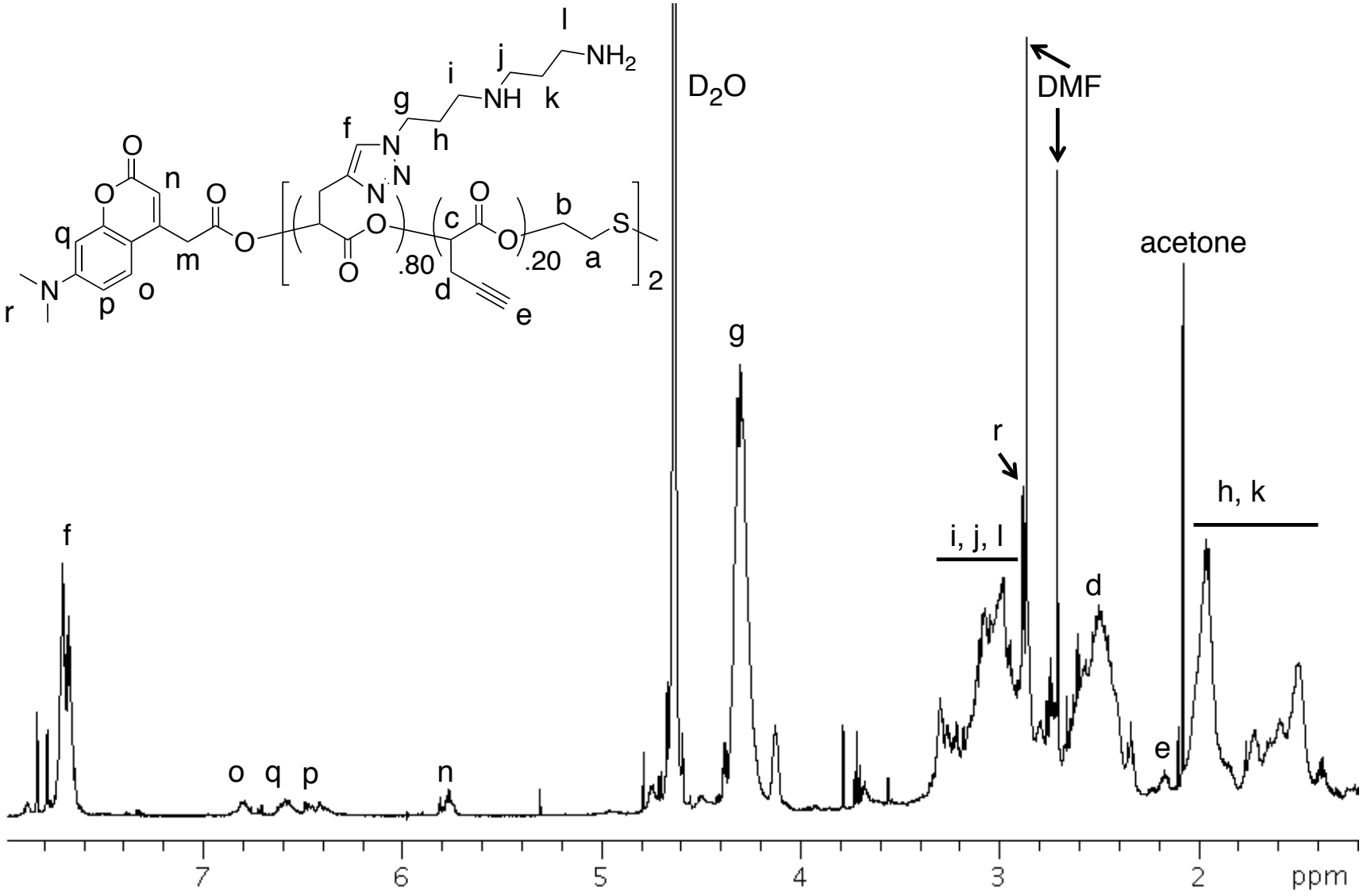

Appendix 17 ^{1}H NMR of Clicked polymer $PG_5SSPG_5[A12_{80}X_{20}]$ in D_2O 500 MHz

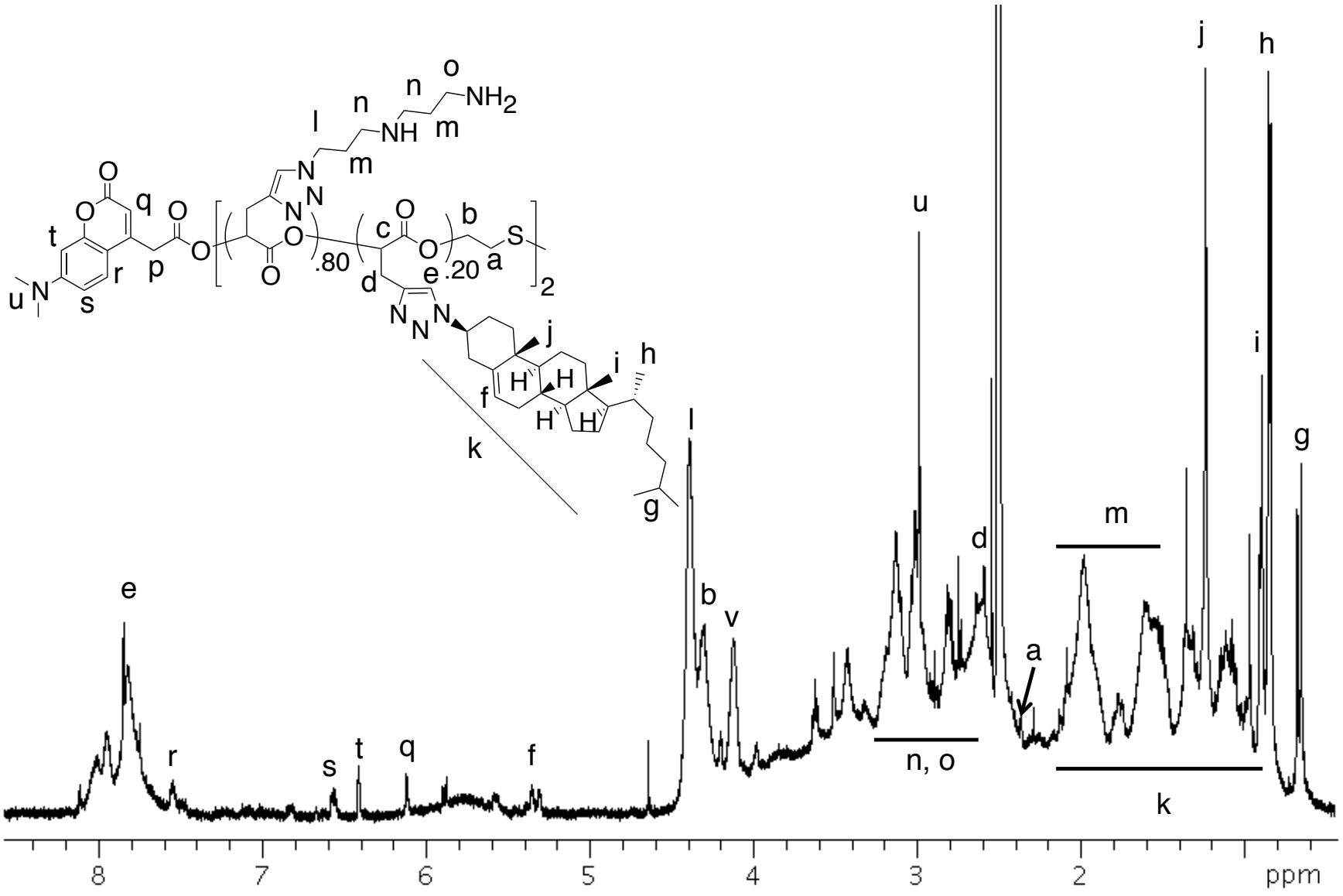

Appendix 18 ^{1}H NMR of clicked polymer $PG_5SSPG_5[A12_{80}Chol(S)_{20}]$ in $CDCl_3/D_2O$ 500 MHz

REFERENCES

1. Middleton, J. C.; Tipton, A. J. *Biomaterials* **2000,** *21* (23), 2335-2346.

2. Cima, L. G.; Vacanti, J. P.; Vacanti, C.; Ingber, D.; Mooney, D.; Langer, R. *Journal of Biomechanical Engineering* **1991,** *113* (2), 143-151.

3. Langer, R. *Accounts of Chemical Research* **1999,** *33* (2), 94-101.

4. Cohen, S.; Yoshioka, T.; Lucarelli, M.; Hwang, L. H.; Langer, R. *Pharmaceutical Research* **1991,** *8* (6), 713-720.

5. Dechy-Cabaret, O.; Martin-Vaca, B.; Bourissou, D. *Chemical Reviews* **2004,** *104* (12), 6147-6176.

6. Jain, R. A. *Biomaterials* **2000,** *21* (23), 2475-2490.

7. De Laporte, L.; Lei Yan, A.; Shea, L. D. *Biomaterials* **2009,** *30* (12), 2361-2368.

8. Houchin-Ray, T.; Swift, L. A.; Jang, J.-H.; Shea, L. D. *Biomaterials* **2007,** *28* (16), 2603-2611.

9. Fu, H.-L.; Cheng, S.-X.; Zhang, X.-Z.; Zhuo, R.-X. *Journal of Controlled Release* **2007,** *124* (3), 181-188.

10. Koby, G.; Ofra, B.; Dganit, D.; Marcelle, M. *Biopolymers* **2007,** *85* (5-6), 379-391.

11. Ikada, Y.; Tsuji, H. *Macromol. Rapid Commun.* **2000,** *21* (3), 117-132.

12. Jing, F.; Smith, M. R.; Baker, G. L. *Macromolecules* **2007,** *40* (26), 9304-9312.

13. Yin, M.; Baker, G. L. *Macromolecules* **1999,** *32* (23), 7711-7718.

14. Vogel, E. B. Synthesis, Characterization, and Applications of Functionalized Polyglycolides. Michigan State University, East Lansing, 2008.

15. Liu, T.; Simmons, T. L.; Bohnsack, D. A.; Mackay, M. E.; Smith, M. R.; Baker, G. L. *Macromolecules* **2007,** *40* (17), 6040-6047.

16. Gerhardt, W. W.; Noga, D. E.; Hardcastle, K. I.; Garcia, A. J.; Collard, D. M.; Weck, M. *Biomacromolecules* **2006,** *7* (6), 1735-1742.

17. Takizawa, K.; Tang, C.; Hawker, C. J. *J. Am. Chem. Soc.* **2008,** *130* (5), 1718-1726.

18. Bertram, J. P.; Jay, S. M.; Hynes, S. R.; Robinson, R.; Criscione, J. M.; Lavik, E. B. *Acta Biomaterialia* **2009,** *5* (8), 2860-2871.

19. Noga, D. E.; Petrie, T. A.; Kumar, A.; Weck, M.; GarcÃ-a, A. s. J.; Collard, D. M. *Biomacromolecules* **2008,** *9* (7), 2056-2062.

20. Zhang, M.; Vedantham, P.; Flynn, D. L.; Hanson, P. R. *Journal of Organic Chemistry* **2004,** *69* (24), 8340-8344.

21. Mathers, R. T.; Coates, G. W. *Chemical Communications* **2004,** (4), 422-423.

22. Jing, F.; Hillmyer, M. A. *J. Am. Chem. Soc.* **2008,** *130* (42), 13826-13827.

23. Tian, D.; Dubois, P.; Grandfils, C.; Jerome, R. *Macromolecules* **1997,** *30* (3), 406-409.

24. Tian, D.; Dubois, P.; Jerome, R. *Macromolecules* **1997,** *30* (9), 2575-2581.

25. Tian, D.; Dubois, P.; Jerome, R. *Macromolecules* **1997,** *30* (7), 1947-1954.

26. Malkoch, M.; Schleicher, K.; Drockenmuller, E.; Hawker, C. J.; Russell, T. P.; Wu, P.; Fokin, V. V. *Macromolecules* **2005,** *38* (9), 3663-3678.

27. Horn, B. A. V.; Wooley, K. L. *Soft Matter* **2007,** *3* (8), 1032-1040.

28. Mecerreyes, D.; Humes, J.; Miller, R. D.; Hedrick, J. L.; Detrembleur, C.; Lecomte, P.; Jérôme, R.; Roman, J. S. *Macromol. Rapid Commun.* **2000,** *21* (11), 779-784.

29. Rieger, J.; Butsele, K. V.; Lecomte, P.; Detrembleur, C.; Jerome, R.; Jerome, C. *Chemical Communications* **2005,** (2), 274-276.

30. Noga, D. E.; Petrie, T. A.; Kumar, A.; Weck, M.; GarcÃ-a, A. J.; Collard, D. M. *Biomacromolecules* **2008,** *9* (7), 2056-2062.

31. Kolb, H. C.; Finn, M. G.; Sharpless, K. B. *Angewandte Chemie International Edition* **2001,** *40* (11), 2004-2021.

32. Tornoe, C. W.; Christensen, C.; Meldal, M. *Journal of Organic Chemistry* **2002,** *67* (9), 3057-3064.

33. van Dijk, M.; Rijkers, D. T. S.; Liskamp, R. M. J.; van Nostrum, C. F.; Hennink, W. E. *Bioconjugate Chemistry* **2009,** *20* (11), 2001-2016.

34. Rostovtsev, V. V.; Green, L. G.; Fokin, V. V.; Sharpless, K. B. *Angewandte Chemie International Edition* **2002,** *41* (14), 2596-2599.

35. Wu, P.; Feldman, A. K.; Nugent, A. K.; Hawker, C. J.; Scheel, A.; Voit, B.; Pyun, J.; Fréchet, J. M. J.; Sharpless, K. B.; Fokin, V. V. *Angewandte Chemie International Edition* **2004,** *43* (30), 3928-3932.

36. Sumerlin, B. S.; Tsarevsky, N. V.; Louche, G.; Lee, R. Y.; Matyjaszewski, K. *Macromolecules* **2005,** *38* (18), 7540-7545.

37. Sperling, L. H., *Introduction to physical polymer science*. Wiley: Hoboken, New Jersey, 2006.

38. Ammendola, P.; Tancredi, T.; Zambelli, A. *Macromolecules* **1986,** *19* (2), 307-310.

39. Mani, R.; Burns, C. M. *Macromolecules* **1991,** *24* (19), 5476-5477.

40. Chien, J. C. W.; Salajka, Z.; Dong, S. *Macromolecules* **1992,** *25* (12), 3199-3203.

41. De Rosa, C.; Auriemma, F. *Progress in Polymer Science* **2006,** *31* (2), 145-237.

42. García, J. M.; García, F. C.; Serna, F.; de la Peña, J. L. *Progress in Polymer Science* **2010,** *35* (5), 623-686.

43. Murthy, N. S. *Journal of Polymer Science Part B: Polymer Physics* **2006,** *44* (13), 1763-1782.

44. Sanda, F.; Endo, T. *Macromolecular Chemistry and Physics* **1999,** *200* (12), 2651-2661.

45. Melis, J.; Zanuy, D.; Alemán, C.; García-Alvarez, M.; Muñoz-Guerra, S. *Macromolecules* **2002,** *35* (23), 8774-8780.

46. Tsuboi, K.; Marcelletti, E.; Matsumoto, H.; Ashizawa, M.; Minagawa, M.; Furuya, H.; Tanioka, A.; Abe, A. *Polym J* **2012,** *44* (4), 360-365.

47. Chamberlain, B. M.; Cheng, M.; Moore, D. R.; Ovitt, T. M.; Lobkovsky, E. B.; Coates, G. W. *J. Am. Chem. Soc.* **2001,** *123* (14), 3229-3238.

48. Ovitt, T. M.; Coates, G. W. *J. Am. Chem. Soc.* **2002,** *124* (7), 1316-1326.

49. Radano, C. P.; Baker, G. L.; Smith, M. R. *J. Am. Chem. Soc.* **2000,** *122* (7), 1552-1553.

50. Fire, A.; Xu, S.; Montgomery, M. K.; Kostas, S. A.; Driver, S. E.; Mello, C. C. *Nature* **1998,** *391* (6669), 806-811.

51. Mello, Craig C. *Angewandte Chemie International Edition* **2007,** *46* (37), 6985-6994.

52. Hannon, G. J. *Nature* **2002,** *418* (6894), 244-251.

53. Siomi, H.; Siomi, M. C. *Nature* **2009,** *457* (7228), 396-404.

54. Barik, S., *RNAi Desing and Application*. Humana Press: New Jersey, 2008; Vol. 442.

55. Ghosh, S.; Gopinath, P.; Ramesh, A. *Applied Biochemistry and Biotechnology* **2006,** *133* (1), 9-29.

56. Mori, T.; Kiyono, T.; Imabayashi, H.; Takeda, Y.; Tsuchiya, K.; Miyoshi, S.; Makino, H.; Matsumoto, K.; Saito, H.; Ogawa, S.; Sakamoto, M.; Hata, J.-I.; Umezawa, A. *Molecular and Cellular Biology* **2005,** *25* (12), 5183-5195.

57. Peng, D.; Qian, C.; Sun, Y.; Barajas, M. A.; Prieto, J. *Journal of Hepatology* **2000,** *32* (6), 975-985.

58. Tao, L.; Liu, J.; Tan, B. H.; Davis, T. P. *Macromolecules* **2009,** *42* (14), 4960-4962.

59. Kaiser, J. *Science* **2007,** *317* (5838), 580-.

60. Lu, C.-Y.; Chou, A.-K.; Wu, C.-L.; Yang, C.-H.; Chen, J.-T.; Wu, P.-C.; Lin, S.-H.; Muhammad, R.; Yang, L.-C. *Gene Therapy* **2002,** *9* (15), 1008-1014.

61. Duvshani-Eshet, M.; Machluf, M. *Journal of Controlled Release* **2005,** *108* (2-3), 513-528.

62. Jeong, J. H.; Mok, H.; Oh, Y.-K.; Park, T. G. *Bioconjugate Chemistry* **2009,** *20* (1), 5-14.

63. Nguyen, J.; Steele, T. W. J.; Merkel, O.; Reul, R.; Kissel, T. *Journal of Controlled Release* **2008,** *132* (3), 243-251.

64. Xiong, X.-B.; Uludag, H.; Lavasanifar, A. *Biomaterials* **2009,** *30* (2), 242-253.

65. Beh, C. W.; Seow, W. Y.; Wang, Y.; Zhang, Y.; Ong, Z. Y.; Ee, P. L. R.; Yang, Y.-Y. *Biomacromolecules* **2008,** *10* (1), 41-48.

66. Meyer, M.; Dohmen, C.; Philipp, A.; Kiener, D.; Maiwald, G.; Scheu, C.; Ogris, M.; Wagner, E. *Molecular Pharmaceutics* **2009,** *6* (3), 752-762.

67. Matsumoto, S.; Christie, R. J.; Nishiyama, N.; Miyata, K.; Ishii, A.; Oba, M.; Koyama, H.; Yamasaki, Y.; Kataoka, K. *Biomacromolecules* **2008,** *10* (1), 119-127.

68. Layman, J. M.; Ramirez, S. M.; Green, M. D.; Long, T. E. *Biomacromolecules* **2009,** *10* (5), 1244-1252.

69. Xu, F. J.; Ping, Y.; Ma, J.; Tang, G. P.; Yang, W. T.; Li, J.; Kang, E. T.; Neoh, K. G. *Bioconjugate Chemistry* **2009,** *20* (8), 1449-1458.

70. Gu, Z.; Yuan, Y.; He, J.; Zhang, M.; Ni, P. *Langmuir* **2009,** *25* (9), 5199-5208.

71. Bivas-Benita, M.; Romeijn, S.; Junginger, H. E.; Borchard, G. *European Journal of Pharmaceutics and Biopharmaceutics* **2004,** *58* (1), 1-6.

72. Tahara, K.; Sakai, T.; Yamamoto, H.; Takeuchi, H.; Kawashima, Y. *Int. J. Pharm.* **2008,** *354* (1-2), 210-216.

73. Hou, X.; Li, Q.; He, Y.; Jia, L.; Li, Y.; Zhu, Y.; Cao, A. *Journal of Polymer Science, Part B: Polymer Physics* **2009,** *47* (14), 1393-1405.

74. Kim, I.-S.; Lee, S.-K.; Park, Y.-M.; Lee, Y.-B.; Shin, S.-C.; Lee, K. C.; Oh, I.-J. *Int. J. Pharm.* **2005,** *298* (1), 255-262.

75. Chang, C.-W.; Choi, D.; Kim, W. J.; Yockman, J. W.; Christensen, L. V.; Kim, Y.-H.; Kim, S. W. *Journal of Controlled Release* **2007,** *118* (2), 245-253.

76. Prabha, S.; Labhasetwar, V. *Pharmaceutical Research* **2004,** *21* (2), 354-364.

77. Mengarelli, V.; Zeghal, M.; Auvray, L.; Clemens, D. *Physical Review E* **2011,** *84* (2), 021805.

78. Ke, J.-H.; Young, T.-H. *Biomaterials* **2010,** *31* (35), 9366-9372.

79. Zhang, W.; Zhang, A.; Guan, Y.; Zhang, Y.; Zhu, X. X. *Journal of Materials Chemistry* **2011,** *21* (2), 548-555.

80. Hao, J.; Yuan, G.; He, W.; Cheng, H.; Han, C. C.; Wu, C. *Macromolecules* **2010,** *43* (4), 2002-2008.

81. Henríquez, C. M. G.; Tagle, L. H.; Terraza, C. A.; González, A. B.; Cabrera, A. L.; Volkmann, U. G. *Journal of Applied Polymer Science* **2012,** *125* (1), 477-487.

82. Brochu, S.; Prud'homme, R. E.; Barakat, I.; Jerome, R. *Macromolecules* **1995,** *28* (15), 5230-5239.

83. Ikada, Y.; Jamshidi, K.; Tsuji, H.; Hyon, S. H. *Macromolecules* **1987,** *20* (4), 904-906.

84. Tsuji, H.; Horii, F.; Hyon, S. H.; Ikada, Y. *Macromolecules* **1991,** *24* (10), 2719-2724.

85. Tsuji, H.; Hyon, S. H.; Ikada, Y. *Macromolecules* **1991,** *24* (20), 5651-5656.

86. Tsuji, H.; Hyon, S. H.; Ikada, Y. *Macromolecules* **1991,** *24* (20), 5657-5662.

87. Tsuji, H.; Horii, F.; Nakagawa, M.; Ikada, Y.; Odani, H.; Kitamaru, R. *Macromolecules* **1992,** *25* (16), 4114-4118.

88. Tsuji, H.; Hyon, S. H.; Ikada, Y. *Macromolecules* **1992,** *25* (11), 2940-2946.

89. Tsuji, H.; Ikada, Y. *Macromolecules* **1992,** *25* (21), 5719-5723.

90. Tsuji, H.; Ikada, Y. *Macromolecules* **1993,** *26* (25), 6918-6926.

91. Tsuji, H.; Ikada, Y.; Hyon, S. H.; Kimura, Y.; Kitao, T. *Journal of Applied Polymer Science* **1994,** *51* (2), 337-344.

92. Tsuji, H.; Ikada, Y. *Journal of Applied Polymer Science* **1995,** *58* (10), 1793-1802.

93. Tsuji, H.; Ikada, Y. *Polymer* **1995,** *36* (14), 2709-2716.

94. Cartier, L.; Okihara, T.; Ikada, Y.; Tsuji, H.; Puiggali, J.; Lotz, B. *Polymer* **2000,** *41* (25), 8909-8919.

95. Tsuji, H.; Okumura, A. *Macromolecules* **2009,** *42* (19), 7263-7266.

96. Fukuzawa, T.; Uematsu, I.; Uematsu, Y. *Polymer Journal* **1974,** *6* (6), 537-541.

97. Hatada, K.; Shimizu, S.-i.; Terawaki, Y.; Ohta, K.; Yuki, H. *Polymer Journal* **1981,** *13* (8), 811-812.

98. Biros, J.; Masa, Z.; Pouchly, J. *Eur. Polym. J.* **1974,** *10* (8), 629-632.

99. Brinkhuis, R. H. G.; Schouten, A. J. *Macromolecules* **1992,** *25* (10), 2725-2731.

100. Chiang, R.; Burke, J. J.; Threlkel.Jo; Orofino, T. A. *J. Phys. Chem.* **1966,** *70* (11), 3591-&.

101. Deboer, A.; Challa, G. *Polymer* **1976,** *17* (7), 633-637.

102. Feitsma, E. L.; Boer, A. D.; Challa, G. *Polymer* **1975,** *16* (7), 515-519.

103. Fazel, N.; Brulet, A.; Guenet, J. M. *Macromolecules* **1994,** *27* (14), 3836-3842.

104. Slager, J.; Domb, A. J. *Biomacromolecules* **2003,** *4* (5), 1308-1315.

105. Slager, J.; Domb, A. J. *Biomacromolecules* **2003,** *4* (5), 1316-1320.

106. Slager, J.; Cohen, Y.; Khalfin, R.; Talmon, Y.; Domb, A. J. *Macromolecules* **2003,** *36* (9), 2999-3000.

107. Slager, J.; Domb, A. J. *Biomaterials* **2002,** *23* (22), 4389-4396.

108. Berkoukchi, M. P.; Helary, G.; Belorgey, G.; Hogenesch, T. E. *Polym. Bull.* **1994,** *32* (3), 297-303.

109. Brinkhuis, R. H. G.; Schouten, A. J. *Macromolecules* **1992,** *25* (21), 5683-5691.

110. Tsuji, H.; Shimizu, K.; Sakamoto, Y.; Okumura, A. *Polymer* **2011,** *52* (5), 1318-1325.

111. Tsuji, H.; Yamamoto, S.; Okumura, A. *Journal of Applied Polymer Science* **2011,** *122* (1), 321-333.

112. Fukushima, K.; Kimura, Y. *Polym. Int.* **2006,** *55* (6), 626-642.

113. Narita, J.; Katagiri, M.; Tsuji, H. *Macromol. Mater. Eng.* **2011,** *296* (10), 887-893.

114. Bishara, A.; Kricheldorf, H. R.; Domb, A. J. *Macromolecular Symposia* **2005,** *225* (1), 17-30.

115. de Jong, S. J.; van Eerdenbrugh, B.; van Nostrum, C. F.; Kettenes-van de Bosch, J. J.; Hennink, W. E. *Journal of Controlled Release* **2001,** *71* (3), 261-275.

116. Hennink, W. E.; De Jong, S. J.; Bos, G. W.; Veldhuis, T. F. J.; van Nostrum, C. F. *Int. J. Pharm.* **2004,** *277* (1-2), 99-104.

117. Nagahama, K.; Mori, Y.; Ohya, Y.; Ouchi, T. *Biomacromolecules* **2007,** *8* (7), 2135-2141.

118. de Jong, S. J.; De Smedt, S. C.; Demeester, J.; van Nostrum, C. F.; Kettenes-van den Bosch, J. J.; Hennink, W. E. *Journal of Controlled Release* **2001,** *72* (1-3), 47-56.

119. Hamada, K.; Yamashita, K.; Serizawa, T.; Kitayama, T.; Akashi, M. *J. Polym. Sci. Pol. Chem.* **2003,** *41* (12), 1807-1812.

120. Fujiwara, T.; Mukose, T.; Yamaoka, T.; Yamane, H.; Sakurai, S.; Kimura, Y. *Macromol. Biosci.* **2001,** *1* (5), 204-208.

121. Lim, D. W.; Park, T. G. *Journal of Applied Polymer Science* **2000,** *75* (13), 1615-1623.

122. Nagahama, K.; Nishimura, Y.; Ohya, Y.; Ouchi, T. *Polymer* **2007,** *48* (9), 2649-2658.

123. Iwakura, Y.; Iwata, K.; Matsuo, S.; Tohara, A. *Die Makromolekulare Chemie* **1969,** *122* (1), 275-280.

124. Iwakura, Y.; Iwata, K.; Matsuo, S.; Tohara, A. *Die Makromolekulare Chemie* **1971,** *146* (1), 21-32.

125. Yin, M. Synthesis and Characterization of Substituted Polylactides. Michigan State University, East Lansing, 2000.

126. Yamagiwa, N.; Tian, J.; Matsunaga, S.; Shibasaki, M. *J. Am. Chem. Soc.* **2005,** *127* (10), 3413-3422.

127. Koppenhoefer, B.; Trettin, U.; Figura, R.; Lin, B. *Tetrahedron Letters* **1989,** *30* (38), 5109-5110.

128. Hou, X.; Li, Q.; He, Y.; Jia, L.; Li, Y.; Zhu, Y.; Cao, A. *Journal of Polymer Science Part B-Polymer Physics* **2009,** *47* (14), 1393-1405.

129. Tsuji, H.; Hyon, S. H.; Ikada, Y. *Macromolecules* **1991,** *24* (20), 5651-5656.

130. Ren, T.-B.; Xia, W.-J.; Dong, H.-Q.; Li, Y.-Y. *Polymer* **2011,** *52* (16), 3580-3586.

131. Thambi, T.; Yoon, H. Y.; Kim, K.; Kwon, I. C.; Yoo, C. K.; Park, J. H. *Bioconjugate Chemistry* **2011,** *22* (10), 1924-1931.

132. Goyal, R.; Tripathi, S. K.; Tyagi, S.; Sharma, A.; Ram, K. R.; Chowdhuri, D. K.; Shukla, Y.; Kumar, P.; Gupta, K. C. *Nanomedicine: Nanotechnology, Biology and Medicine* **2012,** *8* (2), 167-175.

133. Liu, J.; Jiang, X.; Xu, L.; Wang, X.; Hennink, W. E.; Zhuo, R. *Bioconjugate Chemistry* **2010,** *21* (10), 1827-1835.

134. Kuo, W.-T.; Huang, H.-Y.; Chou, M.-J.; Wu, M.-C.; Huang, Y.-Y. *Journal of Nanomaterials* **2011,** *2011*.

135. Anton, N.; Benoit, J.-P.; Saulnier, P. *Journal of Controlled Release* **2008,** *128* (3), 185-199.

136. Soppimath, K. S.; Aminabhavi, T. M.; Kulkarni, A. R.; Rudzinski, W. E. *Journal of Controlled Release* **2001,** *70* (1–2), 1-20.

137. Rolland, J. P.; Maynor, B. W.; Euliss, L. E.; Exner, A. E.; Denison, G. M.; DeSimone, J. M. *J. Am. Chem. Soc.* **2005,** *127* (28), 10096-10100.

138. Sun, H.; Guo, B.; Li, X.; Cheng, R.; Meng, F.; Liu, H.; Zhong, Z. *Biomacromolecules* **2010,** *11* (4), 848-854.

139. Kabanov, A. V. *Advanced Drug Delivery Reviews* **2006,** *58* (15), 1597-1621.

140. Chacko, R. T.; Ventura, J.; Zhuang, J.; Thayumanavan, S. *Advanced Drug Delivery Reviews* **2012,** *64* (9), 836-851.

141. Jiang, X.; Vogel, E. B.; Smith, M. R.; Baker, G. L. *Macromolecules* **2008,** *41* (6), 1937-1944.

142. Portis, A. M.; Carballo, G.; Baker, G. L.; Chan, C.; Walton, S. P. *Microscopy Research and Technique* **2010,** *73* (9), 878-885.

143. Xu, J.; Tao, L.; Liu, J.; Bulmus, V.; Davis, T. P. *Macromolecules* **2009,** *42* (18), 6893-6901.

144. Nakayama, Y. *Accounts of Chemical Research* **2012,** *45* (7), 994-1004.

145. O'Reilly, R. K.; Joralemon, M. J.; Hawker, C. J.; Wooley, K. L. *New Journal of Chemistry* **2007,** *31* (5), 718-724.

146. Xu, P.; Tang, H.; Li, S.; Ren, J.; Van Kirk, E.; Murdoch, W. J.; Radosz, M.; Shen, Y. *Biomacromolecules* **2004,** *5* (5), 1736-1744.

147. Lee, W.-C.; Li, Y.-C.; Chu, I. M. *Macromol. Biosci.* **2006,** *6* (10), 846-854.

148. Thurmond, K. B.; Kowalewski, T.; Wooley, K. L. *J. Am. Chem. Soc.* **1996,** *118* (30), 7239-7240.

149. Zhang, Q.; Remsen, E. E.; Wooley, K. L. *J. Am. Chem. Soc.* **2000,** *122* (15), 3642-3651.

150. Xu, X.; Smith, A. E.; Kirkland, S. E.; McCormick, C. L. *Macromolecules* **2008,** *41* (22), 8429-8435.

151. Sun, G.; Hagooly, A.; Xu, J.; Nyström, A. M.; Li, Z.; Rossin, R.; Moore, D. A.; Wooley, K. L.; Welch, M. J. *Biomacromolecules* **2008,** *9* (7), 1997-2006.

152. Pan, D.; Turner, J. L.; Wooley, K. L. *Macromolecules* **2004,** *37* (19), 7109-7115.

153. Bae, K. H.; Lee, Y.; Park, T. G. *Biomacromolecules* **2007,** *8* (2), 650-656.

154. Xu, B.; Yuan, J. F.; Wang, Z. F.; Gao, Q. Y. *J. Microencapsul.* **2009,** *26* (7), 659-666.

155. Zhang, L.; Liu, W. G.; Lin, L.; Chen, D. Y.; Stenze, M. H. *Biomacromolecules* **2008,** *9* (11), 3321-3331.

156. Talelli, M.; Iman, M.; Varkouhi, A. K.; Rijcken, C. J. F.; Schiffelers, R. M.; Etrych, T.; Ulbrich, K.; van Nostrum, C. F.; Lammers, T.; Storm, G.; Hennink, W. E. *Biomaterials* **2010,** *31* (30), 7797-7804.

157. Abraham, G.; McCarroll, J.; Byrne, F.; Saricilar, S.; Kavallaris, M.; Bulmus, V. *Journal of Biomaterials Science, Polymer Edition* **2011,** *22* (8), 1001-1022.

158. Zhang, Z.; Yin, L.; Tu, C.; Song, Z.; Zhang, Y.; Xu, Y.; Tong, R.; Zhou, Q.; Ren, J.; Cheng, J. *ACS Macro Letters* **2012,** *2* (1), 40-44.

159. Allard, E.; Larpent, C. *Journal of Polymer Science, Part A: Polymer Chemistry* **2008,** *46* (18), 6206-6213.

160. Li, Y.; Du, W.; Sun, G.; Wooley, K. L. *Macromolecules* **2008,** *41* (18), 6605-6607.

161. Huynh, V. T.; Binauld, S.; de Souza, P. L.; Stenzel, M. H. *Chemistry of Materials* **2012,** *24* (16), 3197-3211.

162. Liu, J.; Pang, Y.; Huang, W.; Huang, X.; Meng, L.; Zhu, X.; Zhou, Y.; Yan, D. *Biomacromolecules* **2011,** *12* (5), 1567-1577.

163. Khorsand Sourkohi, B.; Schmidt, R.; Oh, J. K. *Macromol. Rapid Commun.* **2011,** *32* (20), 1652-1657.

164. Khorsand Sourkohi, B.; Cunningham, A.; Zhang, Q.; Oh, J. K. *Biomacromolecules* **2011,** *12* (10), 3819-3825.

165. Wen, H.-Y.; Dong, H.-Q.; Xie, W.-j.; Li, Y.-Y.; Wang, K.; Pauletti, G. M.; Shi, D.-L. *Chemical Communications* **2011,** *47* (12), 3550-3552.

166. Rehor, A.; Hubbell, J. A.; Tirelli, N. *Langmuir* **2004,** *21* (1), 411-417.

167. Li, Y.; Xiao, K.; Luo, J.; Xiao, W.; Lee, J. S.; Gonik, A. M.; Kato, J.; Dong, T. A.; Lam, K. S. *Biomaterials* **2011,** *32* (27), 6633-6645.

168. Barick, K. C.; Singh, S.; Jadhav, N. V.; Bahadur, D.; Pandey, B. N.; Hassan, P. A. *Advanced Functional Materials* **2012,** *22* (23), 4975-4984.

169. Wen, H.; Guo, J.; Chang, B.; Yang, W. *European Journal of Pharmaceutics and Biopharmaceutics* (0).

170. Jiang, X.; Zhang, G.; Narain, R.; Liu, S. *Soft Matter* **2009,** *5* (7), 1530-1538.

171. Mu, B.; Liu, P. *Reactive and Functional Polymers* **2012,** *72* (12), 983-989.

172. Coradeghini, R.; Gioria, S.; García, C. P.; Nativo, P.; Franchini, F.; Gilliland, D.; Ponti, J.; Rossi, F. *Toxicology Letters* **2013,** *217* (3), 205-216.

173. Panyam, J.; Labhasetwar, V. *Advanced Drug Delivery Reviews* **2012,** *64, Supplement* (0), 61-71.

174. Foster, K. A.; Yazdanian, M.; Audus, K. L. *Journal of Pharmacy and Pharmacology* **2001,** *53* (1), 57-66.

175. Maeda, H.; Wu, J.; Sawa, T.; Matsumura, Y.; Hori, K. *Journal of Controlled Release* **2000,** *65* (1–2), 271-284.

176. Lallana, E.; Sousa-Herves, A.; Fernandez-Trillo, F.; Riguera, R.; Fernandez-Megia, E. *Pharmaceutical Research* **2012,** *29* (1), 1-34.

177. Cheng, R.; Feng, F.; Meng, F.; Deng, C.; Feijen, J.; Zhong, Z. *Journal of Controlled Release* **2011,** *152* (1), 2-12.

178. Negoda, A.; Comiskey, G. A.; Baker, G. L.; Worden, R. M. *In Preparation* **2013**.

179. Yacobi, N. R.; Malmstadt, N.; Fazlollahi, F.; DeMaio, L.; Marchelletta, R.; Hamm-Alvarez, S. F.; Borok, Z.; Kim, K.-J.; Crandall, E. D. *American Journal of Respiratory Cell and Molecular Biology* **2010,** *42* (5), 604-614.

180. Ojeda, R.; Terenti, O.; de Paz, J. L.; Martin-Lomas, M. *Glycoconjugate Journal* **2004,** *21* (5), 179-195.

181. Carboni, B.; Benalil, A.; Vaultier, M. *Journal of Organic Chemistry* **2002,** *58* (14), 3736-3741.

182. Withey, A. B. J.; Chen, G.; Nguyen, T. L. U.; Stenzel, M. H. *Biomacromolecules* **2009,** *10* (12), 3215-3226.

183. Saito, G.; Swanson, J. A.; Lee, K.-D. *Advanced Drug Delivery Reviews* **2003,** *55* (2), 199-215.

184. Christensen, L. V.; Chang, C.-W.; Kim, W. J.; Kim, S. W.; Zhong, Z.; Lin, C.; Engbersen, J. F. J.; Feijen, J. *Bioconjugate Chemistry* **2006,** *17* (5), 1233-1240.

185. Ou, M.; Wang, X.-L.; Xu, R.; Chang, C.-W.; Bull, D. A.; Kim, S. W. *Bioconjugate Chemistry* **2008,** *19* (3), 626-633.

186. Breunig, M.; Hozsa, C.; Lungwitz, U.; Watanabe, K.; Umeda, I.; Kato, H.; Goepferich, A. *Journal of Controlled Release* **2008,** *130* (1), 57-63.

187. Breunig, M.; Lungwitz, U.; Liebl, R.; Goepferich, A. *Proceeding of the National Academy of Sciences* **2007,** *104* (36), 14454-14459.

188. Pichon, C.; LeCam, E.; Guerin, B.; Coulaud, D.; Delain, E.; Midoux, P. *Bioconjugate Chemistry* **2001,** *13* (1), 76-82.

189. Kinnane, C. R.; Such, G. K.; Antequera-GarciÌ a, G.; Yan, Y.; Dodds, S. J.; Liz-Marzan, L. M.; Caruso, F. *Biomacromolecules* **2009**.

190. Tsarevsky, N. V.; Matyjaszewski, K. *Macromolecules* **2005,** *38* (8), 3087-3092.

191. Kim, S. H.; Jeong, J. H.; Lee, S. H.; Kim, S. W.; Park, T. G. *Journal of Controlled Release* **2006,** *116* (2), 123-129.

192. Rozema, D. B.; Lewis, D. L.; Wakefield, D. H.; Wong, S. C.; Klein, J. J.; Roesch, P. L.; Bertin, S. L.; Reppen, T. W.; Chu, Q.; Blokhin, A. V.; Hagstrom, J. E.; Wolff, J. A. *Proceeding of the National Academy of Sciences* **2007,** *104* (32), 12982-12987.

193. Endo, K.; Kojima, G.; Yamanaka, T. *Kautschuk Gummi Kunststoffe* **2006,** *59* (1-2), 41-44.

194. Song, L.; Xiao, M.; Shu, D.; Wang, S.; Meng, Y. *Journal of Materials Science* **2007,** *42* (4), 1156-1161.

195. Meng, Y. Z.; Liang, Z. A.; Lu, Y. X.; Hay, A. S. *Polymer* **2005,** *46* (24), 11117-11124.

196. Kalarickal, N. C.; Rimmer, S.; Sarker, P.; Leroux, J.-C. *Macromolecules* **2007,** *40* (6), 1874-1880.

197. Ruano, J. L. G.; Parra, A.; Aleman, J. *Green Chemistry* **2008,** *10* (6), 706-711.

198. Pathak, U.; Pandey, L. K.; Mathur, S. *Synthetic Communications* **2009,** *39* (16), 2923-2927.

199. Dong, W.-L.; Huang, G.-Y.; Li, Z.-M.; Zhao, W.-G. *Phosphorus, Sulfur and Silicon and the Related Elements* **2009,** *184* (8), 2058 - 2065.

200. Sharma, S. P.; Suryanarayana, M. V. S.; Nigam, A. K.; Chauhan, A. S.; Tomar, L. N. S. *Catalysis Communications* **2009,** *10* (6), 905-912.

201. Collman, J. P.; Devaraj, N. K.; Eberspacher, T. P. A.; Chidsey, C. E. D. *Langmuir* **2006,** *22* (6), 2457-2464.

202. Kim, S. Y.; Kim, G. *Bulletin of the Korean Chemical Society* **2008,** *29* (9), 1790-1792.

203. Jocelyn, P. C.; William, B. J.; Owen, W. G., Chemical reduction of disulfides. In *Methods in Enzymology*, Academic Press: 1987; Vol. Volume 143, pp 246-256.

204. Kim, W. J.; Christensen, L. V.; Jo, S.; Yockman, J. W.; Jeong, J. H.; Kim, Y.-H.; Kim, S. W. *Molecular Therapy* **2006,** *14* (3), 343-350.

205. Cook, A. D.; Pajvani, U. B.; Hrkach, J. S.; Cannizzaro, S. M.; Langer, R. *Biomaterials* **1997,** *18* (21), 1417-1424.

206. Sun, S.-W.; Lin, Y.-C.; Weng, Y.-M.; Chen, M.-J. *Journal of Food Composition and Analysis 19* (2-3), 112-117.

207. Cilli, E. M. J., G. N; Ribeiro, S. C; Oliveira, E; Nakai, C. R. *Journal of the Brazilian Chemical Society* **2000,** *11* (5), 474-478.

208. Sashidhar, R. B.; Capoor, A. K.; Ramana, D. *Journal of Immunological Methods* **1994,** *167* (1-2), 121-127.

209. Nimesh, S.; Chandra, R. *European Journal of Pharmaceutics and Biopharmaceutics* **2009,** *73* (1), 43-49.

210. Hill, A. V. *Journal of Physiology* **1910,** *40*, iv-vii.

211. Monod, J.; Wyman, J.; Changeux, J.-P. *Journal of Molecular Biology* **1965,** *12* (1), 88-118.

212. Koshland, D. E.; Némethy, G.; Filmer, D. *Biochemistry* **1966,** *5* (1), 365-385.

213. Scales, C. W.; Huang, F.; Li, N.; Vasilieva, Y. A.; Ray, J.; Convertine, A. J.; McCormick, C. L. *Macromolecules* **2006,** *39* (20), 6871-6881.

214. Posner, G. H.; Ting, J. S.; Lentz, C. M. *Tetrahedron* **1976,** *32* (19), 2281-2287.

215. Li, X.; Xie, Q. R.; Zhang, J.; Xia, W.; Gu, H. *Biomaterials* **2011,** *32* (35), 9546-9556.

216. Hom, C.; Lu, J.; Liong, M.; Luo, H.; Li, Z.; Zink, J. I.; Tamanoi, F. *Small* **2010,** *6* (11), 1185-1190.

217. Viitala, R.; Jokinen, M.; Tuusa, S.; Rosenholm, J.; Jalonen, H. *J Sol-Gel Sci Technol* **2005,** *36* (2), 147-156.

218. Bhattarai, S.; Muthuswamy, E.; Wani, A.; Brichacek, M.; Castañeda, A.; Brock, S.; Oupicky, D. *Pharmaceutical Research* **2010,** *27* (12), 2556-2568.

219. Chen, A. M.; Zhang, M.; Wei, D.; Stueber, D.; Taratula, O.; Minko, T.; He, H. *Small* **2009,** *5* (23), 2673-2677.

220. Hartono, S. B.; Gu, W.; Kleitz, F.; Liu, J.; He, L.; Middelberg, A. P. J.; Yu, C.; Lu, G. Q.; Qiao, S. Z. *ACS Nano* **2012,** *6* (3), 2104-2117.

221. Li, X.; Chen, Y.; Wang, M.; Ma, Y.; Xia, W.; Gu, H. *Biomaterials* **2013,** *34* (4), 1391-1401.

222. Na, H.-K.; Kim, M.-H.; Park, K.; Ryoo, S.-R.; Lee, K. E.; Jeon, H.; Ryoo, R.; Hyeon, C.; Min, D.-H. *Small* **2012,** *8* (11), 1752-1761.

223. Xia, T.; Kovochich, M.; Liong, M.; Meng, H.; Kabehie, S.; George, S.; Zink, J. I.; Nel, A. E. *ACS Nano* **2009,** *3* (10), 3273-3286.

224. Zhang, L.; Wang, T.; Li, L.; Wang, C.; Su, Z.; Li, J. *Chemical Communications* **2012,** *48* (69), 8706-8708.

225. Lee, H.; Sung, D.; Veerapandian, M.; Yun, K.; Seo, S.-W. *Anal Bioanal Chem* **2011,** *400* (2), 535-545.

226. Cohen, J. L.; Schubert, S.; Wich, P. R.; Cui, L.; Cohen, J. A.; Mynar, J. L.; FreÃÅchet, J. M. J. *Bioconjugate Chemistry* **2011,** *22* (6), 1056-1065.

227. Raemdonck, K.; Naeye, B.; Buyens, K.; Vandenbroucke, R. E.; Høgset, A.; Demeester, J.; De Smedt, S. C. *Advanced Functional Materials* **2009,** *19* (9), 1406-1415.

228. Tripathi, S. K.; Goyal, R.; Gupta, K. C. *Soft Matter* **2011,** *7* (24), 11360-11371.

229. Broaders, K. E.; Cohen, J. A.; Beaudette, T. T.; Bachelder, E. M.; Fréchet, J. M. J. *Proceedings of the National Academy of Sciences* **2009,** *106* (14), 5497-5502.

230. Bachelder, E. M.; Beaudette, T. T.; Broaders, K. E.; Dashe, J.; Fréchet, J. M. J. *J. Am. Chem. Soc.* **2008,** *130* (32), 10494-10495.

231. Kamat, M.; El-Boubbou, K.; Zhu, D. C.; Lansdell, T.; Lu, X.; Li, W.; Huang, X. *Bioconjugate Chemistry* **2010,** *21* (11), 2128-2135.

232. Stöber, W.; Fink, A.; Bohn, E. *Journal of Colloid and Interface Science* **1968,** *26* (1), 62-69.

233. Lim, J.; Ha, S.-W.; Lee, J.-K. *Bulletin of the Korean Chemical Society* **2012,** *33* (3), 1067-1070.

234. Nozawa, K.; Gailhanou, H.; Raison, L.; Panizza, P.; Ushiki, H.; Sellier, E.; Delville, J. P.; Delville, M. H. *Langmuir* **2004,** *21* (4), 1516-1523.